2022

Impact of Orthophosphate as a Corrosion Inhibitor and Chloramine Disinfectant on Drinking Water Biofilm Communities

Mitchell Cooke
cook0750@mylaurier.ca

Impact of Orthophosphate as a Corrosion Inhibitor and Chloramine Disinfectant on Drinking Water Biofilm Communities

by

Mitchell Cooke

THESIS

Submitted to the Department of Biology

Faculty of Science

In partial fulfillment of the requirements for the

Master of Science in Integrative Biology

Wilfrid Laurier University

Dedication:

I would like to dedicate this research thesis to my parents, Barb and Glenn Cooke, and sister Katie Caesar. Your restless support of my research and studies, throughout both of my undergraduate and graduate degrees has allowed me to reach goals I once thought were unobtainable. I have you all to thank for sparking my incessant passion for science. A thought once awakened, does not again slumber.

Abstract

A drinking water distribution system (DWDS) must maintain conditions within quality standards which assure the effective and safe transport of finished drinking water from treatment plants to the household tap. Although safe to drink, finished water is not sterile, and may contain hundreds of microorganisms in a single milliliter. These microorganisms are present from the source waters, such as lakes, rivers and aquifers, and have passed through early treatment steps. Final treatment steps, such as the maintenance of disinfectant residuals, are used to further minimize viable cells present and focus on the reduction of harmful organisms. Microbial cells entering the distribution system have the ability to attach to pipe walls, and possibly use what little nutrients are present for growth. Over time, these microbial communities may impact the quality of treated drinking water. As many Canadian DWDSs contain lead service lines, which may slowly solubilize over time, the allowable amount of dissolved lead in treated water has come under restrictive scrutiny, to lower amounts and minimize health concerns. As lead service lines are common, corrosion inhibitors, such as orthophosphate, have been increasingly utilized by municipalities as a means of controlling lead solubility. However, the impact of these corrosion inhibitors on the microorganisms present in a DWDS is not fully understood. This research aims to better understand the impact of orthophosphate, in the presence of a chloramine disinfectant, on bacterial communities in a simulated DWDS. Annular reactors (Ars), fed with treated drinking water, were established in a flow-through design, which allowed for routine microbiological sampling, including an assessment of both genetic and metabolic profiles of suspended and attached microorganisms. During the initial flow-through experiment, ARs dosed with three concentrations of orthophosphate were monitored for microbial profiling over the course of 12 weeks. Viable cell counts for both bulk and coupon-associated microorganisms, along with biofilm reformation potential, increased in the presence of orthophosphate at doses above 1 mg/L. Genetic and metabolic diversity of coupon-associated communities increased in the presence of orthophosphate at concentrations of 2 and 4 mg/L. In the second 12-week experiment, ARs contained a high (3 mg/L) or low (2 mg/L) concentration of chloramine, both in the presence and absence of orthophosphate at 2 mg/L. Bulk phase and coupon-associated samples again exhibited higher viable cell counts and biofilm reformation potential in the presence of orthophosphate, with only minor differences being dependent on chloramine dose. Metabolic activity and diversity was highest for coupon-associated microorganisms exposed to orthophosphate. Genetic diversity was lower for communities exposed to chloramine in the absence of orthophosphate, as well as those exposed to the higher chloramine concentration in the presence of added orthophosphate, indicating the selective pressure associated with this disinfectant residual. An opportunity to assess microorganisms collected at the end of a long-term pipe loop study of different corrosion inhibitors indicated that orthophosphate increases viable cell counts of microorganisms collected from pipe walls, when compared to sodium-silicate alternatives. Overall, this research shows that the use of orthophosphate as a corrosion inhibitor at or above 2 mg/L allows for microorganisms in a DWDS to replicate to higher levels and, as a consequence, reform more biomass as biofilm material. These OP-exposed biofilms have shown an increased resistance to the chloramine disinfectant residual and are likely to impact the profile of bulk phase microorganisms in a distribution network.

Acknowledgments:

I want to extend my most sincere and permanent gratitude towards my research supervisor, Dr. Robin M. Slawson. Over the past 4 years of research in her laboratory, she has shown me schools of thought which have impacted how I view the world in the best of ways. By catering to my runaway ideas of research, through careful support, she kept me dedicated and excited about a future of academics. Her mentorship has felt more like a friendship, through which she encourages independent thought, effort and a healthy environment for budding scientists. I would also like to extend my deepest appreciation towards my co-supervisor Dr. Peter Huck, and committee members Dr. Joel Weadge and Dr. Sigrid Peldszus. Our meetings typically consisted of encouraging expertise, which spanned across multiple disciplines. The countless hours of expert knowledge they have given to me just scrapes the surface of their ability as mentors.

I would like to acknowledge the Natural Sciences and Engineering Research Council of Canada (NSERC), and the Ontario Clean Water Agency (OCWA).

This research was part of a larger overall project, aimed at investigating key aspects of drinking water quality. Mahmoud Badawy, a PhD Candidate at the University of Waterloo, spearheaded the major aspects of this project, such as experimental design and setup. Other researchers associated with this project, Kimia Aghasadeghi and Vedika Bakshi, were integral in its completion. Thank you for your time and endless effort.

Along with other collaborators, I would like to thank the water utility from Southern Ontario, and its staff, who have allowed for this project to take place.

Lastly, I would like to extend my thanks to my friends and co-workers, for their support and appreciation of my goals. In no particular order; Brian Lowrance, Joel Mitchell, Sam Snider, Dom Daniels, Shayne Oberhoffner, Wesley Daniels, Aaron Lewis, Natasha Hannan, Sam Lum, Chris Bartlett, Emily McConnell, James Bannister, Megan Gordon, Pat Strzalkowski, Dylan Guillemette, Becca Fievoli, Joe Lass, James Rabbets, Devin Saatchi, and so many more.

Table of Contents

List of Tables

List of Figures

List of Abbreviations

Adenosine Triphosphate (ATP)

Annular Reactors (ARs)

Average Well Colour Development (AWCD)

Colony Forming Units (CFU)

Community-Level Physiological Profile (CLPP)

Crystal Violet (CV)

Denaturing Gradient Gel Electrophoresis (DGGE)

Deoxyribonucleic Acid (DNA)

Drinking Water Distribution System (DWDS)

Ethidium Bromide (EtBr)

Exopolysaccharide (EPS)

Guanine-Cytosine (GC)

Heterotrophic Plate Count (HPC)

Lead Service Line (LSL)

Operation Taxonomic Units (OTUs)

Orthophosphate (OP)

Peptone Buffered Saline (PBS)

Polymerase Chain Reaction (PCR)

Polymerase Chain Reaction-Denaturing Gradient Gel Electrophoresis (PCR-DGGE)

Polyvinylchloride (PVC)

Reasoner's 2A agar (R2A)

Unweighted Pair Group Method with Arithmetic Mean (UPGMA)

Chapter 1: Introduction and Background

1.1 Overview

Being of primary concern for many, access to clean drinking water is essential. The distribution and retention of water, and the assurance of its quality is multi-faceted, and constantly changing. Aspects of drinking water research can span from branches of civil engineering, water chemistry, and microbiology. Many Canadian drinking water distribution systems (DWDS's) may contain at least some lead service lines (LSLs), primarily in older areas of the system, which can release solubilized lead into treated water after it leaves the treatment plant. Additional sources of lead may be some types of solder and brass fittings. The addition of corrosion-inhibiting treatments to finished water has been demonstrated to reducing the amount of dissolved lead, yet the impacts of these treatments on the microbial community, especially in the presence of disinfectant residuals, within a DWDS are not fully understood. The scope of this research focused on the impact of orthophosphate on microbial communities which are present in a DWDS. In doing so, we took an integrative approach, through community profiling of the microorganisms in a simulated DWDS, to help understand key gaps in knowledge associated with these drinking water treatments.

1.2 Background

1.2.1 Introduction to Drinking Water Distribution

The purpose of all drinking water treatment and distribution systems is to operate within a standard practice to create safe, potable water. When source water is utilized from groundwater aquifers, rivers, or lakes, treatment processes are put in place to ensure low enumeration of microorganisms and remove contaminants. Many of these treatment processes physically remove microorganisms, including filtration and flocculation/sedimentation of suspended solids. Although effective, these physical barriers do not remove 100% of all organisms and secondary treatment steps are used to further reduce viable microbial cell counts (Liao et al. 2015).

Recently, regulations are being scrutinized and modified to lower the maximum allowable lead concentration out of the tap in households. Canadian regulations place the maximum amount of allowable lead at 5 µg/L (Health Canada, 2019). Regulation changes begin at the Federal level, which are then implemented at the Provincial and Territorial level. These changes require either the costly removal and replacement of LSLs, or the addition of corrosion inhibitors, such as silicates or orthophosphate (OP) compounds, to control lead solubilization (Schock 1989). Other issues surrounding LSPs are related to location of the lines. Municipalities may replace LSLs until the private property line, at which point, the property owner is responsible. Due to the lower cost of corrosion inhibitors (Schneider et al. 2007), many municipalities have begun dosing drinking water with OP. Typically, these doses range from concentrations above 1 mg/L, to over 3.5 mg/L of orthophosphate.

Orthophosphate contains a single phosphorus atom, which is able to react with lead pipelines in older distribution systems. The oxidation of lead creates an insoluble lead phosphate, which acts

as a scale to seal in any soluble lead compounds, preventing their introduction into the drinking water (Nriagu 1972; Schock 1989). Another advantage of OP is that it can easily be added to the water systems as a routine part of the water treatment process (Schneider et al. 2007).

Although OP is a possible solution to the issue of lead in finished drinking water, there are some discussed disadvantages associated with its use. A disadvantage of using OP is that phosphorous can be the most limiting nutrient for microbial growth in source waters. A ratio of 10:4:1 of carbon, nitrogen and phosphorous is often required for optimal microbial growth (Casida, 1960; Miettinen, Vartiainen, & Martikainen, 1997), and the introduction of phosphorous-containing corrosion inhibitors in drinking water systems enhances the ratio of these compounds, which can allow for higher rates of microbial growth. (Berman 1988; Miettinen et al. 1997). For example, bacteria can use the phosphate compounds as a source of phosphorus for common metabolites including adenosine triphosphate ATP (Faust and Correll 1976; Berman 1988). When there is higher availability of phosphates for these metabolites, growth is advanced (Jansson 1988).

The potential for increased microbial growth in a DWDS is cause for concern, and some microbiological aspects of drinking water are regulated through guidelines. The Federal Guidelines for Canadian Drinking Water Quality address that drinking water leaving a treatment plant must have no detectable cell counts of coliform bacteria per 100mL of treated water tested (Health Canada 2012). Coliform bacteria are bacteria that are used as indicators for human and animal fecal contamination, and can give evidence towards bacterial regrowth in the DWDS or the intrusion of untreated water. However, coliform and fecal contaminants are not the only microorganisms that pose a threat (Szewzyk et al. 2000).

To combat the presence of potentially harmful microorganisms, municipalities routinely treat drinking water with disinfectant chemicals. Of these treatments, chlorination is among the most

common in North American, and one of the oldest practices when discussing drinking water treatment (Pasteur 2000). The use of chlorine-based compounds, including chloramine, allows for the degradation of cells through disruption of membrane proteins. These cells are effectively killed, and pose a minimized threat to public safety (Berry et al. 2006a). However, due to the high levels of microbial diversity found in source waters, bacteria that have higher resistance profiles to treatment steps are typically present (Levy et al. 2016; Douterelo et al. 2017). These bacteria, which are only damaged or relatively unharmed by chlorine compounds, are able to spread through the distribution system and can have observable impacts on drinking water quality (Douterelo et al. 2016).

To assure that disinfectants are effective, treatments are dosed in such a way to assure that residual amounts are present throughout the entire distribution system. Chlorine-based disinfectants, such as chloramine, are often nitrogen-bound, which allow for longer retention times through a more stable chemical presence (Ozekin et al. 1996; Zhang et al. 2009). The production of these compounds occurs through the addition of both ammonia and chlorine to treated water, allowing for the formation of chloramine. These chloramines, most commonly in the form of monochloramine, can be decomposed by bacteria present in the DWDS (Wilczak et al. 1996). Decomposition of monochloramine by bacteria is an example of nitrification, wherein nitrates and nitrites are released through microbial metabolism of free ammonia (Zhang and Edwards 2009; AWWA 2013). The initial presence of free ammonia allows for residual chloramine levels throughout the DWDS, however unintentional increases may be due to improper treatment protocols, lowered pH of the treated water, or the chemical degradation of chloramine (Sawade et al. 2016). As free ammonia is metabolized by bacteria present in the system, the increase of nitrates and nitrites can act as a catalyst for further disinfectant residual degradation. This, in turn, can

lower disinfectant impacts, and pose a risk to public safety (Wolfe et al. 1988; Zhang et al. 2009; Zhang and Edwards 2009). The increase of disinfectant residual metabolism is referred to as a "Nitrification Event" and can give evidence towards increased presence of microbial communities in a DWDS (Gomez-Alvarez and Revetta 2020). To combat these events, levels of free ammonia, nitrites and nitrates are measured to act as an indicator.

1.2.2 Low Nutrient Environments

Nutrients are present in environments in different ratios, dependant on the environment and the interactions within. Typically, phosphorous is thought to be the limiting nutrient in many environments, however due to the relatively low level of organic carbon in many raw waters and the removal of organic material during drinking water treatment, carbon may actually be the most limiting nutrient in a DWDS (Volk and LeChevallier 1999).

As per standard water quality assurance practices, some removal of organic carbon may occur through drinking water treatment regimes. The presence of organic materials gives way to higher potential for microbial adherence, growth and regrowth in a DWDS (LeChevallier et al. 1991). The removal of organic matter through primary treatments is not absolute, as some dissolved organic matter (DOM) still may enter the distribution network. When the DOM enters the system, deposits may form along pipe wall material, further inducing the growth of biofilm communities. Typically, DOM is from the raw source water itself, and conditions the surface of pipe material for initial colonizing bacteria to adhere (Emmanuelle I. Prest et al. 2016). With the adherence of microorganisms on pipe material, the degradation of service pipes through microbial and biochemical interactions at the interface of the pipe material may release organic compounds into

the water (Szewzyk et al. 2000; Fish and Boxall 2018). Pipe material and deposited minerals from source waters can become dislodged and dispersed throughout the network, providing essential nutrients for microbial communities. The release of these compounds can have a domino effect for microbial growth, allowing for the dispersal of cells and regrowth of biofilm communities from the bulk phase. By limiting nutrients present in a system, some level of microbial control can be achieved. However, some bacteria may be able to utilize chemicals from treatment regimes, such as the nitrification of chloramine, for metabolic activity (Wilczak et al. 1996; Boe-Hansen et al. 2002; Park et al. 2008).

Conversely, the over-enrichment of nutrients in an ecosystem is referred to as "nutrient loading", where an excess of nutrients is present (Liu et al. 2018). In the case of nutrient loading, metabolic activity and community composition of present bacteria may be impacted (Bannister et al. 2021). The impacts of nutrient loading in relation to microbial communities in a DWDS are not fully understood, as the presence of these nutrients are commonly understood to be limiting.

1.2.3 Microbial Presence in a DWDS

Bulk water is the treated water which passes through a DWDS. Although in lowered numbers when compared to source waters, bacteria are still present in the bulk phase of treated water. The lowered cell count of treated water decreases diversity, as cells that are more susceptible to treatment are killed or removed (Farkas et al. 2012). The surviving and damaged cells that pass through the system through the bulk phase are typically thought of as low concern, as it is commonly understood that their metabolic activity is decreased, to focus on cell survival and repair and the vast majority of present microorganisms are not pathogenic. Bulk phase microorganisms

have major implications on biofilm diversity and structure, and may still act as a community, however low cell counts and metabolic activity may be reduced when compared to biofilm communities attached to pipe wall materials (Douterelo et al., 2019). These bulk phase microorganisms, which have been impacted by treatment regimes, are typically less metabolically active, and being damaged, focus on cellular repair once adhered to a biofilm. Bacterial populations, including those in a DWDS, can be profiled based on their respective metabolic and genetic attributes, such as which carbon sources they can metabolize, and the presence or absence of specific genetic sequences. The presence or absence of specific structural and functional profiles in the bulk phase shape the diversity of the biofilms communities (Boe-Hansen et al. 2002; Martiny et al. 2003).

As mentioned, microbial communities are found through all DWDS. These communities contain various species, typically reflective of the source water which the systems draw from. As source water is treated through various stages, damaged and resistant cells are able to pass through in low concentrations, staying well below an acceptable range for treated water (Li et al. 2017). However, once these cells have entered the distribution systems, they may adhere to pipe material or enter biofilms which are already present. Due to the ability of many bacteria to form these biofilms, pockets of higher concentrations of microorganisms can form (El-Chakhtoura et al. 2015).

1.1.4 Biofilm Formation

Biofilms are structures that are created by bacteria which have typically adhered to a surface, and in the case of DWDS, this surface is the pipe material used to distribute treated water (Berry et al. 2006a). These biofilms are created through the production of polymers and exopolysaccharides,

which create a protective barrier for bacteria to reside in. These biofilms can be extremely diverse, and contain both extra and intracellular constituents including amino acids, proteins, deoxyribonucleic acid (DNA) fragments, and both live and dead cells (Martiny et al. 2003; Douterelo et al. 2014). Biofilms act not only as a protectant from the environment, but also provide a higher opportunity for the transfer of genetic information through horizontal gene transfer between species. Drinking water biofilms are rarely monocultural, and reflecting the inocula of the source can, therefore, contain a vast array of species and strains of bacteria (Kelly et al. 2014)

Biofilm development occurs in a number of defined stages. Initial colonization of a surface occurs when planktonic cells adhere to the pipe wall surface. Rough surfaces allow for microscopic pockets of lower flow rate, where cells can attach using adhesion structures including pili (Liu et al. 2013a). As more planktonic cells adhere, irreversible attachment occurs, wherein cells begin to produce polysaccharide material and planktonic growth is halted. These bacteria, which begin the formation of biofilms, are commonly referred to as “Initial Colonizers”, as they introduce the first steps in biofilm production (Martiny et al. 2003; Liu et al. 2013a). While these cells produce biofilm material, more cells from the environment may become attached nearby, or even to the initial colonizing cells themselves (Hwang et al. 2012a). Communication between cells increases the production of biofilm material, forming a matrix as the biofilm matures (Douterelo et al. 2014). Over time, as these biofilms mature, and as bacteria from the environment adhere to, enter, and multiply within the structure, an increase in overall diversity is typically seen (Martiny et al. 2003; I. Douterelo et al. 2018).

Environmental conditions play a major role in biofilm formation. Factors including temperature, pH, water availability, nutrient presence and physical barriers, such as flow dynamics in aquatic environments determine biofilm structures through their impact on the microorganisms present

(Fish and Boxall 2018). Of these conditions, the varied flow rates in a DWDS can have major implications on biofilm structures present. As these biofilms mature and grow in size, higher levels of force are applied to the surface, and can increase potential for sloughing and dispersal events (Tsvetanova 2020).These occur when sections of biofilm material are disturbed, releasing bacteria and biofilm material which still contains cells (Farkas et al. 2012; Liu et al. 2013b). These released bacteria may go on to form new biofilms, and sloughed sections may adhere to pipe material further throughout the distribution network. This regrowth can allow for the spread of bacteria throughout the network, and increase biofilm presence along the majority of pipe material.

In a DWDS, where microbial diversity of the bulk phase is lowered through treatments, such as chloramine disinfection, biofilms act as a harbour for damaged and repairing cells (Akin et al. 1982). These cells enter biofilm structures and have a chance to repair and replicate, and the biofilm material acts as a barrier from disinfectants and environmental pressures present. The major force impacting the diversity of the microorganisms in the bulk phase in DWDS is secondary treatment residuals. Once the cells are exposed to these disinfectant residuals, they are either damaged or killed. Dead cells may lyse and release constituents, such as DNA, ATP or proteins, which can be taken up by biofilm communities. Extracellular DNA, released during cell death or through metabolic activity, has been shown to persist in these systems, and may impact studies which focus on genetic profiling (Sakcham et al. 2019).

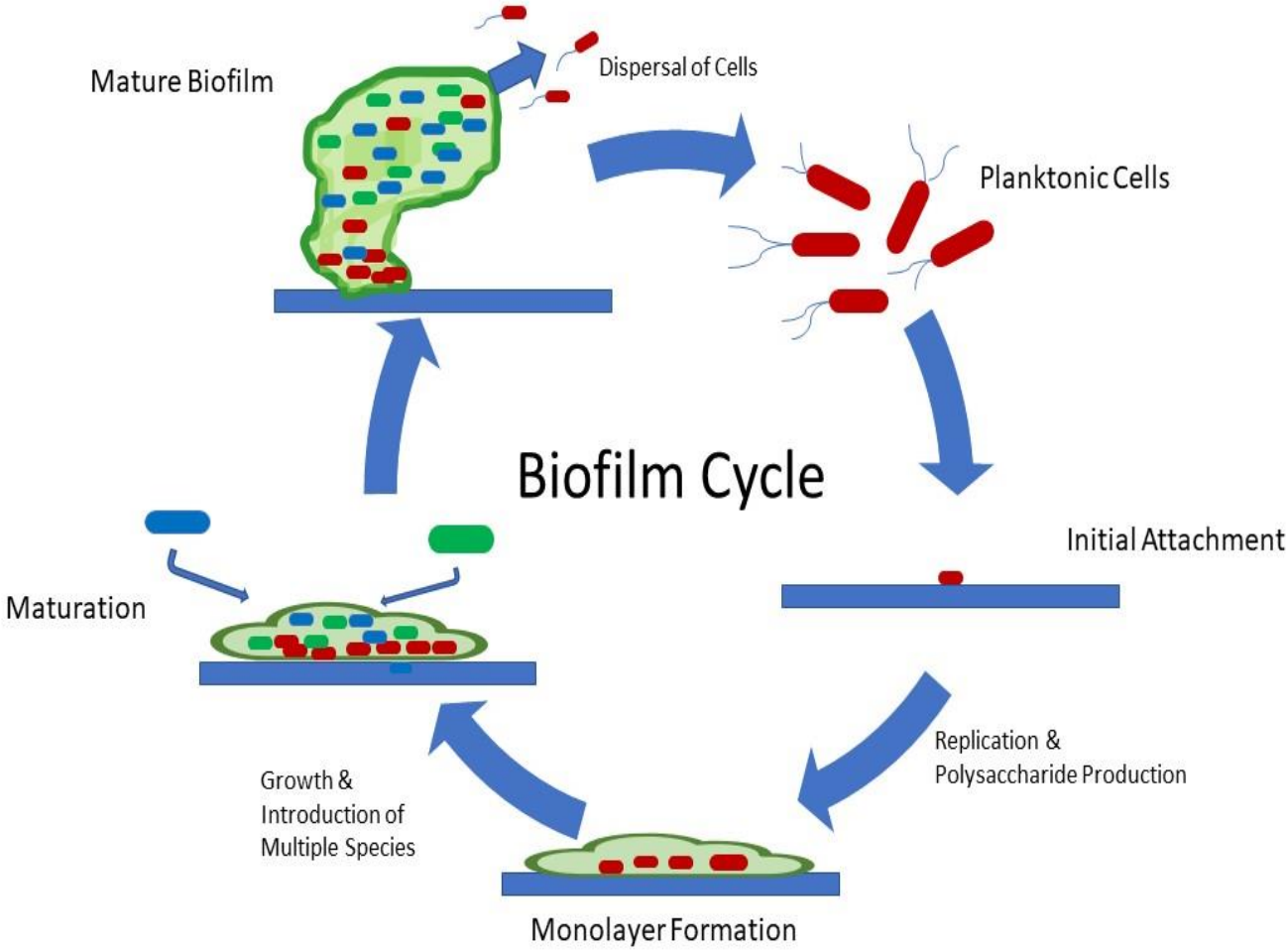

Figure 1.1: The formation of diverse drinking water biofilms. Note the initial attachment, and the possibility of dispersal and reintroduction into new environments. Environmental biofilms are rarely comprised of only one species (Adapted from Don, 2007).

1.1.5 Biofilm Diversity

Biofilm communities can contain metabolic and structural profiles which can vary widely in diversity. As biofilms mature and more cells enter from the bulk phase, shifts in diversity can occur to become more reflective of the bulk phase (Chan et al. 2019). DWDS biofilm diversity has been

shown to increase over time, shifting from species which are classified as initial colonizers, towards a community mirroring that of the bulk phase (Martiny et al. 2003). The biofilms are then comprised of unique communities of bacteria, where species presence can vary between areas of each biofilm. These communities may be reflective of the environment, but due to the transience of many species, are typically more diverse. The diversity of biofilms is commonly studied, as they have major implications in food, medical and drinking water safety (Liu et al. 2013a).

Biofilm communities are of primary focus when discussing DWDS, as the metabolic potential for compounds, including disinfectant residuals, may be increased when compared to bulk phase communities. Studies have shown that biofilm communities can make up to 95% of the active biomass in a DWDS (Flemming et al. 2002). Along with comprising the majority of biomass, these biofilm communities are typically shown to be more metabolically active than the cels which are suspended in the bulk phase. The role that these communities play in water quality means that researching and monitoring their presence and diversity is essential.

Studies have typically focused on genetic diversity of these communities. DNA is extracted from biofilm material and sequenced to determine either species or operational taxonomic units (OTUs) present. With this information, general inferences can be made as to the overall species diversity, and overarching potential for metabolic diversity. As source water, treatment regimes, system engineering and location of the biofilms all impact their diversity, the assessment of these communities may widely differ between DWDSs. Biofilm diversity, both metabolic and species, can have implications on resistance to environmental pressures including treatment regimes (X. Li et al. 2010; Van Blerk et al. 2011; Hwang et al. 2012a; Kelly et al. 2014).

The primary focus for these studies weighs heavily on the presence or absence of specific species or strains of bacteria as dependant on genetic material. *Pseudomonas*, *Firmicutes*, *Legionella* and

ammonia oxidizing bacteria are all of considerable focus due to their impacts on biofilm formation, disinfectant resistance, disease and nitrification events (Kwon et al. 2011; I. Douterelo et al. 2018; Keshvardoust et al. 2020). Although commonly thought that the presence of these bacteria significantly determines the metabolic profile of a community, this may not be the case, as various studies have shown that metabolic diversity and structural diversity of a community can shift independently of one another (Frąc et al. 2012; Clairmont and Slawson 2020). These community shifts may be due to changes in environmental pressures, the time of year, and the introduction of new bacterial cells from the bulk phase.

As more cells enter a developing biofilm, specific environmental niches can arise. The size of biofilms can play a major role in these niches, as the proximity to the surface of the structure can impact nutrient presence, oxygen availability, and competition for resources. Typically, slower-growing bacteria are found deeper in these biofilms, while the more metabolically active and faster-growing cells are found closer to the surface interface (Cruz et al. 2020). Due to the presence of these different niches in a biofilm, interactions between the microorganisms and their environment may be missed in investigations which rely solely on genetic analyses.

While the genetic profiling of these biofilms is widely studied, further research into the metabolic functionality of these communities may lead to further insight towards understanding the community shifts present over the lifetime of these biofilms. These metabolic niches have yet to be fully studied in a DWDS and may play key roles in overall water quality.

1.1.6 Factors Influencing Regrowth

As previously mentioned, events such as sloughing can impact biofilm diversity, as the removal of sections may remove entire environmental niches from the community. These sloughing events can allow for the spread of diversity in a DWDS, and many factors, such as flow rate, can play a role in the sloughing and regrowth of biofilms (Fish et al. 2016; Fish and Boxall 2018). Flow rate can vary, even in direction, among areas of a DWDS, as dead-end pipe caps and elevation changes impact overall flow dynamics (Manuel et al. 2007). Flow rates have been shown to impact biofilm structure, and communities which form biofilms in areas of higher flow rate have been shown to create biofilms which are more resistant to shear force. Cell density has also been identified as being directly dependant on shear force from flow rates (Fish et al. 2017).

Disinfectant residuals have also been shown to impact biofilm structure, and decrease biofilm regrowth potential. Chlorine-based disinfectants have been shown to reduce overall mass of biofilms, by increasing the likelihood of sloughing events (Fish et al. 2020). This, in combination with the bactericidal effects of chlorine-based treatments, decreases overall cell count and diversity in the biofilms.

When considering regrowth potential of biofilms, pipe material also plays a role. Surface texture of pipe material varies and can allow or inhibit the attachment of sloughed material or released cells (Lehtola et al. 2006). Rough surfaces, such as corroded lead pipes or stainless steel, have been shown to increase potential for biofilm regrowth shortly after attachment. Compared to materials such as polyvinylchloride (PVC) and polyethylene, where biofilm regrowth potential is decreased (Lehtola et al. 2006; Liu et al. 2013b). This potential for sloughing events and regrowth plays major roles in the overall diversity of a DWDS. As mentioned, more metabolically active

cells are typically found closer to the interface of the biofilm (Cruz et al. 2020). As biofilm material close to the interface is dislodged and cells eventually reattach, those with higher levels of metabolic activity may initially dominate the early biofilm, before the uptake of bulk phase microorganisms takes place.

1.1.7 Drinking Water Quality Assurance: Microbiological Aspects

To properly ensure water is kept at a safe standard for consumption, microbiological presence is routinely tested. These tests provide feedback on the presence or absence of potentially pathogenic bacteria, the amount of bacteria which are able to enter the distribution system (Rose and Grimes 2001), and the presence of basic metabolites, such as ATP. Standard heterotrophic plate count (HPC) provides insight into the amount of colony forming units (CFU), or viable cells, which have a heterotrophic metabolism, and can replicate in low-nutrient conditions (Deininger and Lee 2001; Delahaye et al. 2003). Media used for HPC-enumeration mirror nutrient loads present in drinking water, and allow for the visible determination of CFU, which can be monitored and recorded. Dramatic changes in CFU can help identify nitrification events and periods of higher or lower microbial growth (LeChevallier et al. 1980).

These methods can also determine the presence of coliform bacteria, which are indicator organisms for the presence of pathogens including *Salmonella* sp. and *Escherichia* sp. The presence of coliform bacteria may not be of major concern, however, once levels cross an acceptable threshold, the risk of pathogenesis and disease outbreak increases (Ozekin et al. 1996; Szewzyk et al. 2000).

Extracellular ATP is a metabolite produced when bacteria are actively metabolising or reproducing, which can be tracked using luciferase enzyme testing. Due to the removal of most microorganisms during the treatment process, it is largely assumed that the vast majority of ATP molecules in these systems can be directly attributed to bacterial regrowth within the distribution network (Liu et al. 2013a). Filters placed in pipelines can be removed and processed, and the amount of extracellular ATP measured using a luminometer. Luminometers measure the amount of light produced during a reaction of ATP and a standard luciferase enzyme, which can then be related to theoretical ATP concentrations (Delahaye et al. 2003). However, metabolic functionality is very dynamic between microorganisms, and ATP levels vary widely throughout species (Deininger and Lee 2001). Large amounts of bacteria can be metabolising at very low rates and can produce similar ATP levels compared to lower amounts of microorganisms which are metabolising at a higher rate. With this is in mind, some issues arise with the accuracy of quality assurance which ATP testing provides.

Typically, both HPC and ATP testing are performed in conjunction, allowing for a relationship between microbial presence and ATP concentrations to be determined (Deininger and Lee 2001). With these tests being completed routinely, levels of bacteria in drinking water systems can be monitored and safe levels ensured more accurately.

1.1.8 Microbial Community Profiling

A typical environmental microbial biofilm can include countless species and strains. Each and every biofilm is a unique environment, containing varying nutrient loads, polysaccharide

structures, extracellular constituents and bacterial species. These variations impact the functional and genetic profile of these communities (Clairmont & Slawson, 2019).

Drinking water biofilm communities tend to be less diverse and contain fewer viable bacteria when compared to biofilms found in sediment, soil or even surface waters. This is in part due to the treatment processes involved in drinking water distribution, including filtration and disinfection steps (Berry et al. 2006a).

However, these communities have an increased potential to influence the quality of treated water when environmental shifts occur. These shifts could include temperature range increases, a decrease in disinfectant residual, as well as the possibility of higher nutrient loads. If environmental conditions shift towards a more favourable opportunity for the microorganisms present in these communities, there could be a shift in the overall genetic and metabolic community profile (Berry et al. 2006a; Hwang et al. 2012b).

Microbial communities can be profiled both structurally and functionally, which allows for further investigation into the impact of their presence, and potential profile shifts in a DWDS. These profiles can be created in multiple ways, typically through genetic techniques and functional assays. Structural, or genetic profiles focus primarily on the DNA present in each community. DNA from samples can be replicated and multiplied to higher magnitudes for further analysis. These samples of amplified DNA can be used in techniques which allow for visualization of shifts in the community (Lührig et al. 2015), including Denaturing Gradient Gel Electrophoresis (DGGE). DGGE differentiates DNA samples based on G:C content, as well as overall DNA segment size. (Eichner et al. 1999). The multi-level differentiation gel can be stained to visualize any bands present (Figure 1.2). The differentiation of DNA based on the guanine-cytosine (G-C) content and band length can give distinct structural profiles for each community.

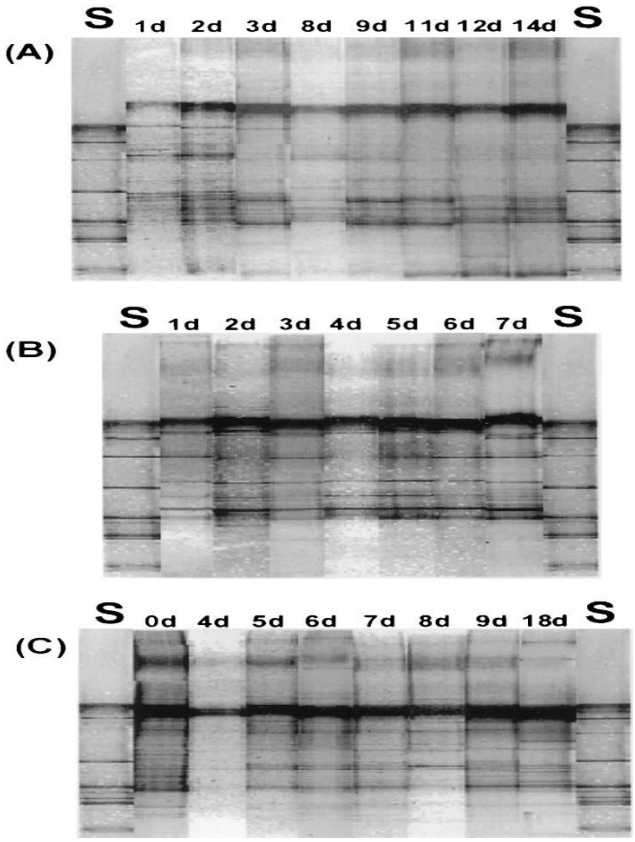

Figure 1.2: Wastewater sludge microbial diversity after chemical treatment. Three DGGE gels (A,B and C), with bands representing shifts in microbial genetic profiles in wastewater sludge over time. Each lane represents a distinct time after chemical treatment, while each band represents a grouping of DNA with similar G:C content and overall length. Retrieved from https://aem.asm.org/content/65/1/102

Functional profiles refer to the ability of a community to metabolize or degrade an array of metabolite sources. The functional metabolism of a community, similar to the structural profile, can readily shift in response to environmental changes (Clairmont & Slawson, 2019). These shifts, however, tend to be a direct result of structural shifts in the community. Functional profiles depend on the genetic sequences being expressed in a community at a given point in time, and can shift rapidly in response to structural profile changes (Hwang et al. 2012b).

The functional profiles of communities also depend heavily on the presence or absence of specific species and strains, as they can be altered by aspects such as competition and syntrophic relationships. These community-level physiological profiles are of great interest in environmental microbiology (Frąc et al. 2012).

A multitude of assays exist which can provide a functional community profile. Such assays are intended to determine the metabolic capabilities of a community and can vary in the metabolite sources being profiled. For example, carbon, nitrogen and phosphorous utilisation profiles are scientifically important in microbially-driven remediation of damaged soils and wetlands (Frąc et al. 2012; Clairmont and Slawson 2020), but can also provide important community dynamics in drinking water networks, where organic nutrient loads are much lower (AWWA 2013). BIOLOG EcoPlates^{TM} are one such assay, where sole organic carbon nutrient sources are bound to a reducible dye, which is released if the nutrient source is metabolized. These assays provide community profiles which can be compared through functional richness, diversity and total nutrient usage.

When compared together, both functional and structural profiles provide further understanding into the specific community-level interactions taking place in drinking water distribution networks. These underlying interactions can drastically alter the quality of treated water, and are subject to shifts due to environmental changes (Berry et al. 2006a).

1.3 Research Need

Studies specifically associated with drinking water biofilm community dynamics are sparse, as research on drinking water networks traditionally focuses on the physico-chemistry of treated water. The lower microbial loads, along with a potential for decreased diversity in these communities could easily be discounted as less important when discussing treated water. However, it has been shown through previous studies that biofilm communities in drinking water distribution networks have greater impacts on treated water than might have once been expected (Ashbolt 2015). These impacts include nitrification of chloramine disinfectant residual, degradation of network pipe material, potential for spread of disease and overall reduction of water quality (AWWA 2013). With new regulations and treatments being put in place to limit the amount of lead present in treated water, biofilm communities present in distribution networks are likely to be impacted. Corrosion inhibitors, including orthophosphate, are fairly understudied from a microbial perspective. Literature seems somewhat conflicting on the impacts of these corrosion inhibitors on biofilm communities, and how these impacted communities change (Faust and Correll 1976; Berman 1988; Jansson 1988; Schock 1989). There has also been very little research into the role that these corrosion inhibitors play in the reduction of chloramine residuals, which are put in place to reduce the presence of disease causing organisms such as *Escherichia, Salmonella* and *Legionella* species (Rusin et al. 1997). These key knowledge gaps require further study, as they potentially influence the overall quality of treated drinking water.

1.4 Research Question and Objectives

The goal of this research is to answer the question: how do corrosion control measures, specifically the use of orthophosphate, impact profiles of microorganisms in drinking water distribution systems? Using a community profiling approach along with standard microbial assessments (HPCs), this research will investigate the impact of orthophosphate dosages on bulk phase microorganisms and biofilms grown under flow-through conditions which simulate a full-scale distribution network using chloramine as a disinfectant residual. The impact of these biofilms on chloramine residual decay will also be investigated to provide an improved understanding of microbial influences on chloramine stability in DWDSs.

Specific research objectives to answer this question are;

1) Using culture and molecular-based approaches, assess microbial response to the presence and absence of orthophosphate as a corrosion inhibitor.
2) Establish microbial response to the presence and absence of chloramine as a disinfectant through culture and molecular-based approaches.
3) Compare and contrast biofilm response to chloramine in the presence of orthophosphate by comparing community profiles.

Chapter 2: Methodology

2.1 Experimental Design

In studies which focus on the DWDS', many applicable experimental approaches exist, which represent the conditions of a full-scale distribution system. These can range from benchtop, batch experiments to pilot-plants containing representative pipe loops. A common experimental approach, used in this study involved annular reactors (ARs). Microbial growth was established and monitored in bench-scale reactors as part of an experimental set-up designed by collaborators in the Faculty of Engineering at the University of Waterloo, intended to reflect full-scale distribution pipelines. The ARs were manufactured by BioSurface Technologies Corporation (Bozeman, Montana, USA). These reactors are designed to simulate sections of distribution systems where flow and shear force can be controlled (Gomes et al. 2014). Each AR is comprised of three concentric cylinders: two stationary glass cylinders (internal and external), and a rotating inner polycarbonate drum. Each AR contains 20 removable strips, "coupons" which are suspended within the inner chamber. Coupons used in this design were made of polycarbonate, which is optimal for biofilm growth and removal (Ollos et al. 1998), while avoiding any impacts of metal corrosion. Each coupon has a surface area of 17.5 cm^2 exposed to water to allow for microbial adhesion and biofilm formation. The rotational speed of the internal drum was set to 50 rpm for all experiments in this project to get a shear force equal to the shear force of a pipe of 100 mm in diameter under a velocity of 0.3 m/s. Water, along with disinfectant and corrosion inhibitor, was pumped into these reactors, where it was mixed at a constant rotational speed to simulate water flowing throughout distribution pipelines. Reactors were set up in parallel, and flow rates adjusted to a retention time of 10 days, each with a distinct set of coupons (Figure 2.1). Water retention

time was considered to represent more extreme scenarios which can at times be observed in distribution reservoirs or specific areas of the network. Temperatures used were intended to represent those most typically found in the Ontario distribution network in the peak of summer (18-22^{o}C).

All water used was collected from a Canadian drinking water treatment plant, unchlorinated, post-filtration. Surface water was sourced from one the Great Lakes, Lake Ontario. Prior treatment consisted of screening, flocculation and sedimentation, and filtration.

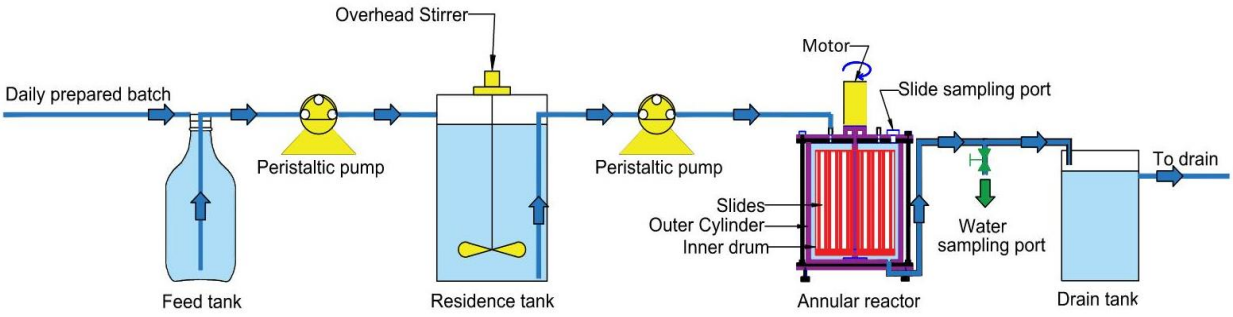

Figure 2.1: Detailed design of the reactor setup used to simulate full-scale distribution systems. Flow direction of treatments is indicated. (Courtesy of Mahmoud Badawy, 2020).

2.1.1 Batch Experiments

Prior to each phase of flow-through experiments, batch tests took place to confirm efficacy and theory of experimental design, and for quality assurance and control purposes.

Batch tests were conducted in 250mL Erlenmeyer flasks, using 50mL of collected feed water. pH and OP treatments were dosed into individual flasks at the beginning of the batch test and incubated in a benchtop shaker at 50rpm. Flasks were covered with tinfoil to remove the potential of

autotrophic growth and incubated at 20°C, +/- 2°C for 21 days. Subsamples were created based on addition of monochloramine at 0, 1, 2 and 4 mg/L OP and pH adjustment to 7.40 and 7.95, as well as samples without pH adjustment. Samples from each flask were removed aseptically, every 3 days, and processed immediately for microbial growth response.

2.1.2 Flow-through Design: Phase 1

Phase 1 of this investigation focused on the impact of different orthophosphate doses on overall biofilm community development. Four ARs were set up in parallel, and dosed with orthophosphate at 1,2, and 4 mg/L (0.33, 0.66 and 1.32 mg/L as phosphorus, respectively), with the fourth AR receiving no added orthophosphate as a control (Figure 2.2). Monochloramine was created through the addition of 2.2 mg/L of chlorine, and 0.50 mg/L of ammonia, for a final measured concentration of ~1.9-2.0 mg/L. Free ammonia, nitrites, nitrates, free and combined chlorine concentrations, and pH were monitored throughout.

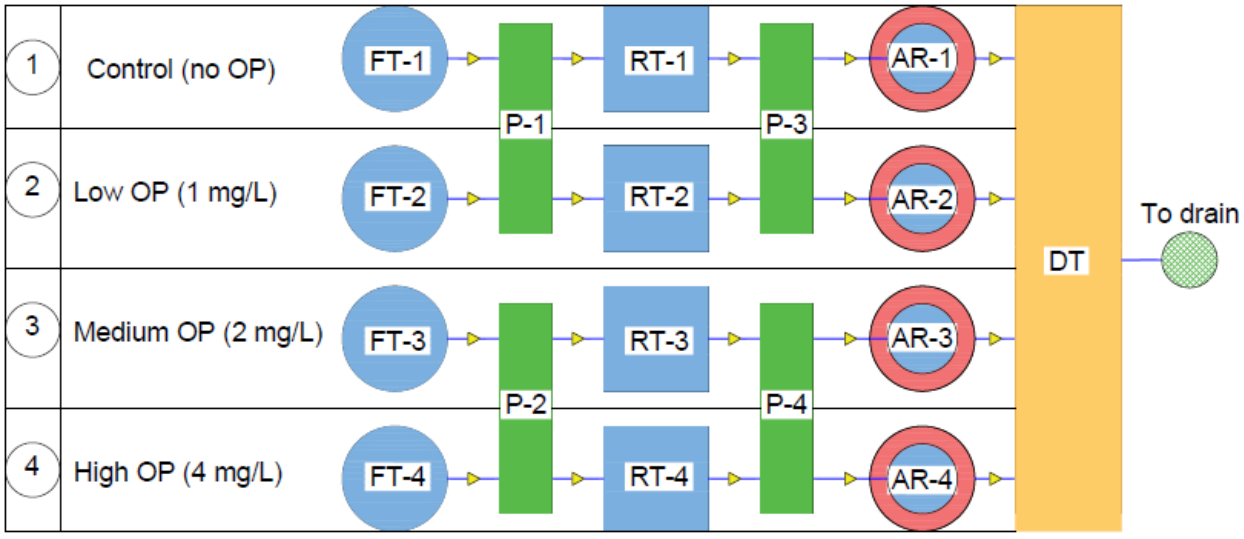

Figure 2.2: Experimental design of Phase 1. FT= Feed Tank, P= Pump, RT= Retention Tank, P= Pump, AR= Annular Reactor, DT= Drainage Tank (Courtesy of Mahmoud Badawy, 2020).

All systems were run for over 12 weeks, whereby sampling of coupons took place weekly, for the first 21 days, and then every 10 days thereafter, allowing for optimal utilisation of the 20 available coupons in each reactor. Following coupon removal, replacements were inserted to maintain flow and hydraulic conditions but were not subsequently used. Coupons were removed in duplicate for a total of 10 sampling events.

2.1.3 Flow-through Design: Phase 2

Phase 2 of this investigation focused on the impact of varying chloramine concentrations on bulk phase and coupon-attached microbial community development in the presence and absence of orthophosphate at a fixed concentration, based on data acquired in Phase 1. Four ARs were set up in duplicate, and run in parallel, and dosed with varied chlorine and ammonia levels to create a high (3.00 mg/L) and low (2.00 mg/L) monochloramine system, with and without the addition of orthophosphate (Figure 2.3).

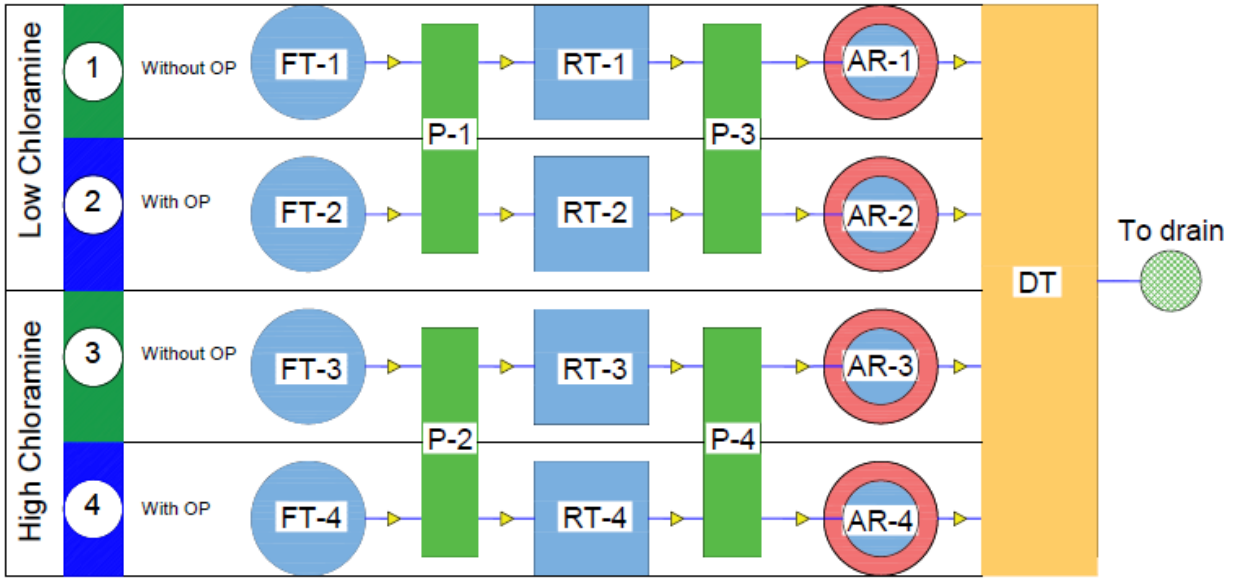

Figure 2.3: Experimental design of Phase 2. FT= Feed Tank, P= Pump, RT= Retention Tank, P= Pump, AR= Annular Reactor, DT= Drainage Tank. (Courtesy of Mahmoud Badawy, 2020).

All systems were run for over 15 weeks, with sampling of coupons taking place every 7-14 days, allowing for optimal utilisation of the 20 available coupons in each reactor. Following coupon removal, replacements were inserted to maintain flow and hydraulic conditions but were not subsequently used. Coupons were removed in duplicate for a total of 10 sampling events.

2.2 Materials and Methods

2.2.1 Sample Processing

Coupons were removed from each AR using sterile forceps and placed in sterile stomacher bags containing 100mL of sterile 0.9% NaCl diluent. Coupons were removed with as little air exposure as possible, to limit the impact of oxygen on anaerobic organisms. 100mL of bulk water was also removed from each reactor at the outflow and placed in sterile bottles during coupon removal. Samples were stored at $4^{O}C$ for no more than 48 hours before processing, with the majority of sample processing occurring 1-2 hours following sample collection.

To resuspend attached microorganisms from the coupons, the stomacher bag was placed in the stomacher (Stomacher 400 Lab Blender, Seward, London, UK) for processing. The stomacher was operated at normal speed (230 rpm±5%) for 2 min (Gagnon and Slawson 1999). The resuspended biofilm material was then processed for viable plate count (HPCs), functional (Biolog) and structural (DGGE) microbial community profiles as described below.

Culturable Assessment

2.2.2 Heterotrophic Plate Count

Resuspended microorganisms and bulk water samples were serially diluted in physiological saline solution, and 100uL were spread onto Reasoner's 2A agar (R2A agar), intended to represent the conditions present in treated drinking water. After 5-to-7 days incubation at $22^{o}C$, colonies were enumerated, and CFU/mL^{2} calculated for each coupon.

2.2.3 Crystal Violet Assays

To assess biofilm reformation potential of the attached and bulk water microbial communities, standard crystal violet (CV) assays were modified and optimised from a variety of protocols (O'Toole 2010; Merritt 2015; Shukla and Rao 2017). As microbial numbers in drinking water are lower than sample types on which traditional protocols are based, 50uL of resuspended biofilm diluent or bulk water was inoculated into 5mL of R2A broth, in pre-sterilized glass test tubes in triplicate. The samples were then incubated for 7 days at 20^{o}C (+/- 2^{o}C) under static conditions. Following 7 days of incubation, the broth, including planktonic (suspended) growth, was aseptically aspirated. The remaining growth attached to the glass tube was considered biofilm material. This was gently washed with peptone buffered saline (PBS) twice to remove any loosely attached cellular material and allowed to air dry. After air-drying, 5mL of 0.1% (w/v) CV was added and allowed to stain the biofilm material for 5 min. After staining, the CV was removed, and biofilms were washed in a similar fashion.

Following the final washing and air-drying, the CV bound to the biofilms was solubilized with 5mL of 33% (v/v) acetic acid. This acetic acid, now containing the previously bound CV, was transferred into 96-well microtiter plates for analysis. Analysis took place using an xMark™ Microplate Absorbance Spectrophotometer (Bio-Rad Laboratories Inc., Hercules, CA, USA), measuring absorbance at 590nm wavelengths (O'Toole 2010). The absorbance concentration reflected the amount of total biofilm material present.

2.2.4 Community-Level Physiological Profiling

BioLog EcoPlates ™ are 96-well microtiter plates, which can be utilized for metabolic assays. Each 96-well plate contains 31 unique, sole carbon sources in triplicate, in separate wells and includes water controls for each set. Each carbon source is bound to a colourless tetrazolium-based dye. When inoculated with available microbial material, any reduced molecules formed during the metabolization of carbon sources utilized by the microorganisms, interact with the bound dye. In doing so, the reduced tetrazolium dye forms a purple colour in the well, which is quantifiable using a spectrophotometer and reflects the extent of carbon utilization. Statistical analyses of the carbon-level physiological profiles (CLPPs) of each community can then be undertaken (Garland and Mills 1991) generating a community "fingerprint", or metabolic profile.

150uL of bulk water or biofilm resuspension samples were aseptically transferred into each well of individual BIOLOG EcoPlates™ (Biolog, Hayward, CA, USA), and absorbance measured in an xMark™ Microplate Absorbance Spectrophotometer (Bio-Rad Laboratories Inc., Hercules, CA, USA), at 590nm wavelengths, at times of 0, 24, 48, 72 and 96 hours (Weber et al. 2008; Bannister et al. 2021). Incubation of these plates took place at 20^{o}C (+/- 2^{o}C). Absorbances readings were then used for statistical analyses, including AWCD, Shannon Diversity of metabolic potential, and carbon source guild analysis. Shannon Diversity ($H' = -\sum pi \ln pi \; n \; i$=1, where n represents the carbon sources utilized, and pi is the proportion of their utilization) is typically represented as species diversity through the evenness and richness of specific species, strains or subcultures within a community. However, this can also be applied to carbon source utilization from BIOLOG EcoPlates™. To do so, species richness and evenness were used to represent carbon source utilization and proportional usage of carbon sources, respectively (Zak et al. 1994;

Bannister et al. 2021). This provided an H’ index, which was used to visualize overall metabolic diversity between communities.

Lastly, carbon source guilds were created, based on the 5 categories of carbon substrates found in the BIOLOG EcoPlates^{TM}. The 31 carbon sources were categorized into the 5 groups; polymers, carbohydrates, carboxylic and ketonic acids, amino acids, and amines and amides (Table 2.1), and their percent usage over time compared (Oszust et al. 2014; Bannister et al. 2021).

Table 2.1: Carbon Sources in Biolog Ecoplates™ Organized by Compound Group

Carbon Source	Compound Group
Tween 40 Tween 80 Glycogen α-Cyclodextrin	Polymers
Pyruvic acid methyl ester Carbohydrates D-Cellobiose α-D-Lactose β-Methyl-D-glucoside D-Xylose i-Erythritol D-Mannitol N-Acetyl-D-glucosamine Glucose-1-phosphate D,L-α-Glycerol phosphate	Carbohydrates
D-Glucosaminic acid D-Galactonic acid-γ-lactone D-Galacturonic acid 2-Hydroxybenzoic acid 4-Hydroxybenzoic acid γ-Hydroxybutyric acid Itaconic acid α-Ketobutyric acid D-Malic acid	Carboxylic and Ketonic acids
L-Arginine L-Asparagine L-Phenylalanine L-Serine L-Threonine Glycyl-L-glutamic acid	Amino Acids
Phenylethylamine Putrescine	Amines and Amides

Structural Community Profiling

2.2.5 DNA Isolation

DNA was isolated from bulk water and biofilm diluent from the same samples used for culture-based analysis. Approximately 80mL of remaining sample water was filtered through 0.22uM cellulose filters. DNA extractions took place using a Qiagen DNeasy PowerWater kit (Qaigen, Hilden, Germany), and DNA was stored in -80^{O}C freezers until analysis.

2.2.6 Polymerase Chain Reaction-Denaturing Gradient Gel Electrophoresis

Polymerase Chain Reaction- Denaturing Gradient Gel Electrophoresis (PCR-DGGE) is a technique commonly used to visualize the representative diversity of genetic sequences within a microbial community. Through DGGE, PCR amplified regions of 16s ribosomal DNA can be separated based on their GC content and visualized through staining and UV imaging. Using a gradient of denaturing chemicals, specifically urea and formamide, in a polyacrylamide gel, community fingerprints at specific timepoints can be created based on banding size, pattern, and intensity. Individual bands can be described as operational taxonomic units (OTUs), with band intensity being representative of the prevalence of that OTU in the community (Muyzer et al. 1993).

One drawback of PCR-DGGE is the inability to differentiate specific species presence or absence, meaning true species diversity cannot be evaluated. Since PCR-DGGE focuses on the content of DNA in the amplified samples, rather than the specific sequences, comparisons between samples and the formation of OTUs based on GC content are required. Despite this, PCR-DGGE is still

highly specific, with the ability to discriminate between genetic OTUs which make up only 1% of the community profile (Muyzer et al. 1993; Muyzer 1999).

To perform PCR-DGGE, the highly-variable V3 region of the 16s bacterial rDNA was amplified using universal primers 314F (5'- CCTACGGGAGGCAGCAG-3`) and 518R (5`-ATTACCGCGGCTGCTGG- 3`) (Muyzer et al. 1993; Green et al. 2010), with an additional GC clamp (CGCCCGCCGCGCCCCGCGCCCGTCCCGCCGCCCCCGCCCG) on the 5' end of the 341F primer (Sigma Aldrich, Oakville, Ontario CA). Due to the denaturant method-of-action for PCR-DGGE, a GC clamp is required to stop the loss of denatured strands from the gel by binding them to the gel itself. PCR supermix (Bioline, Memphis, TN, USA) was used to assure accurate, stable DNA amplification.

The DNA was amplified through the following PCR conditions in a thermocycler (iCycler iQ™ Multicolor Real-Time PCR Detection System, Bio-Rad Laboratories Inc., Hercules, CA); an initial denaturation of 94°C for 5 min, followed by 20 cycles of 94°C denaturation, 65°C annealing and 72°C elongation for 1 min each. The initial annealing temperature of 65°C was decreased every 2 cycles by 1°C to a final temperature of 56°C on the 20th cycle. This final annealing step was followed by 10 additional cycles of 94°C, 55°C and 72°C for 1 min each. The final elongation step consisted of 7 min at 72°C, after which the final PCR product was held at 4°C until storage at -20°C (Bannister et al. 2021).

The final PCR product was subjected to electrophoresis in a 1.8% (w/v) agarose gel, stained with ethidium bromide (EtBr), before DGGE took place. This was to assure the presence of amplified genetic material, with size corresponding to the targeted region of the 16s ribosomal DNA sequence (233 bp) (Muyzer et al. 1993; Green et al. 2010).

15 µL of PCR product were run on 20mL, 8% (w/v) acrylamide gels with a 25-70% denaturing gradient (5-14mL of formamide and 3.15-14.7g of urea) (Green et al. 2010) formed with a peristaltic pump gradient former (VWR Mini Pump Variable Flow, VWR Scientific, Radnor, PA, USA) for 19 hours at 65 °C on a CBS Scientific TM DGGE-2401 machine (CBS Scientific Inc., Del Mar, CA, USA) powered using a PowerPac™ Basic Power Supply (Bio-Rad Laboratories Inc., Hercules, CA, USA).

The gels were then stained with EtBr (Thermo Fisher Scientific, Waltham, MA) while shaking at 50 rpm on an orbital shaker (VWR Orbital Shaker, VWR Scientific, Radnor, PA) for 30 min. Staining was followed by a destaining step, where gels were placed in 1xTAE buffer for 5 min, to dilute any excess EtBr. After destaining steps, gels were imaged with UV light (Gel Doc™ XR+ Gel Documentation System, Bio-Rad Laboratories Inc., Hercules, CA). Images were analysed using the gel comparison software GelCompar II (Applied Maths © , Belgium). Similarity matrices (Dice-Sorensen Index) and UPGMA dendrograms were created based on banding patterns and band intensity generated in GelCompar II.

Chapter 3: An Investigation of the Impact of OP Addition on Drinking Water Microbial Communities

3.1 Overview:

To understand the impact of OP dosage on microbial communities in distributed drinking water, a 12-week flow-through experimental design was established using annular reactors (ARs) run in parallel (Section 2.1.1). Four conditions were tested exposing the system to 1, 2 and 4 mg/L OP, plus a control system with no added OP. Over these 12 weeks, coupons were removed in duplicate

at timepoints ranging from 7 to 10 days apart, with bulk water removal occurring at the same time (Section 2.2.1). Biofilm and bulk water microbial profiles were created using the monitoring methods previously outlined (Section 2.2). At the same time, physico-chemical analyses were performed at the University of Waterloo **(**Appendix A**).** These parameters were monitored more frequently over the 12-week study period, and include concentration data for compounds such as nitrite, nitrate, ammonia, free and combined chlorine, and pH.

The primary objective of this phase of the research was to assess microbial response to the presence and absence of OP at different concentrations as a corrosion inhibitor. To do so, both cultural and molecular-based approaches (Section 2.2) were utilized.

3.2 Results and Discussion

3.2.1 OP impact on culturable microbial growth and biofilm formation potential

HPC data was monitored for both bulk water and biofilm samples from the flow-through system. The bulk water samples had lower culturable cell counts overall, when compared to corresponding biofilms samples for each treatment (Figures 3.1 and 3.3). Differences in HPCs between OP doses were seen across all sampling dates for bulk phase microorganisms. The most notable differences in HPCs occurred between 1 and 2 mg/L of added OP, with an increase of 0.3 log units in the bulk water samples (Figure 3.1). A plateau in overall HPCs is seen in samples taken from day 52 onwards.

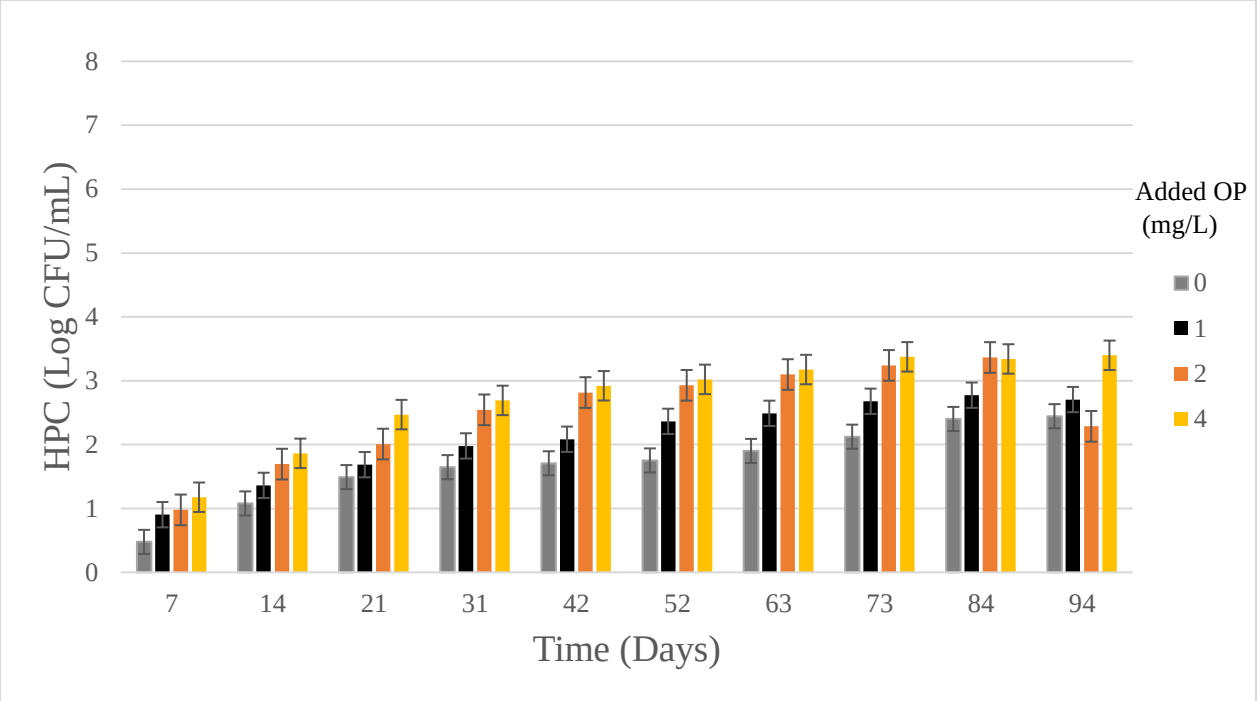

Figure 3.1: Heterotrophic plate count (HPC) of bulk phase microorganisms. All samples were plated in duplicate, on R2A agar. Error bars represent standard error (n=2). OP= orthophosphate

.

Along with HPC, biofilm reformation potential was monitored through crystal violet assays (as described in Section 2.2). These assays are used to determine the potential for detached or suspended cells to reform biofilms and can provide insight into potential metabolic or genetic shifts in a community (Kragh et al. 2019). The ability to form or reform biofilm material in these assays will vary depending on the communities' utilization of available nutrients in a DWDS under static conditions (O'Toole 2010).

Bulk phase microorganisms were able to reform more biomass as biofilm material, in relation to increasing OP doses (Figure 3.2). Between day 14 and day 42, biofilm reformation potential decreased for all OP exposures. On day 52, 1, 2 and 4 mg/L OP-exposed communities showed comparable absorbance, followed by a decrease similar to that observed for biofilm communities

(Figures 3.2 and 3.4). An increase in biofilm formation potential was seen following the noted decrease, however it was less noticeable than that seen from attached cells recovered from the coupons (Figure 3.4).

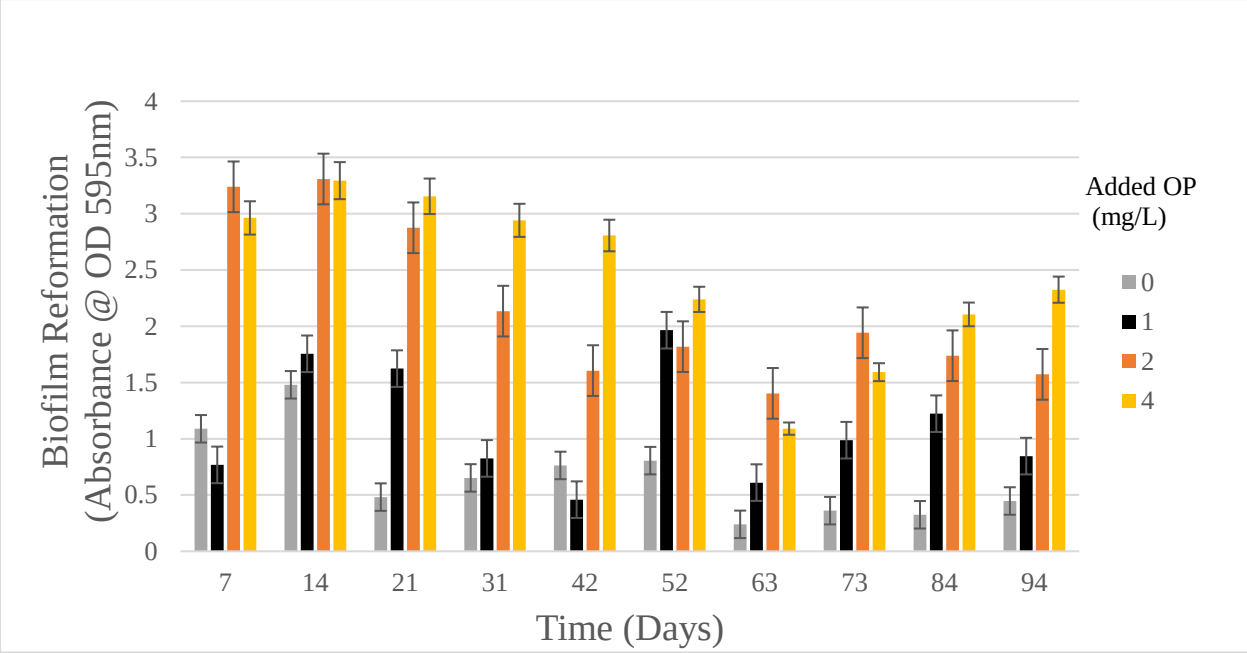

Figure 3.2: Biofilm reformation potential of bulk phase communities, as measured through absorbance of CV-stained biofilm material. Samples were incubated for 7 days in static R2A broth before staining occurred. Error bars represent standard error (N=2). OP = orthophosphate

HPCs from biofilm material removed from coupons showed the greatest increase from 1 and 2 mg/L of OP, with no notable differences between 0 and 1 mg/L added OP (Figure 3.3). Highest levels of HPCs were noted in communities exposed to 4 mg/L OP, reaching over 3 log units higher than systems exposed to 0 and 1 mg/L on days 73 and 84. Viable cell counts from attached biofilms increased between days 7 and 63, with a plateau, and even a slight decrease in the 1 and 2 mg/L OP-exposed systems from day 73 onward. No notable differences were noticed between coupon replicates over the experiment duration.

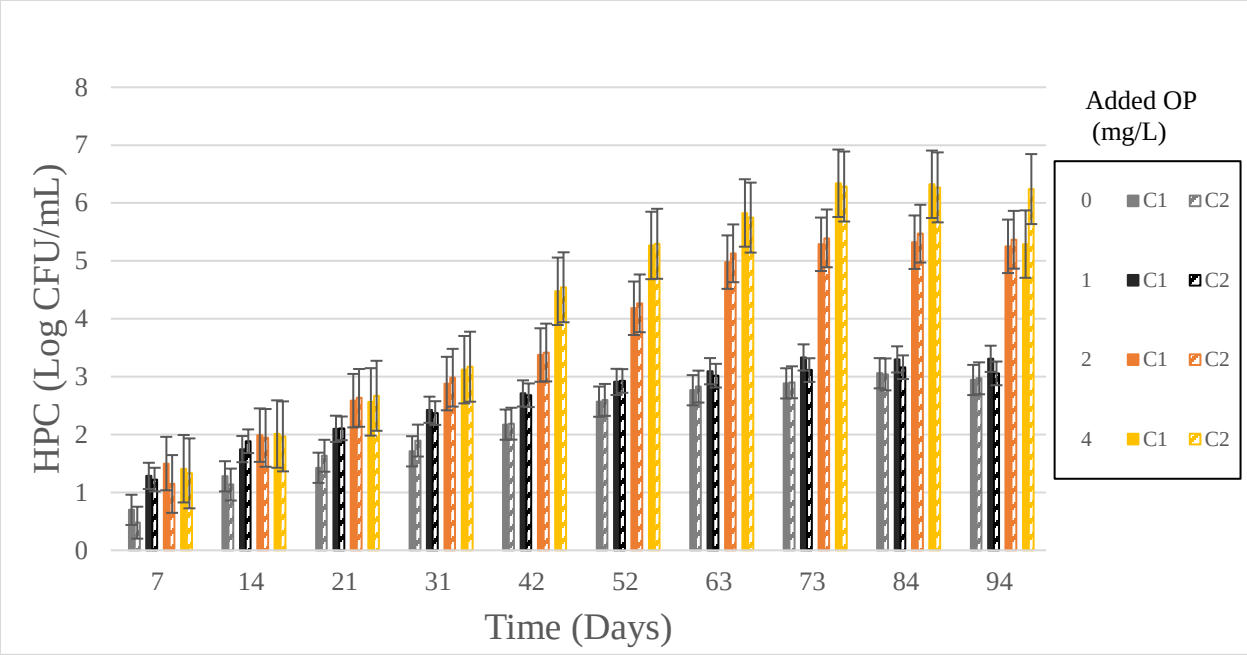

Figure 3.3: Heterotrophic plate count (HPC) of removed biofilm communities. All samples were plated in duplicate, on R2A agar. Error bars represent standard error (n=2). C1 and C2 refer to coupon 1 and 2, respectively. Duplicate coupons were not averaged and are shown for each sampling event. OP = orthophosphate.

Coupon-associated communities exposed to higher concentrations of OP (2 and 4 mg/L) were able to reform higher amounts of biofilm material under static conditions than those exposed to lower doses (0 and 1 mg/L) (Figure 3.4). Between day 7 and day 42, communities exposed to 2 mg/L OP formed the most biomass as biofilm material comparative to communities exposed to all other doses, measured through indirect quantification of absorbance (described in Section 2.2). An initial increase in absorbance was seen for all communities excluding the control, which showed an overall decrease in reformation potential. Between days 14 and 31, samples from 0, 2, and 4 mg/L OP-exposed reactors showed relatively stable absorbance values, only slightly decreasing (Figure 3.4), indicating little change overall. Contrary to this, the cells recovered from 1 mg/L OP-exposed biofilms steadily increased. Between days 31 and 52, biofilm reformation potential for most coupon-associated communities rapidly decreased for all doses tested. Following day 52, a steady

increase in absorbance was seen for coupon-associated cells exposed to 1, 2 and 4 mg/L OP. It appears that these trends, although similar, were delayed in samples from the bulk phase, as the lowest absorbance values were measured on day 63, 11 days after the lowest values from the biofilm communities were seen (Figure 3.4). The decrease in biofilm formation potential was also not as pronounced, with a more noticeable decrease occurring between days 14 and 42.

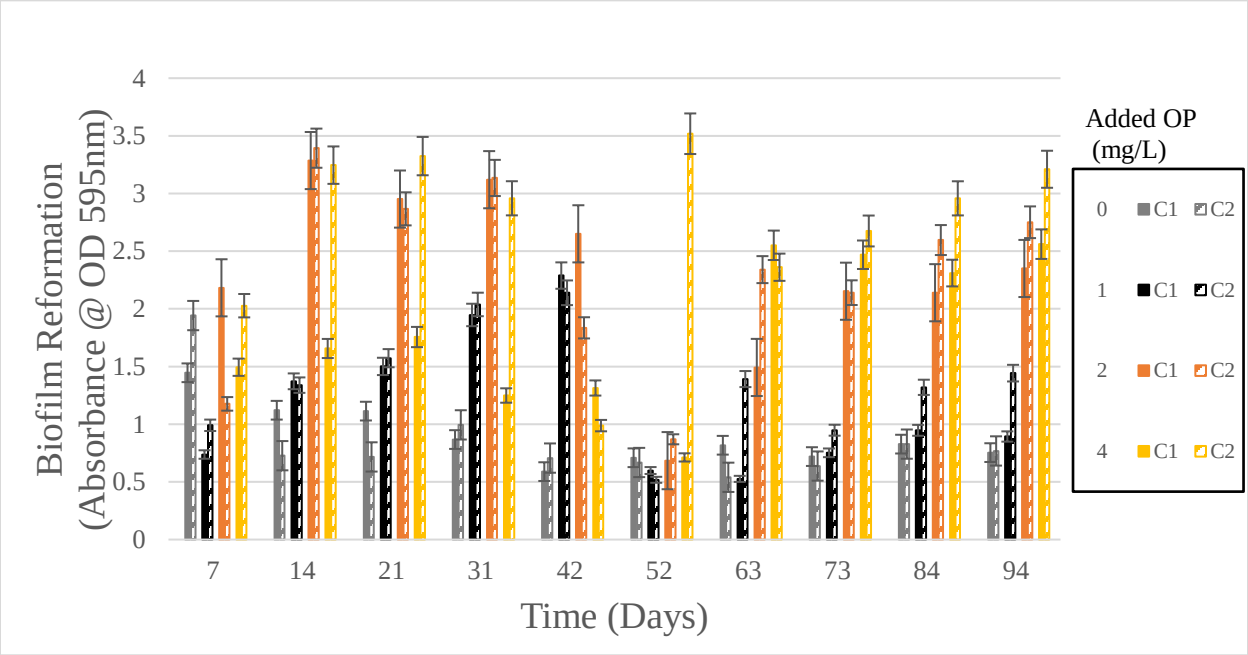

Figure 3.4: Biofilm reformation potential of coupon-associated communities, as measured through absorbance of CV-stained biofilm material. Samples incubated for 7 days in static R2A broth before staining occurred. Error bars represent standard error (N=9)C1 and C2 indicate coupons 1 and 2, respectively. OP = orthophosphate

As mentioned previously, phosphorus may be a limiting nutrient at concentrations typically seen in a DWDS (Correll 1999). If this is the case, noticeable changes in growth would be associated with increasing concentrations of OP (Javier et al. 2021).In this study, an increase in biologically available phosphorus through exposure to OP corresponded to an increase in viable cell counts,

as measured by HPC (Figures 3.1 and 3.3). An increase in biologically-available phosphorus would provide an advantage to cellular growth and, allow cells to replicate to higher viable counts (Del Olmo et al. 2020). As all ARs were supplied with the same source water, the bacterial cells entering each reactor system would have been under similar metabolic conditions where phosphorus was likely a limiting nutrient. This means that coupon-associated cells exposed to >/= 2mg/L OP were able to uptake more phosphorus and proceed with cellular processes, such as replication and biofilm formation, at an increased level (Figure 3.3 and 3.4).

As external phosphorus has been shown to be incorporated by exopolysaccharide (EPS) material, and utilized as a minor structural component (Zhang, Fang, Wang, Sheng, Xia, et al. 2013; Zhang, Fang, Wang, Sheng, Zeng, et al. 2013), microbial communities growing in systems with higher OP levels may not only be able to metabolize more, but also be exposed to more phosphorus in more interior levels of the biofilms. As biofilms form, there is potential for EPS material to capture and retain nutrients from the bulk phase, which may remain until metabolized by inhabitants found at more interior levels of the biofilm (Goller and Romeo 2008). Typically, cellular activity and metabolism is higher at the interfaces of biofilm surfaces, where nutrient exposure is higher (Martiny et al., 2003). However, if phosphorus exposure is increased during the early stages of biofilm formation, it may be possible that the integration of phosphorus into EPS allows for increased microbial activity in the interior of biofilm structures (Rooney et al. 2020). The porous nature of biofilms may also play a role in this, as phosphorus may integrate deeper into the biofilm as increases in concentration are seen. The enhanced P exposure to typically less metabolically active cells in interior levels of the biofilm could possibly increase overall cell counts seen in these biofilms (Rooney et al. 2020; Salgar-Chaparro et al. 2020) as observed in our study (Figure 3.4).

The eventual plateau of biofilm HPC samples observed in this study is also typical of a maturing biofilm (Muhammad et al., 2020). Environmental pressures, such as flow rate, chloramine presence and temperature, all play a role in the limitations imposed on biofilm development as they age and increase in size. As chloramine has been shown to degrade biofilm material, it's possible that the upper limitations of biofilm biomass and cell count were being reached at the later sampling dates of this study (Lehtola et al. 2006; Ling and Liu 2013).

The trends observed in both the bulk phase and coupon biofilm HPCs were expected (Figure 3.1 and 3.3). Later-stage biofilms, which have been studied in DWDSs, have been shown to significantly influence the type of microorganisms found in the bulk (suspended) phase (Liu et al. 2013a; Fish and Boxall 2018). In some studies, bulk phase bacteria have been shown to make up less than 5% of total biomass in a DWDS (Martiny et al. 2003; Ling and Liu 2013). This lower cell count when compared to biofilms communities is expected, as there is less exposure to nutrients, and more exposure to environmental pressures, such as flow rate and disinfectant residual (Srinivasan et al. 2008; Mirjam Blokker and Van Der Wielen 2018).

In a new system, such as the ARs during the initial days of this study, the bulk phase microorganisms consist mainly of those from the influent water. During subsequent stages where biofilm communities are forming or have already formed, bulk phase communities are reflective of not only the influent water, but the biofilm communities as well (Fish and Boxall 2018; Schleich et al. 2019; Tsvetanova 2020). This can include planktonic cells which have detached from the pipe wall, including cells which have been sloughed from biofilm material or entirely disrupted biofilm communities. These detachments occur constantly, and cells which were once encapsulated in a biofilm become part of the bulk phase community (Farkas et al. 2012), and during analysis, may represent cells which may no longer be part of the influent or source water

community, but have survived and evolved by entering and replicating in biofilms adhered to pipe wall material. The similarity of trends between the biofilm and bulk phase HPC observed in our study may be due to this near constant exchange of cells from biofilms into the bulk phase of treated water (Schmeisser et al. 2003; Farkas et al. 2012).

The ability for these communities to reform a biofilm is essential in a DWDS, where sloughing events are frequent, and surface material is abundant. As these disrupted cells attach to pipe material, they begin to reform biofilm material (Douterelo et al. 2016). In this investigation, cells exposed to higher levels (2 and 4 mg/L) of OP were able to form greater amounts of biofilm biomass in the same time frame as those exposed to 1 mg/L OP (Figure 3.2). An initial increase in biofilm reformation was expected, as early colonizers typically seen in a DWDS, such as *Pseudomonas* or *Actinomyces*, are common in the bulk phase (Wingender and Flemming 2004; Revetta et al. 2013). These initial colonizers have been shown to form more robust biofilms in short periods of time and form the early biofilms found in a DWDS. These initial colonizing bacteria are suggested to be the most numerous, or metabolically active, in these communities and benefit from the addition of phosphorus compounds (Del Olmo et al. 2020). Once the early stages of biofilm formation are underway, bacteria in the bulk phase have a higher chance of attachment to pipe material and subsequent integration into the biofilms. This increases overall microbial diversity, as well as competition for resources and space (Kelly et al. 2014; Reuben et al. 2019). As the biofilms begin to diversify, so do the metabolic profiles of the communities (Zak et al. 1994; Button et al. 2016; Cruz et al. 2020). Bacteria which favour nutrient uptake and replication may become dominant in the biofilms, overtaking the initial colonizers. This expanding diversity is a sign of a maturing environmental biofilm (O'Toole 2010; Beitelshees et al. 2018).

Biofilms formed in a DWDS, do so at a relatively slower pace compared to those formed in other environments, such as wastewater or soil systems. This is most likely due to the lower nutrient concentrations, exposure to disinfectant treatments, lower temperatures and higher shear force of the bulk phase water (Martiny et al. 2003). Multiple studies have indicated that biofilm formation can take upwards of 60 days to develop and mature, at which time, more pronounced diversity is often seen (Martiny et al. 2003; Liu et al. 2013b; Aggarwal et al. 2018). In this study, the maturation of the biofilm, and corresponding changes in the genetic makeup of the community, such as the potential loss or decrease of initial colonizers, may be the cause of the decrease in reformation potential seen from the coupon-associated communities on day 52 (Figure 3.4). Coupon replicate 2 of the 4 mg/L exposed communities showed a noticeable increase in biofilm reformation, most likely due to the formation of a large pellicle, almost 1mm thick (Data not shown). These pellicles were not seen before this date and after day 52, those which formed were noticeably thinner. After day 52, absorbance values were more constant over time, indicating a potentially mature biofilm, with a more stable microbial diversification (Figure 3.4) (De la Fuente-Núñez et al. 2013; Li et al. 2019).

As seen in Figures 3.2 and 3.4, biofilm reformation potential showed similar trends between bulk phase and biofilm communities. However, these similar trends in the bulk phase seem to be delayed in comparison to those seen in coupon-associated communities. For example, the lowest reformation potential for biofilm communities is seen on day 52, however these values are not reflected in the bulk community until the sampling on day 63.

As it has been noted in literature, the activity and composition of bulk phase microorganisms heavily relies on those of the biofilm communities. Micro-sloughing, as well as the natural occurrence of planktonic cells exiting in a biofilm, would introduce cells found in the biofilm

community into the bulk phase in higher concentration than that found in the original influent water (Fish and Boxall 2018; Lee et al. 2018). Although the cells present in a biofilm are initially from the bulk phase, these specific genetic or metabolic profiles may not be present in high concentration in the bulk phase until the biofilms mature and further cell release occurs (Douterelo et al. 2013; Fish and Boxall 2018). In our study, the lag time observed in trends between biofilm and bulk community biofilm reformation is possibly due to the retention of cells in biofilms, which have not been released into the bulk phase (Fang et al. 2009a; Chan et al. 2019; Tsvetanova 2020).

The sharp decrease in biofilm reformation potential being based on metabolic or genetic shifts in the community is further supported by evidence that no noticeable sloughing events occurred. A sloughing event would be indicated by a noticeable decrease in overall cell count in biofilm communities, reflected by an equally noticeable increase in cell count in the bulk phase (Kaplan 2010). As seen in Figures 3.1 and 3.3, the occurrence of a sloughing event is highly unlikely, as no noticeable or distinct changes were seen in HPC for either bulk or biofilm communities. Following this decrease, a rise is again seen biofilm reformation potential. This increase may be due to the introduction of bacteria which have similar biofilm formation patterns as those from the initial colonizers, reflecting higher amounts of biomass as biofilm material being formed.

3.2.2: Impact of OP dose on microbial community profiles

Functional Profiling by CLPP:

Further functional monitoring performed using metabolic assays allows for a range of assessment opportunities for the microbial community at each sampling time (Clairmont and Slawson 2020). As previously stated, BioLog EcoPlates™ were used to determine the community-level physiological profile (CLPP) through average well colour development (AWCD), Shannon

Diversity, and carbon guilding (see Section 2.2). AWCD of each EcoPlate™ was measured after 5 days of sample incubation and provides insight into the carbon metabolism occurring within a community over time.

In all instances (Figure 3.5), bulk (suspended) phase microbial profiles did not surpass the threshold level of carbon utilization, an absorbance value of 0.250, as described in section 2.2. Suspended phase microorganisms exposed to 4 mg/L OP generally showed the highest carbon utilization (reflected by higher OD readings). At day 42, the AWCD of the 4 mg/L exposed community reached the highest OD for all timepoints, at an absorbance of 0.194. Qualitatively, plates inoculated with samples from day 42 onward did appear to have minor tetrazolium reduction when plates were placed on an illuminating board for contrast. However, due to the absorbance readings consistently being below threshold, no significance between the different OP doses on carbon utilization within bulk phase microorganisms can be highlighted. This indicates that microorganisms in the bulk phase, regardless of exposure to OP, are noticeably less metabolically active than those from coupon-associated communities.

The attached coupon-associated biofilm communities generally showed higher carbon utilisation profiles with AWCD (Figure 3.6) following a similar trend seen in both HPC and CV assays (Figures 3.3 and 3.4), where exposure to higher concentrations of OP resulted in higher levels of microbial activity. On day 14, biofilm communities exposed to 4 mg/L of OP were the only ones which surpassed the threshold, where EcoPlate™ readings from coupon replicates had an AWCD reading of roughly 0.750 and 0.42, respectively (Figure 3.6). At day 21, biofilm cells from the 2 mg/L exposed AR surpassed the threshold, showing comparable carbon utilization to biofilm material removed from the 4 mg/L AR. All monitored biofilm communities exposed to 2 and 4 mg/L showed signs of active metabolism as evidenced by increases in AWCD. Overall,

AWCD of communities exposed to 2 mg/L of added OP surpassed those of communities exposed to only 1 mg/L of added OP. On Day 52, a noticeable increase in AWCD for communities exposed to 2 and 4 mg/L of OP was observed. Following day 52, coupon duplicates from respective ARs mirrored each other more closely, and AWCD decreased for each sample. This trend inversely follows that of the biofilm reformation assays (Figure 3.4), where day 52 had the lowest overall reformation potential, followed by a steady increase. Throughout the entire experiment, no microbial communities exposed to 1 or 0 mg/L of OP crossed the AWCD threshold for positive metabolic response, an absorbance value of >0.250, for both bulk phase and attached microorganisms.

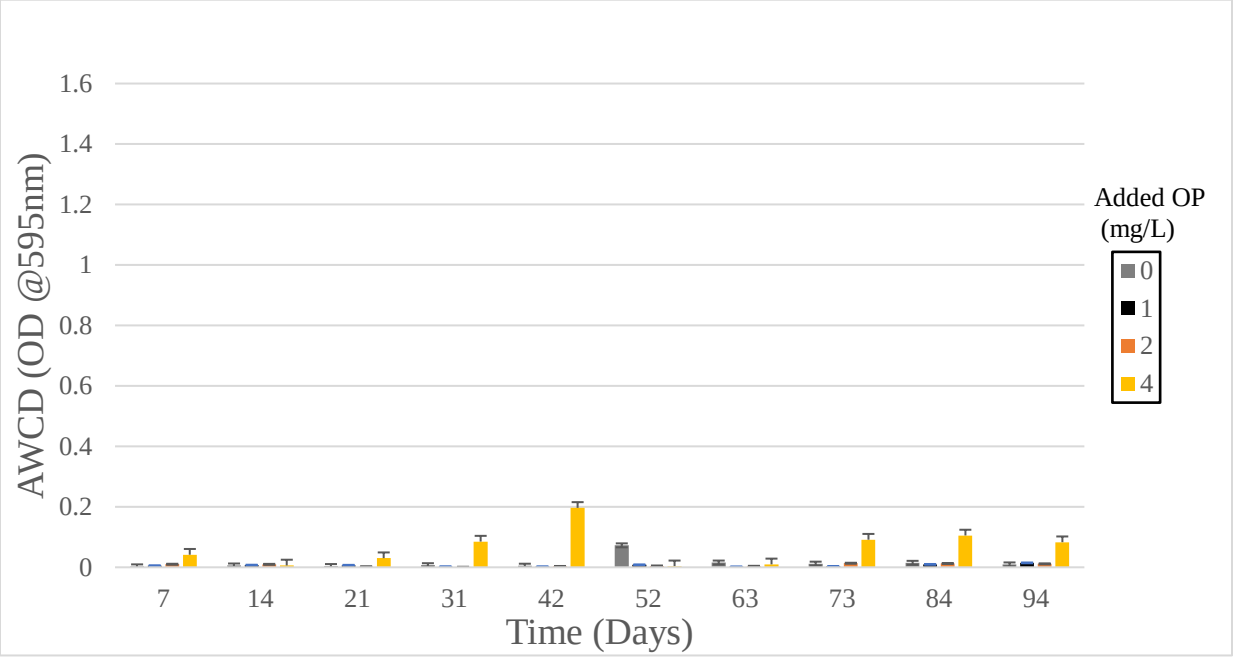

Figure 3.5: Metabolic activity of bulk phase microorganisms, as measured by AWCD of BioLog Ecoplates™. Error bars represent standard error (n=3).

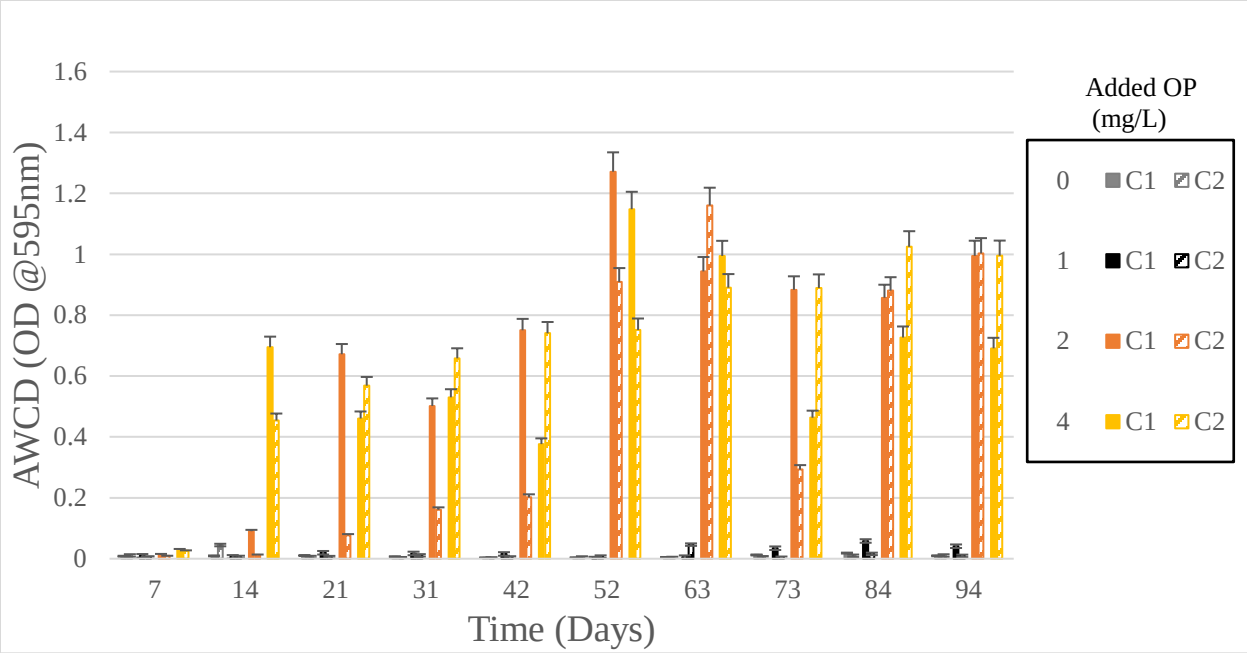

Figure 3.6: Metabolic activity of resuspended coupon-associated communities, as measured through AWCD. Error bars represent standard error (n=3). C1 and C1 represent coupon replicate 1 and 2, respectively.

Shannon Diversity (H') was also calculated based on the carbon utilization data monitored from the EcoPlates™. Shannon diversity could not be calculated for any of the bulk water microorganisms, or coupon-associated biofilms from reactors dosed with 1 or 0 mg/L added OP, as the metabolic response was too weak (absorbance values below 0.250). Consequently, data is shown only for the coupon-associated biofilm communities from reactors exposed to 2 and 4 mg/L OP. As seen in Figure 3.7 the H' of coupon replicates remained similar between biofilm communities exposed to the same OP concentration over time. After a slight increase in diversity between day 7 and 21, communities exposed to 2 and 4 mg/L added OP maintained a stable profile (H' 2.50-3.25).

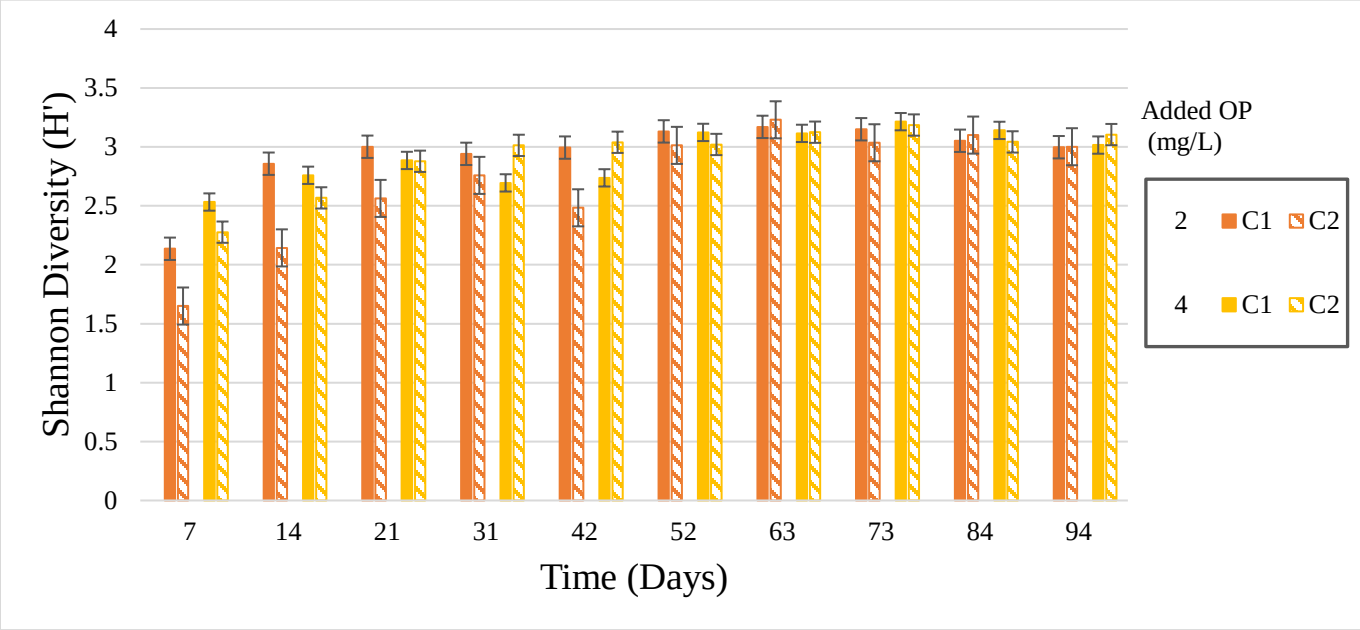

Figure 3.7: Metabolic diversity of removed biofilm communities' carbon source utilization, measured through Shannon Diversity (H') based on absorbance readings of BioLog Ecoplates™. Error bars represent standard error (n=3). C1 and C1 represent coupons 1 and 2, respectively. Data from 1 and 0 mg/L OP exposed communities omitted, as absorbance readings did not surpass metabolic thresholds of 0.250. A higher H' is indicative of greater carbon utilization diversity. OP= orthophosphate

To further investigate the metabolic profiles of these communities, the proportion of carbon sources utilized within a carbon group (guild) was compiled. As each EcoPlate™ contains carbon sources associated with a different guild, the ratio of reduction for these compounds can be monitored to help in assessing profiles (Sofo and Ricciuti 2019; Clairmont and Slawson 2020; Bannister et al. 2021). Carbohydrates, carboxylic acids, amino acids, polymers and amines/amides represent the 5 guilds from which carbon utilization was determined (Figure 3.8).

Between days 7 and 94, a noticeable decrease in overall polymer utilization was seen for 2 and 4 mg/L OP-exposed communities (Figure 3.8). This was in conjunction with a 15% increase in carboxylic acid utilization after day 52, and a 5 to 7% increase in amines/amides utilization. Excluding some inconsistency of amino acid utilization between coupon replicates in the 2 mg/L

OP-exposed AR from days 7 to 52, no noticeable difference in metabolic profiles were seen for the 2 and 4 mg/L OP-exposed communities over the 94 days of the experimental run.

For biofilm communities exposed to 1 mg/L added OP, over 50% of all carbon utilization was from carbohydrate and polymer sources, across all sampling times (Figure 3.8). This trend was similarly observed in the control (0 mg/L added OP) communities as well, where, on day 94, coupon-associated communities exhibited 48% of their carbon utilization between carbohydrate and polymer sources, and 43% of carbon utilization being attributed to carboxylic acids. Overall, carbon guilding of these community profiles indicated a more evenly distributed of carbon utilization over time for 2 and 4 mg/L OP-exposed communities as compared to the 1 mg/L and control communities.

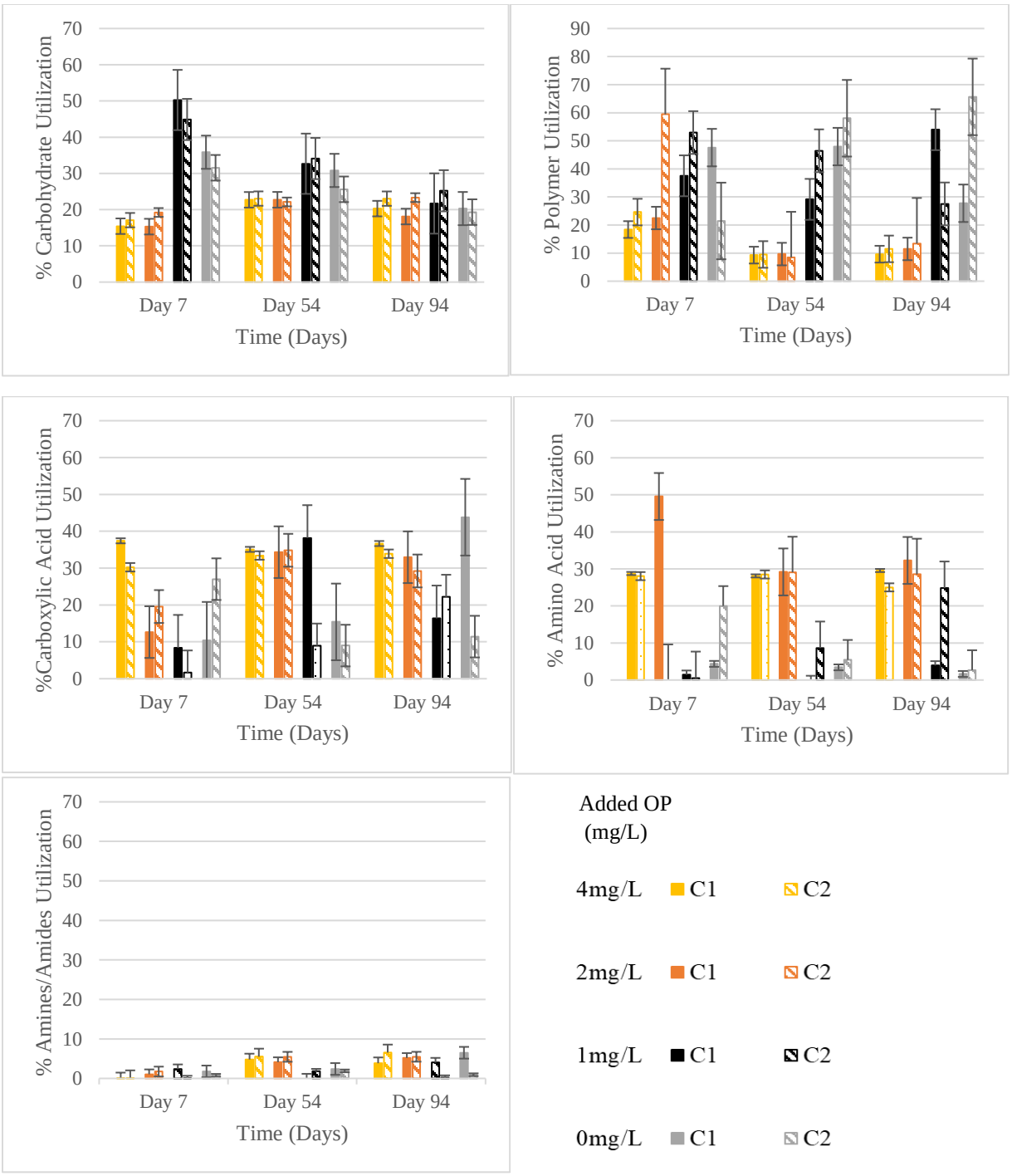

Figure 3.8: Percent usage of carbon substrates (grouped by polymers, carbohydrates, carboxylic and ketonic acids, amino acids, and amines and amides) on Biolog™ Ecoplates by coupon-associated bacterial communities. Each bar represents the average usage (%) for a group of carbon substrates. Error bars represent standard error (n=3). C1 and C2 represent coupon replicate 1 and 2, respectively.

As previously mentioned, biofilms formed in environmental settings with external pressures, form at different paces (Chandki et al. 2011). A wide range of factors, including community composition, nutrient availability, environmental temperature and the presence of other stressors all influence the time required to reach a mature biofilm (Goller and Romeo 2008). Maturation of biofilms can be indicated by a diversifying community, steady metabolic profiles, and increasing cell counts (Araya et al. 2003; Chandki et al. 2011; Kwon et al. 2011). In diverse microbial environments, initial colonizers are typically seen as main contributors to both biofilm formation and early population diversity, as such early biofilms tend to be made of few species which dominate both genetically and metabolically (Pisithkul et al. 2019; Salgar-Chaparro et al. 2020). In doing so, diversity, both genetically and metabolically, is often low. These bacteria, such as *Pseudomonas* spp., have a niche which is filled early in the lifecycle of the biofilms. Often composed of a rigid metabolic profile (Mouchet et al. 2012; Flynn et al. 2017), these communities form the foundation of the early biofilm profile. Over time, as exposure to bulk-phase microorganisms increases, these biofilms will take in and harbour many bacteria with which they may come in contact (Elias and Banin 2012; Y. Li et al. 2015; Douterelo et al. 2016). Within the protection of the biofilm, these new cells from the environment may replicate, which allows for new populations and ecological microniches to arise. Typically, these niches can be defined based on nutrient composition, oxygen gradients, and predation from other cells (Depetris et al. 2021).

A mature biofilm is one which has allowed different niches to form, wherein the initial colonizers may not be present to the same degree they once were. As such, the presence or absence of taxa can shift the dominance towards species initially found in low counts. These

community shifts can sometimes be determined through metabolic profiling (Button et al. 2016; Clairmont and Slawson 2020).

A less mature biofilm may have lower levels of metabolism, such as those seen in this study from communities exposed to lower OP doses (Figure 3.5 and 3.6), or they may exhibit a more strict nutrient utilisation range (Sofo and Ricciuti 2019; Joshi et al. 2021). As the population potentially diversifies, as in the case of bulk phase microorganisms entering biofilms in a DWDS, these metabolic niches expand, as a greater variety of microorganisms allows for the utilization of a wider range of nutrient sources (Martiny et al. 2003).

This diversification is a probable reason for the results observed in Figure 3.6. On day 7, the low AWCD is most likely due to the low cell count (Figure 3.3), as the bacteria would not be present in high enough numbers, or were too damaged by initial treatment operations , to actively metabolize the carbon sources (Boe-Hansen et al. 2002). From days 14 to day 43, AWCD is consistent for the 2 and 4 mg/L OP-exposed coupon-associated communities, but not yet at the highest measured levels, indicating a lower metabolic activity than exhibited from communities at later sampling dates. The noticeable increase on day 52 indicates a more actively metabolic community, followed by a decrease, although levels remain higher than those observed from days 0 to 42.

Although below the positivity threshold, the bulk phase AWCD from the 4 mg/L OP-exposed community followed a similar trend. It is possible that the presence of the metabolically dominant taxa in the bulk phase was able to enter the biofilm and affect the community profile between sampling dates, or a niche in the biofilm had formed which could support the replication of metabolically active subgroups (Liu et al. 2013a). This is further supported when considering Figure 3.4, where a noticeable decrease in biofilm formation potential was seen for these

coupon-associated communities. Predation and competition in a biofilm allow for dominance to be more fluid than static, as cells are constantly interacting with both the environment, and other microorganisms present (Banks and Bryers 1991; Douterelo et al. 2016; Yuan et al. 2020). As these metabolically active strains are becoming more present, outcompeting the initial colonizers, the metabolic profile would change to reflect this, which could also affect biofilm formation potential as the community changes.

The lower metabolic activity seen in the control and 1 mg/L OP-exposed communities (Figure 3.6) corresponds with the lowered cell counts and lower biofilm reformation potential discussed previously (Figure 3.3 and figure 3.4). This evident increase in growth response associated with higher OP concentrations further supports the concept that OP can be metabolised as a growth nutrient. Higher nutrient levels have been routinely associated with higher levels of cellular replication, biofilm formation, and diversity (Fang et al. 2009b; Jang et al. 2012; Huang et al. 2016; Del Olmo et al. 2020). Stepwise increases in biofilm biomass may continue to trap higher levels of nutrients, such as OP, from the bulk water (Fang et al. 2009a; Zhang, Fang, Wang, Sheng, Xia, et al. 2013), thus building the community over time.

Results based on the carbon guilding in Figure 3.8 shows a more stable metabolic range for biofilm communities exposed to 2 and 4 mg/L of OP. These stable metabolic ranges indicate the potential for a more diverse community, as rates of co-metabolism and higher amounts within specific ranges are more likely to be present (Joshi et al. 2021). Comparatively, lower levels of diversity and robustness in a biofilm may lead to a very strict metabolism, that could fluctuate widely over time, depending on internal microbial interactions. Products similar to EcoPlates™ can be used to identify microorganisms from microbial communities with low-diversity, based

on a more strict metabolic profile (Stefanowicz 2006; Kela P. Weber and Legge 2010; Sofo and Ricciuti 2019). Figure 3.9, modified from Flynn, 2017, helps to describe this:

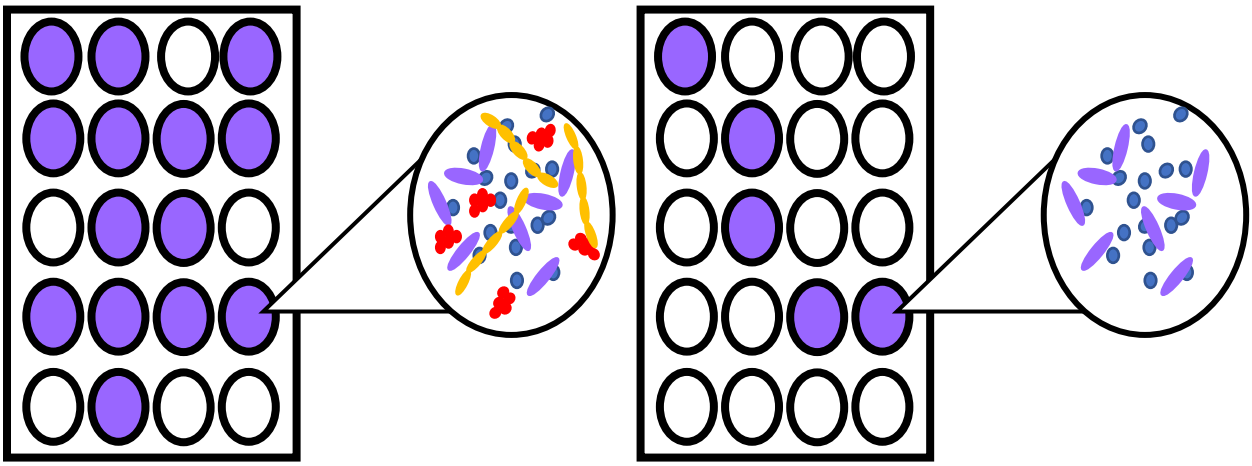

Figure 3.9: Examples of microbial diversity impacting metabolic profiling through CLPP. Image adapted from Flynn, 2017.

Differences in metabolic diversity between OP doses of 2 and 4 mg/L are not seen in Figure 3.7, as measured through H' values. Shannon diversity does not reflect the noticeable variation between sampling dates that is seen in the AWCD or biofilm reformation potential data, such as the sharp decrease in AWCD see on day 52 (Figure 3.4). It does indicate that increasing the concentration of OP, to which these communities are exposed increases metabolic diversity, as reflected through higher H' values of carbon utilization (Clairmont and Slawson 2020; Bannister et al. 2021).

Another possibility is an increase in metabolic activity of specific carbon sources, rather than metabolic diversification from a maturing biofilm, as Shannon diversity indices and carbon

source guilding do not indicate changes in metabolic diversity (Figures 3.6 and 3.2.6), the differences in AWCD and biofilm formation potential may reflect initial bacteria adapting to the environment, and beginning to metabolize more actively within the support or protection of a more stable biofilm, (Pisithkul et al. 2019)

Structural profiling was also performed to provide further insight into these concepts, as a noticeably changing genetic profile may be indicative of diversification of taxa, rather than a change in metabolic activity levels of the initial colonizers (Konstantinidis and Tiedje 2004; Mouchet et al. 2012).

Structural Profiling using DGGE:

Structural profiling took place using denaturing gradient gel electrophoresis (DGGE) as a means of assessing genetic shifts within the coupon-associated communities over the course of the experimental period. Similarity was compared using hierarchical clustering analysis through GenCompare II, to generate an unweighted pair group method with arithmetic mean (UPGMA) dendrograms (Németh et al. 2014). These dendrograms are then compared for each treatment to visualize the communities' changing profiles over the sampling period.

The coupon-associated community exposed to 4 mg/L OP has a low similarity between clusters, at only 4.5% (Figure 3.10). This is the lowest similarity seen throughout all communities, and clustering seems to be related to the date of sampling, with samples from nearby dates exhibiting higher genetic similarity, comparative to samples from further dates. Throughout days 7 to 42, coupon-associated communities exposed to 4 mg/L of added OP exhibited 66.7% overall similarity, and can be seen as a distinct cluster. At day 52, a decrease in genetic similarity accounts for another distinct cluster. These biofilms then continue to exhibit a pattern of low

similarity throughout the final sampling dates, with day 94 biofilms only sharing 14.8% similarity to other clusters.

Coupon-associated communities exposed to 2 mg/L OP demonstrated much higher overall similarity (49.4%) when compared to those exposed to 4 mg/L (Figure 3.10), and, as seen in Figure 3.11, had more similar clustering between sampling dates. Three major clusters are apparent, and are grouped into sampling dates before and following day 52 which share 68.2% genetic similarity with each other, and the third cluster solely comprising the coupon-associated communities sampled on day 52. Similarity between coupons remained high compared to communities exposed to 4 mg/L OP (Figure 3.10), with the lowest occurrence of genetic similarity being from biofilms sampled on day 52.

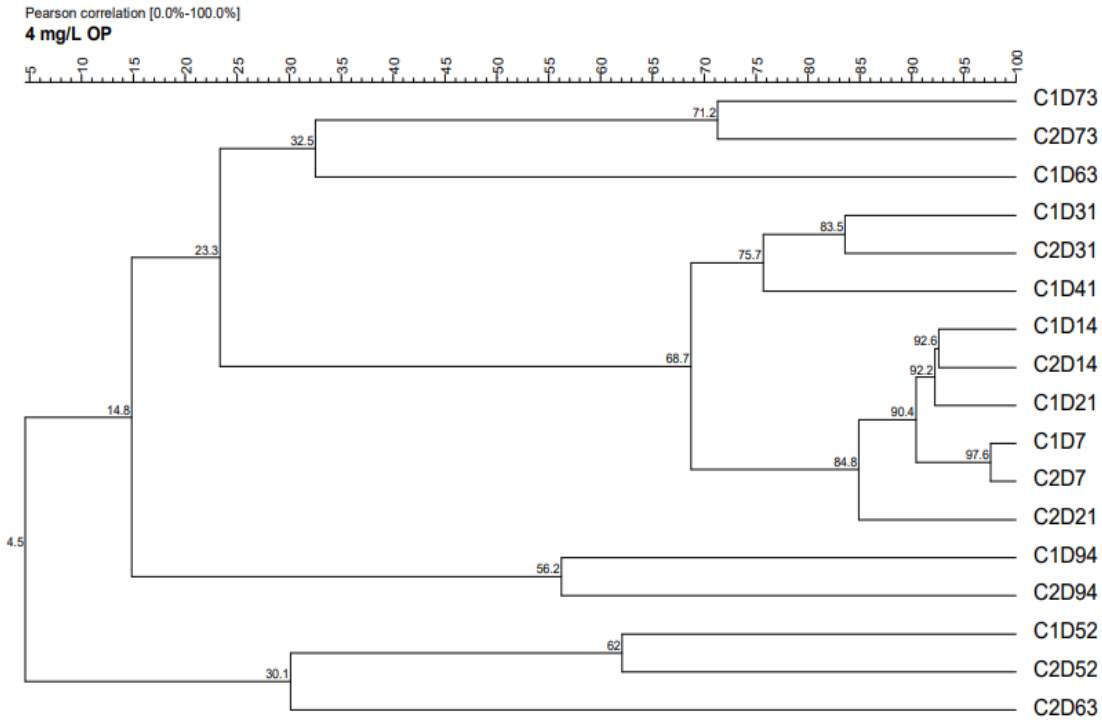

Figure 3.10: Hierarchical cluster analysis of banding patterns obtained from denaturing gradient gel electrophoresis (DGGE) of PCR amplified 16 rDNA extracted from coupon-associated biofilms after exposure to 4 mg/L of OP, rendered graphically as an UPGMA dendrogram. C= Coupon replicate, D= Isolation day

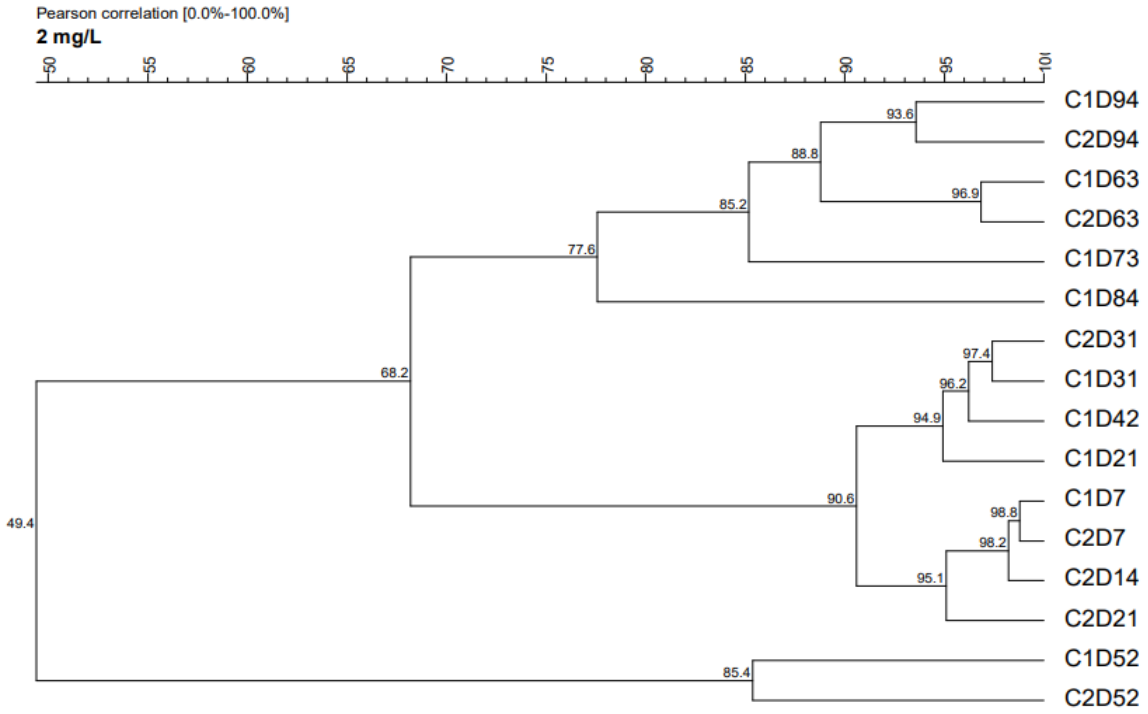

Figure 3.11: Hierarchical cluster analysis of banding patterns obtained from denaturing gradient gel electrophoresis (DGGE) of PCR amplified 16 rDNA extracted from coupon-associated biofilms after exposure to 2 mg/L of OP, rendered graphically as an UPGMA dendrogram. C= Coupon replicate, D= Isolation day

Unlike the dendrograms created for 4 and 2 mg/L OP-exposed coupon-associated communities (Figures 3.10 and 3.11), those exposed to 1 and 0 mg/L of added OP exhibit less distinct cluster patterns (Figures 3.12 and Figure 3.13). As seen in Figure 3.12, overall similarity between samples is 42.7%, with mainly two distinct clusters. For these treatments, genetic similarity of coupon-associated communities differentiates more between sampling dates. For example, C1D14 and C1D21, while only being 7 days apart, exhibit the lowest levels of genetic similarity. It becomes more difficult to discern patterns from these clusters, as DNA extractions from these communities routinely failed to yield sufficient viable DNA for accurate processing.

Interestingly, the control biofilm communities, exposed to no additional OP, show highest overall similarity between clusters when compared to OP-exposed systems, at 54.7% (Figure 3.13). With similarity being relatively high within control communities, it is difficult to draw concise conclusions. Regardless, similarity does show some signs of decreasing over time, such as the 94% similarity between D21 and D42 coupons, compared to the 68.9% between D52 and D73 coupons (Figure 3.12).

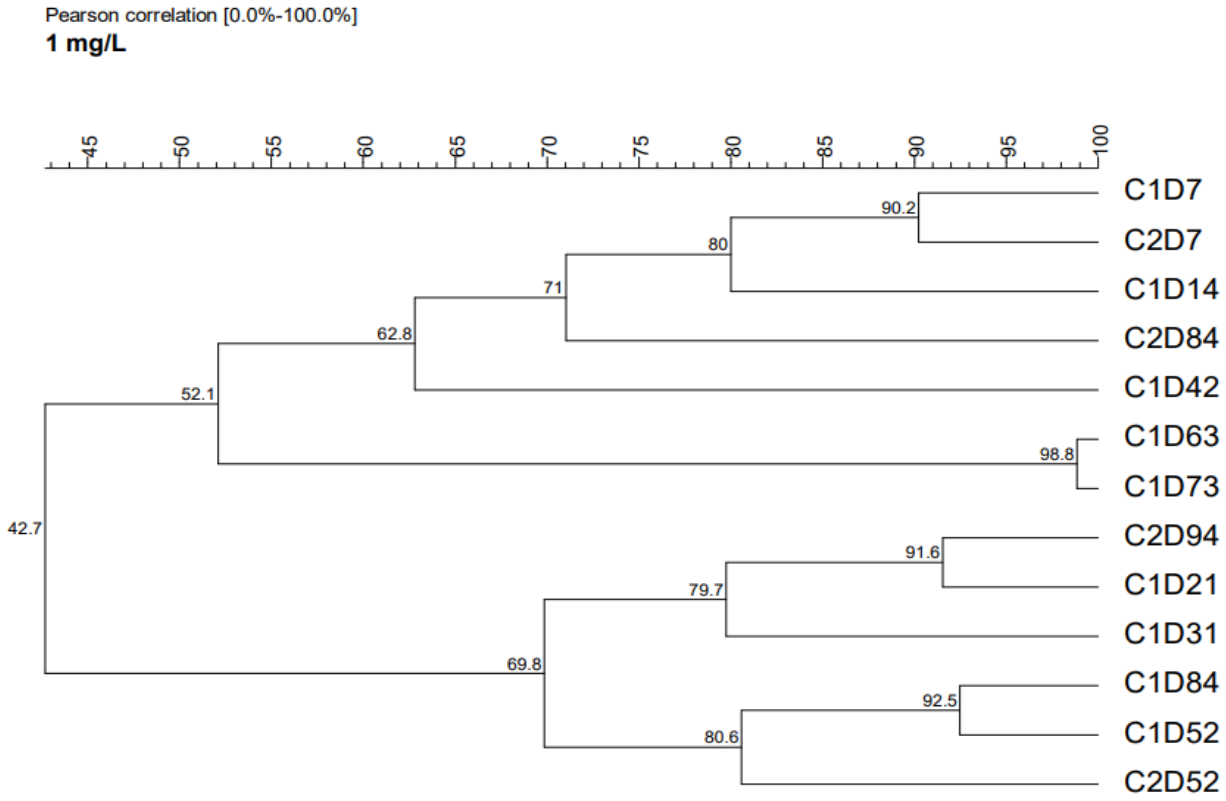

Figure 3.12: Hierarchical cluster analysis of banding patterns obtained from denaturing gradient gel electrophoresis (DGGE) of PCR amplified 16 rDNA extracted from coupon-associated biofilms after exposure to 1 mg/L of OP, rendered graphically as an UPGMA dendrogram. C= Coupon replicate, D= Isolation day

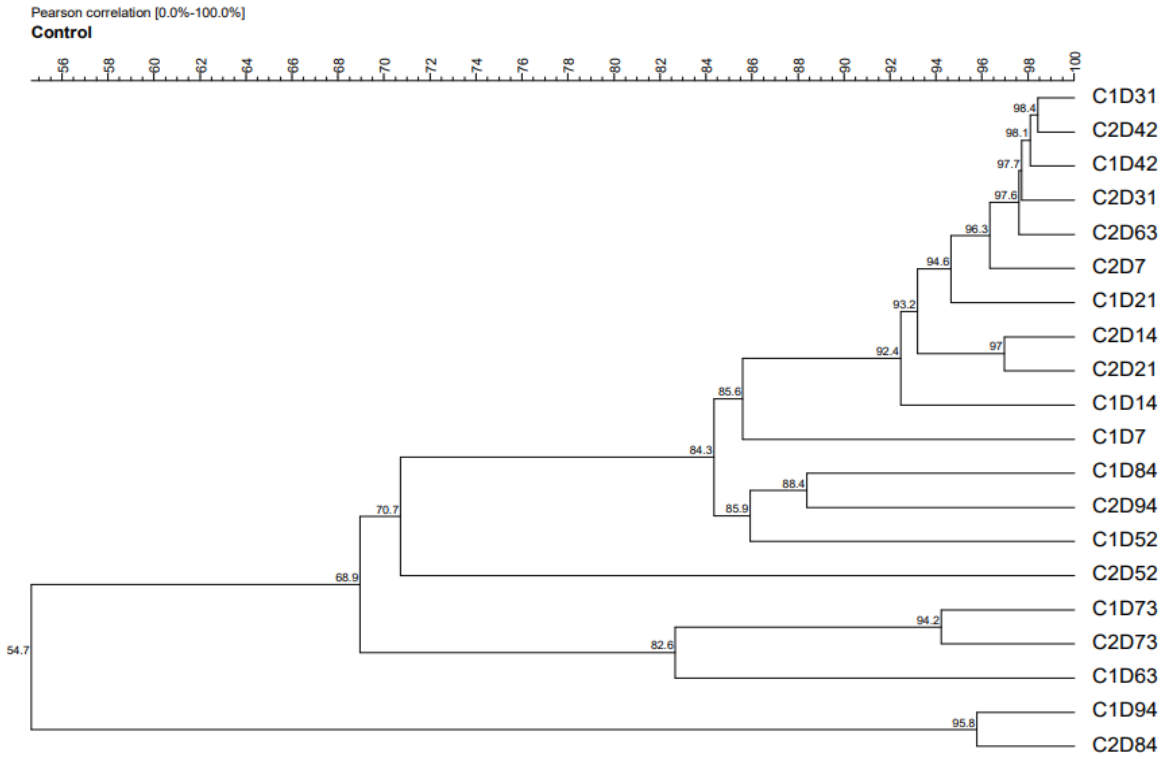

Figure 3.13: Hierarchical cluster analysis of banding patterns obtained from denaturing gradient gel electrophoresis (DGGE) of PCR amplified 16 rDNA extracted from coupon-associated biofilms after exposure to 0 mg/L of additional OP, rendered graphically as an UPGMA dendrogram. C= Coupon replicate, D= Isolation day

Overall, exposure to increased OP concentrations has impacted coupon-associated microbial community structure, dependant on the OP concentration. Clear distinctions can be observed between sampling dates for coupon-associated communities exposed to 4 and 2 mg/L OP which reflected trends in metabolic activity, including the changes in AWCD being dependent on sampling date (Figure 3.6). The lower similarity observed between clusters associated with sampling date for these communities reflects a shift in genetic profiles present in the biofilm (Leflaive et al. 2008; Mouchet et al. 2012). Whether these changes are reflective of a shift in taxa, or metabolic sequences, cannot be discerned through DGGE analysis. Although shifts in

taxa and metabolism are not mutually exclusive, it can be speculated that due to the low level of similarity based on G-C content, these shifts are based on a major genetic variation of the communities, more likely a diversification of species, rather than metabolic sequences, which have been shown to make up only a small portion of microbial genomes (Konstantinidis and Tiedje 2004).

Although differences in genetic similarity were exhibited throughout each biofilm community, those exposed to higher levels of OP (2 and 4 mg/L) have clearer distinctions between clusters, based on sampling dates (Figure 3.10 and 3.11). Earlier dates, before day 52, seem to be clustered together with high similarity for 2 and 4 mg/L OP-exposed communities, which then begin to diversify following day 52. For these higher OP concentrations, day 52 had the lowest overall similarity, potentially due to a shift in community structure. This shift in community structure would be indicative of a maturing biofilm community, where genetic diversity is increased, and conditions on the interior of the biofilm are more stable (Martiny et al. 2003). The control communities and those exposed to 1 mg/L exhibited higher genetic similarity over time, with patterns between sampling dates that are more difficult to discern (Figure 3.12). This further supports the previously discussed observation that OP acts as a nutrient for growth and potential diversification within bacterial communities (Rickard et al. 2004). The genetic similarity for the communities exposed to 2 and 1 mg/L OP maintained similar ranges, from roughly 50 to 99%, compared to the control system with similarities almost exclusively above 80% (Figures 3.11 and 3.12). This trend is also reflected in the biofilm communities exposed to 4 mg/L OP (Figure 3.10), with higher nutrient availability being associated with greater clustering, linking shifts in structural profiling to OP exposure (Leflaive et al., 2008; Xue et al., 2008).

Comparing Microbial Profiles

When comparing both structural (DGGE) and metabolic (CLPP) profiles, the key impact of OP on drinking water-associated microorganisms and communities can be identified (Clairmont and Slawson 2020; Bannister et al. 2021). Over the course of the initial phase of this experiment, both metabolic and structural data indicate that OP serves to enhance the ability of microorganisms in a DWDS to form more robust biofilms, higher in both genetic and metabolic diversity, as well as metabolic activity. Previous research has shown that growth of biofilm communities in a DWDS is slow, due to lack of nutrients, lowered temperatures, and the presence of environmental pressures. As mentioned previously, biofilm maturation, described as a point of stable diversity, can take upwards of months in these environments (Zak et al. 1994; Martiny et al. 2003; Douterelo et al. 2014; E. I. Prest et al. 2016).

This research shows that OP at concentrations higher than 1 mg/L enhances the ability of microorganisms in the bulk phase of a DWDS, which then attach to pipe material, to replicate to higher numbers (Figures 3.1 and 3.3), with an increased potential to form stronger biofilms (Figure 3.2 and 3.4). In doing so, nutrient loads which are potentially captured during biofilm formation are also increased, and transient inhabitants have an increased likelihood of exposure to these nutrients (Boe-Hansen et al. 2002; Revetta et al. 2013; Reuben et al. 2019). This increase in nutrient exposure may be what led to a higher level of both genetic and metabolic diversity, as seen in Figures 3.7 and 3.11**,** respectively (Fang et al. 2009a; Mouchet et al. 2012; Liu et al. 2018).

As the transient cells are hosted by more robust biofilms, reducing external pressures, the cells can replicate to higher numbers, and impact overall diversity through competition and predation (Brileya et al. 2014; Cruz et al. 2020). As such, a biofilm which is robust enough, may reach a

state of maturation in a shorter time span than those which are not exposed to excess nutrient loads.

In our study, samples isolated on day 52 showed noticeable metabolic and genetic differences from communities exposed to higher concentrations of OP (Figures 3.6, 3.10 and 3.11). Biofilm formation potential drastically decreased, which was accompanied by a sharp increase in overall metabolic activity (Figure 3.4 and Figure 3.6). Samples collected on this date also shared little similarity in community structure (Figures 3.10 and 3.11) This trend is not seen for the control communities, where there is little variation in overall metabolic activity and genetic similarity (Figures 3.6 and 3.13). Following this date, AWCD and biofilm reformation potential seemed to return to measurements which were seen in samplings from day 7 to 42, however, the structural profiles for these communities did not return to earlier profiles (Figure 3.5). The potential for the profile of a biofilm community to show greater diversity increases in the presence of more cells (I. Douterelo et al. 2018) and, as seen in Figure 3.1.1, communities exposed to OP exhibited higher viable cell counts overall. One suggested reasoning for this is the decreased prevalence of initial colonizers, related to an increase of transient or bulk phase microorganisms which begin to inhabit biofilms after their formation (Martiny et al. 2003; Schmeisser et al. 2003). This would explain why the structural profiles generated from later sampling dates do not return to a profile that is comparable to those generated from earlier sampling dates (Figure 3.10). As these biofilms matured, and more cells were present, the metabolic diversity, as measured through H' indices, may still mirror those of early-stage biofilms, while being comprised of different genetic and metabolic profiles. Genetic and metabolic profiles are not mutually exclusive, and as such similar results have been seen in other studies focused on biofilm community profiling (Mouchet et al. 2012). It is possible, that the slight increase in metabolic activity, as measured through

AWCD, and changes in genetic diversity, seen after day 52 (Figure 3.6 and 3.10), are due to a shift in prevalence of taxa, which have Shannon diversity indices that reflect those of early biofilm colonizers. The more noticeable differences in biofilm formation, AWCD and genetic diversity from coupon-associated communities sampled on day 52 may indicate a period of time where these shifts were occurring in the biofilms, and as such, less stable conditions are seen.

As mentioned previously, maturing biofilms typically exhibit a wide metabolic profile, when compared to younger and less stable biofilm communities (Kwon et al. 2011; Elias and Banin 2012). This is, in part, due to a higher diversification of the community. As seen in Figure 3.8, the carbon guilds of biofilms exposed to 2 and 4 mg/L of OP had less variation over time in comparison to systems with lower OP exposure. This again supports the idea that OP can act as a nutrient for growth and allow for biofilms to become more stable and robust in shorter periods of time. This might also indicate that the control and 1 mg/L OP-exposed communities have not yet reached a state of maturation. The genetic profiling patterns seen in the biofilm communities of this study, are shown to be dependent on OP exposure. As such, communities which are exposed to higher concentrations of OP can form more diverse and robust biofilms.

Higher OP doses also corresponded with higher levels of measured nitrogen species (Appendix A). This might be expected because, since monochloramine stability is pH-associated, it is possible that the increase of monochloramine decay (Appendix A1) was driven through physico-chemical interactions, instead of potential microbial degradation (Fehér et al. 2019). The decreasing pH, relative to an increase in OP dose (Appendix A2), would have driven dichloramine to become a more chemically-favoured chloramine species. In doing so, the ratio of free, unbound ammonia would have been seen to increase, much like was seen in Appendix A5,

as free chlorine molecules would be more stable in binding to ammonia at a ratio of 2-to-1, rather than 1-to-1 (Khiari 2016).

3.3 Investigation Into pH Impact on Microbial Activity in Sampled Water (Batch Test)

The pH of treated water has been shown to significantly impact the degradation of chlorine-based disinfectant residuals, such as monochloramine (Yee et al. 2008). At an acidic pH, below 7.00, the production of dichloramine and trichloramine are more chemically favoured. In fact, acid-mediated conversion of monochloramine to dichloramine occurs at pH values between 6.00 and 6.60 (Trogolo and Arey 2017). Unfortunately, these secondary chloramine species are less stable and decay more rapidly than monochloramine. The upkeep of a more alkaline system, above pH values of 7.5, allows for a more stable disinfectant residual (How et al. 2016).

Additional parallel analyses at the University of Waterloo allowed for an opportunity to investigate potential impacts of a pH adjustment on the microbial communities present in the water used for these studies. Subsamples were created based on addition of monochloramine at 0, 1, 2 and 4 mg/L OP and pH adjustment to 7.40 and 7.95, as well as samples without pH adjustment. HPC and CV assays were performed on samples at 7, 14 and 21 days of incubation. Both HPC and CV assays were conducted to understand the potential impacts of a pH adjustment on the bacteria present in the experimental water. Slight differences in HPC occurred between the tested OP doses or pH adjustments (Figure 3.14). Over the span of 21 days, it can be seen that the bacteria present were able to utilize the available nutrients present in the experimental water for growth, but cell counts remained similar at all tested pH values.

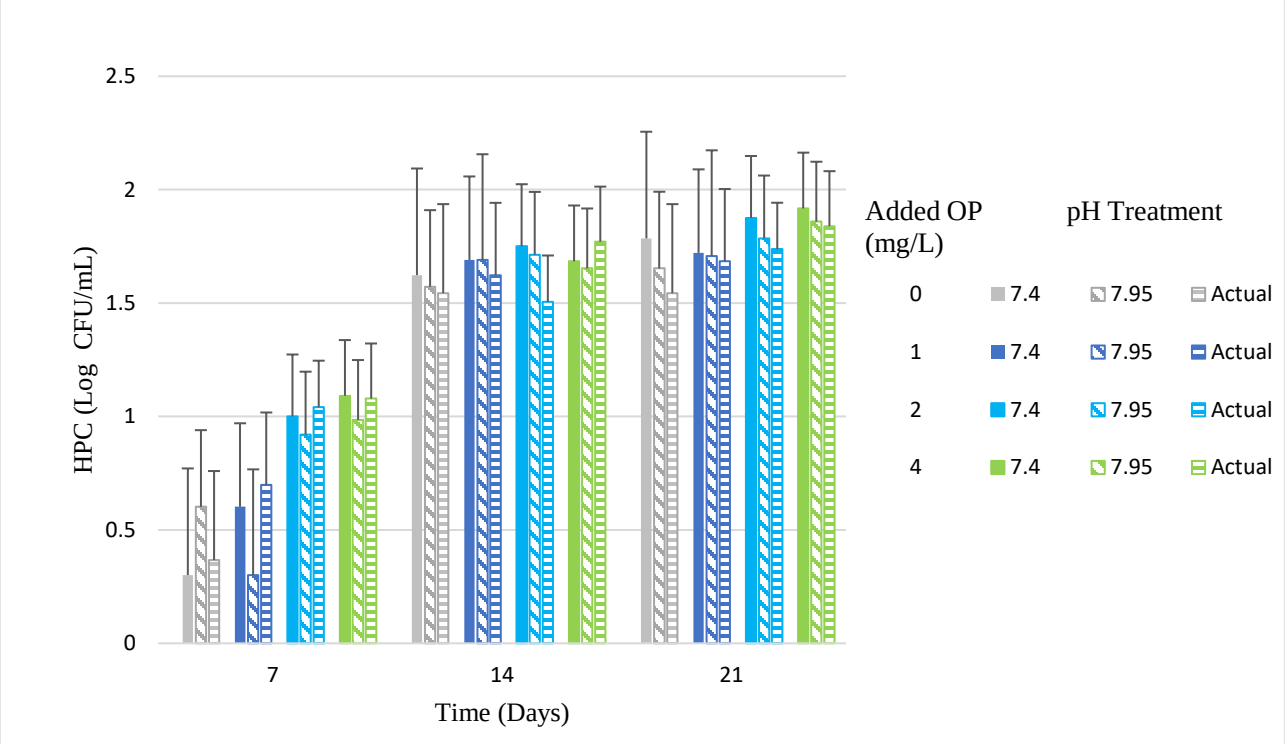

Figure 3.14: Heterotrophic plate counts (HPCs) of batch test to determine the impact of pH adjustment on bulk water microbial communities. Error bars represent standard error (n=2).

In contrast to the HPC results from this batch experiment (Figure 3.14), CV assays show much more notable differences in biofilm reformation potential at different OP doses (Figure 3.15). Similar to HPC results, however, CV assays indicated little difference in biofilm reformation potential at the different pHs tested, as seen in Figure 3.15. Overall, biofilm reformation potential decreased over the duration of the experiment, with highest levels of biofilm reformation potential for samples with 0,1 and 4 mg/L OP occurring on day 7. Samples with 2 mg/L experienced highest levels of reformation potential on day 21, while also exhibiting the highest similarity of reformation potential between different pH levels tested. Samples exposed to 4 mg/L OP showed initially higher biofilm reformation potential at a more neutral pH of 7.4. However, samples on day 21 indicate that biofilm reformation potential is increased at a more alkaline pH of 7.95, and biofilm formation potential of microorganisms exposed to a pH of 7.4 noticeably dropped.

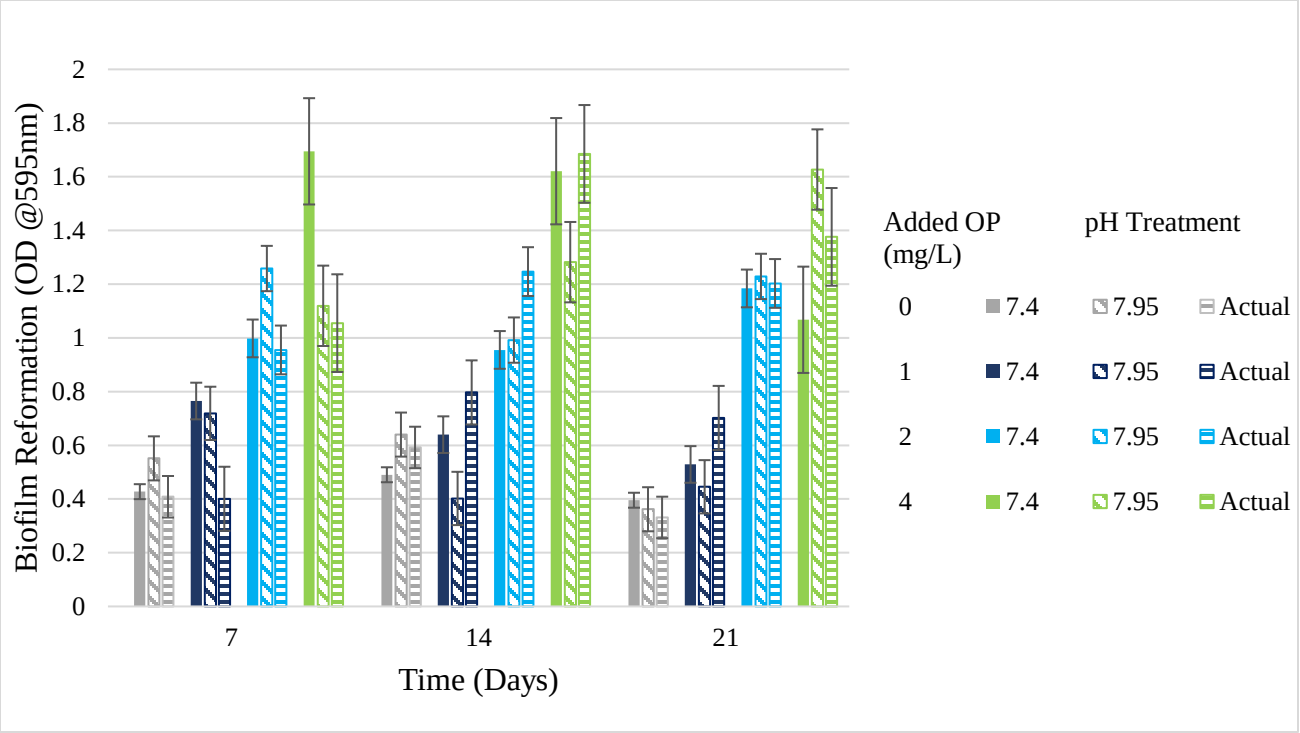

Figure 3.15: Biofilm reformation potential of batch test to determine the impact of pH adjustment on bulk water microbial communities. Error bars represent standard error (n=3).

The ability for bacteria to survive and thrive within a range of pH is common (Jin and Kirk 2018). Environmental conditions can vary significantly over a short period of time, and the bacteria in these environments have become accustomed to these changes. Typically, bacteria prefer pH conditions near neutral, but acidophilic and alkaliphilic bacteria exist which have adapted to more extreme ranges (Bååth and Kritzberg 2015; Jin and Kirk 2018). The pH of treated drinking water is commonly near or somewhat above neutral, to maintain water quality and chemical stability. However, some treatments may alter the pH of finished water, to either more acidic or alkaline conditions (Mohammed and Ismail 2021). Several studies have shown that optimal pH ranges for bacterial growth are varied based on genus, species or strain, and growth curves for bacteria along these ranges are usually bell-shaped, with optimal growth occurring in the span of a single pH unit (Stefanowicz 2006; Marois-Fise et al. 2013; Chao et al. 2015; Jin and Kirk 2018).

The ability of bacteria to survive within environmental conditions where pH may vary is essential. Fluctuations observed in a DWDS are typically within a single pH unit and are constantly monitored to assure finished water quality (Li and Wu 2019). With this in mind, considering the collected water had an original pH near neutral, the adjustments made for this experiment (within 0.5 pH units) were not expected to adversely affect the indigenous bacteria (Marois-Fise et al. 2013).

In this test, the observed increase in biofilm formation potential, without a corresponding change in overall cell count, may at first seem contrasting, however bacteria in low-nutrient systems such as a DWDS can upregulate their production of EPS in times of stress. The maintenance of stress-associated genetic sequences can also allow for a rapid re-entry to a logarithmic state of growth once more optimal conditions arise (Kolter et al. 1993). Our data shows that while the overall number of cells remained comparable at the different pH values tested, there was an effect on the generation of biofilm-forming material which may reflect a protective stress response by the bacteria. For example, nutrient-starved bacteria have been shown to have less susceptibility to environmental influences, including the presence of antibiotic compounds (Nguyen et al. 2011). This increased tolerance in response to nutrient limitation, is through a pathway known as the Stringent Response (SR) (Kjelleberg et al. 1993; He et al. 2012).

The SR acts as a regulator for unnecessary pathways under times of starvation or stress, which may be seen in a DWDS. Common impacts include either an increase or decrease in biofilm development, which may be species-dependent, a decrease in DNA replication and decreases in cell wall synthesis (Kjelleberg et al. 1993; Honsa et al. 2017; Salzer et al. 2020). Although species dependent, an increase in biofilm production and decrease in cell wall synthesis could be a possible explanation for the results shown in both Figures 3.14 and Figure 3.15 (He et al. 2012; Honsa et

al. 2017; Salzer et al. 2020) where we observed an increase in biofilm reformation potential but no obvious increase in cell count. *Vibrio cholerae*, the causative agent of the disease cholera, is one such bacterial species which has been shown to upregulate biofilm formation as a response to stress (Kjelleberg et al. 1993; He et al. 2012).

As introduced previously, it has been shown that phosphorus can be assimilated into EPS matrices, which comprise the major structure of biofilms (N. Li et al. 2010; Zhang, Fang, Wang, Sheng, Xia, et al. 2013). In fact, research has shown that bacteria which produce EPS at higher rates are able to solubilize and assimilate phosphorus at higher efficiencies (Javier et al. 2021).It has been suggested that these initial colonizers may have an SR system which upregulates biofilm formation and nutrient uptake, among other survival responses (Schofield et al. 2018). However, it should be noted the CV assays conducted in our study focused on biofilm reformation, in which samples were allowed to grow in media with nutrient concentrations much higher than those used during the experiment . It is possible that the water used for the batch test contained microorganisms from the bulk (suspended) phase that were not actively forming biofilms to full potential. Conditions of the batch test (Section 2.2) were such that the opportunity of attachment to surface material and with it, the upregulation of biofilm formation material for microorganisms was decreased through the disruption and mixing of samples from the shaking incubator.

3.4 Summary and Conclusions

The experimental design with ARs used in this study allowed for an integrative and highly applicable view of a simulated DWDS. The exposure to OP has been seen in previous research to have conflicting impacts on microbial communities (Faust and Correll 1976; Park et al. 2008;

Jang et al. 2012; Aghasadeghi et al. 2021). Consequently, our initial major experiment was used to investigate the impact of three different OP concentrations, which are in the general ranges of those used in a DWDS. In conclusion, this portion of the research addressed the first objective, of using culture and molecular-based approaches to assess microbial response to the presence and absence of OP as a corrosion inhibitor. In doing so, we can provide insight to the question of the impact of OP addition on microbial communities in a DWDS. The monitored community profiles of microorganisms, from both the bulk and attached phases of the system were seen to be dependent on OP dose. At 4 and 2 mg/L of OP, overall metabolic diversity, biofilm reformation potential and cell count increased when compared to only 1 mg/L of OP. Higher doses of additional OP were also shown to impact genetic diversity, forming a more mature, genetically diverse biofilm in a shorter period of time, most likely due to the increased proliferation of cells and biofilm material through the utilization of OP as a nutrient. It can be said that this research shows that the use of OP as a corrosion inhibitor, in concentrations at, and above 2 mg/L has impacts on microbial communities which allow for the formation of more diverse and potentially robust biofilms.

Chapter 4: An Investigation of the Impact on Drinking Water Microbial Communities of Chloramine Concentration in the Presence and Absence of Orthophosphate

4.1 Overview

To understand the impacts of monochloramine concentration on orthophosphate (OP)-exposed microbial communities in a drinking water distribution system (DWDS), a 12 week flow-through experiment was established, as outlined in Section 2.1.4. Annular reactors (ARs) were dosed

with either a low and high concentrations of chloramine (1.9-2.0, and 2.9-3.0 mg/L, respectively), in the presence and absence of OP at a concentration of 2 mg/L. pH adjustments were made to the influent water to maintain a pH of 7.4, to mitigate pH-mediated monochloramine decay. During these 12 weeks, coupons were removed in duplicate at timepoints ranging from 7 to 14 days apart, with bulk water removal taking place at the same time for microbial analysis (Section 2.2.1). Coupon-associated community and bulk phase microbial profiles were created using monitoring techniques previously outlined in Section 2.2. At the same time, physico-chemical analyses at the University of Waterloo (Appendix B) were performed. These parameters were monitored more frequently over the 15-week study period, and include concentration data for compounds such as nitrite, nitrate, ammonia, free and combined chlorine.

The primary objective of this research was to determine microbial response to the presence of chloramine as a disinfectant in the presence of OP. Culture and molecular-based approaches were used to compare bulk phase and biofilm response under these conditions.

4.2 Results and Discussion

4.2.1 Chloramine impact on culturable microbial growth and biofilm formation potential in the presence and absence of orthophosphate

Heterotrophic plate counts (HPCs) were monitored over the course of this second major experiment for both bulk phase microorganisms and coupon-associated communities. Bulk phase samples (Figure 4.1) indicate that microorganisms exposed to lowered levels of chloramine, in addition to OP, had noticeably higher viable cell counts by day 7. By day 21, all bulk phase

samples exhibited an increase of HPCs. Beyond day 21, increased levels of growth are more noticeable in systems exposed to added OP. Bulk phase microorganisms exposed to OP, in the presence of either high or low levels of chloramine, exhibited higher viable cell counts after 35, eventually plateauing from day 94 onwards, at 3.1 log units. Bulk phase microorganisms exposed to the lower level of chloramine and no added OP exhibited viable cell counts which reached a maximum of 1.66 log units on day 108, reflecting the impact of added OP, as seen in Section 3. Those exposed to the highest concentrations of chloramine, without added OP, had lowest viable cell counts overall, reaching a maximum of 1.54 log units, showing that without added nutrients, the impact of disinfectant is more pronounced.

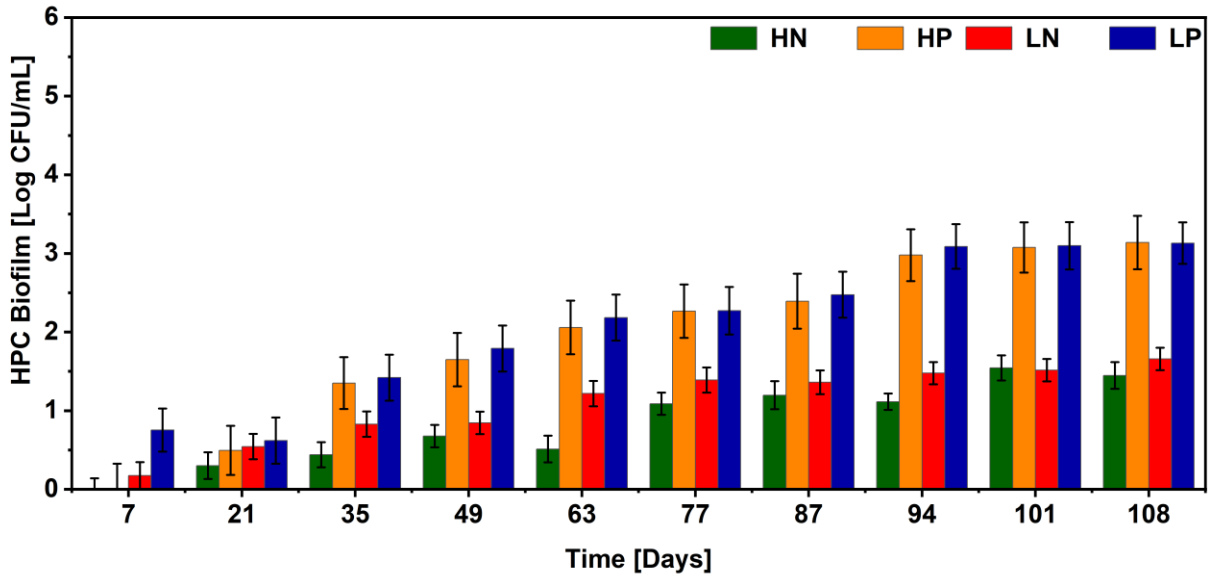

Figure 4.1: Heterotrophic plate count (HPC) of bulk phase microorganisms, sampled from reactors at time of coupon removal. Samples were plated in duplicate. Error bars represent standard error (n=2). L and H represent low (2.0 mg/L) and high (3.0 mg/L) chloramine dose, while P and N represent the addition of orthophosphate and no additional orthophosphate.

As shown in Figure 4.2, bulk phase microorganisms exhibited a higher potential for biofilm reformation in the presence of OP. Microorganisms exposed to the higher chloramine dose and OP had slightly decreased biofilm reformation potential after day 35, compared to those exposed

to a lower chloramine dose in the presence of OP. A decrease was observed in reformation potential for microorganisms exposed to added OP, from a range of 2.77 and 2.41 on day 49, to 2.16, and 0.43 at day 63, for low and high chloramine exposure, respectively. These decreases were not seen as early on in bulk phase microorganisms from ARs exposed to no added OP, however, a decrease in biofilm reformation potential for these cells was observed at day 87. Biofilm reformation potential slowly increased for the microorganisms exposed to lower concentrations of chloramine and no added OP following this increase, but those exposed to higher disinfectant did not recover as well. (Figure 4.2).

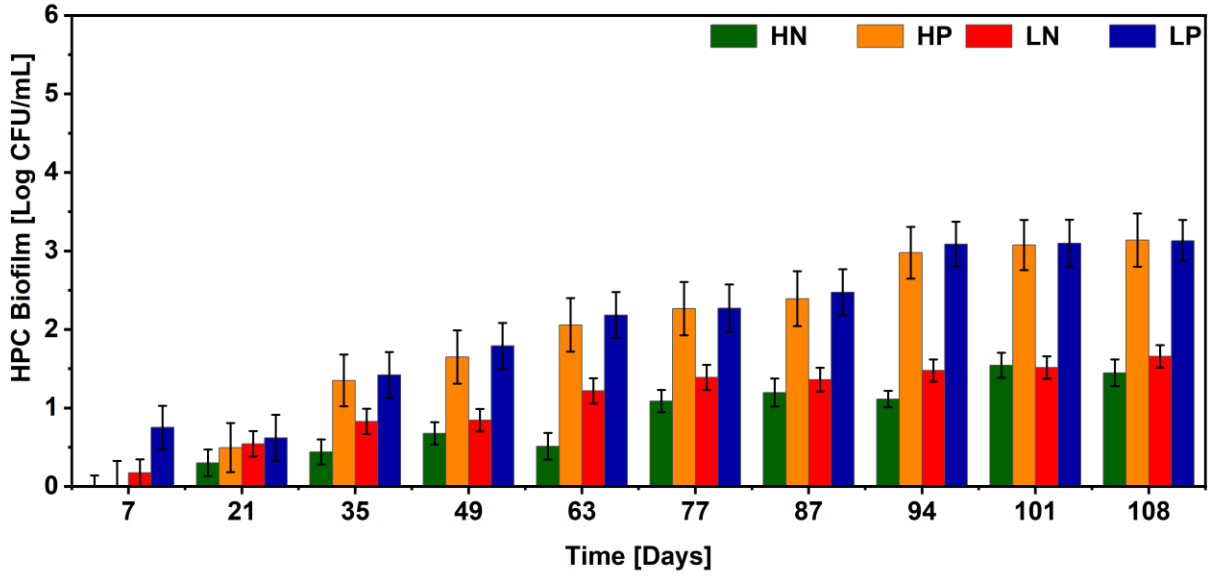

Figure 4.2: Biofilm reformation potential of sampled bulk phase microorganisms, as measured through absorbance of CV-stained biofilm material. Samples incubated for 7 days in static R2A broth before staining occurred. L and H represent low (2.0 mg/L) and high (3.0 mg/L) chloramine dose, while P and N represent the addition of orthophosphate and no additional orthophosphate. Error bars represent standard error (n=3).

As shown in Figure 4.3, viable cell counts for coupon-associated biofilms which were not exposed to added OP were lower than those exposed to OP, regardless of disinfectant dose. Coupon-associated biofilm communities exposed to added OP exhibited overall higher cell

counts than those seen from bulk phase microorganisms (Figure 4.1), yet those which were unexposed to added OP were comparable to HPCs of the bulk phase (Figure 4.3). The difference in HPCs for microorganisms exposed to OP and those left unexposed becomes more noticeable after day 49. Coupon-associated communities exposed to the lower chloramine concentration had slightly higher viable cell counts, when compared to communities exposed to the higher concentration of chloramine. These differences in HPCs between chloramine dose are not seen for communities exposed to OP (Figure 4.1), which might suggest the influence of nutrient addition is greater than the impact of the disinfectant residual. No notable differences were seen for viable cell counts between coupon replicates.

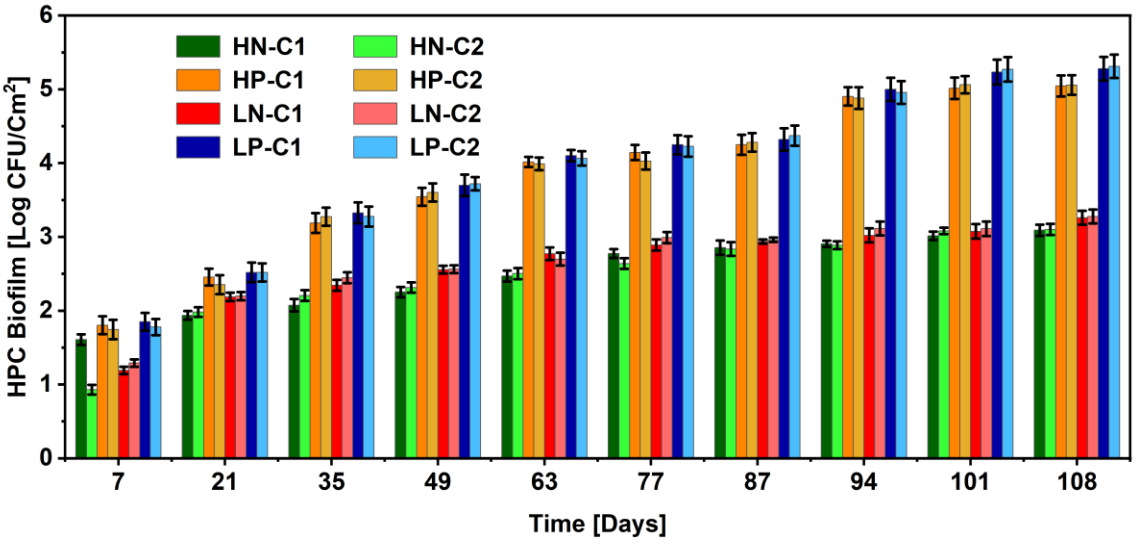

Figure 4.3: Heterotrophic plate counts (HPCs) of coupon-associated microorganisms, sampled from reactors at time of coupon removal. Samples were plated in duplicate (n=2). Error bars represent standard error. L and H represent low (2.0 mg/L) and high (3.0 mg/L) chloramine dose, while P and N represent the addition of orthophosphate and no additional orthophosphate. C1 and C2 represent coupon replicate 1 and 2, respectively.

Biofilm reformation potential data indicates that microorganisms exposed to OP exhibited increased biofilm formation in the coupon-associated samples (Figure 4.4), as was observed for

the bulk phase microorganisms (Figure 4.2). Similar to the trends observed with HPCs (Figures 4.1 and 4.3), differences in biofilm reformation potential are more likely attributed to the added OP, than chloramine concentration.

Differences in biofilm reformation potential between low and high chloramine doses are more pronounced in the absence of OP. For example, on day 87, cells exposed to the high chloramine concentration exhibited higher potential for biofilm regrowth when compared to those exposed to lower chloramine concentrations in the presence of OP. At day 63, a noticeable decrease in biofilm reformation potential is again observed for coupon-associated communities exposed to added OP. Overall, microbial communities exposed to the low chloramine concentration in addition to OP experienced the greatest potential for biofilm reformation.

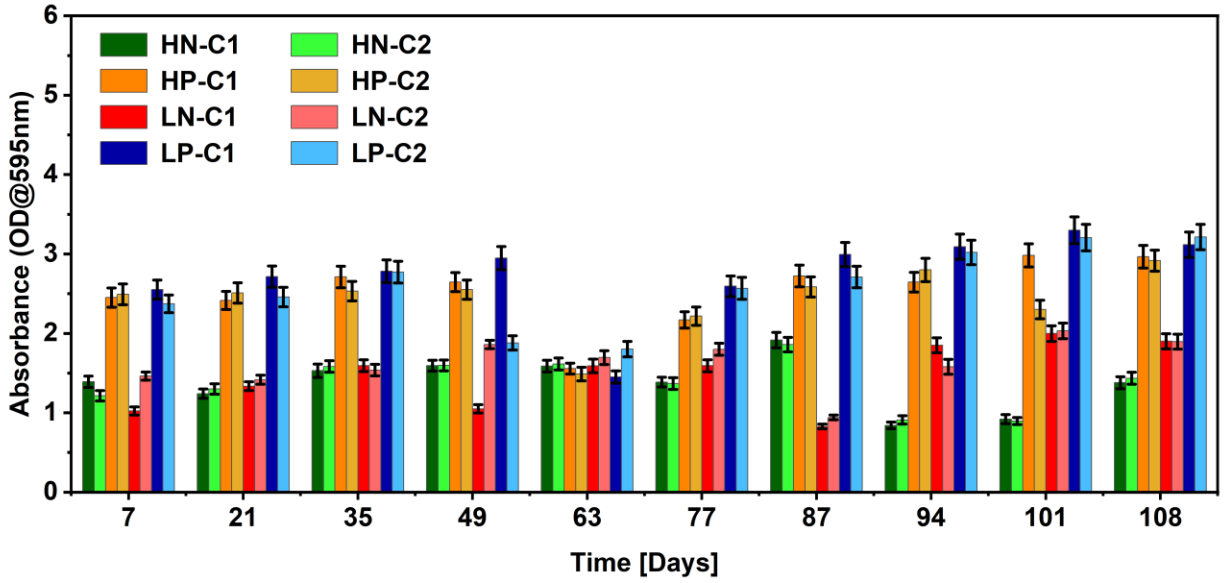

Figure 4.4: Biofilm reformation potential of removed biofilm communities, as measured through absorbance of CV-stained biofilm material. Samples incubated for 7 days in static R2A broth before staining occurred. L and H represent low (2.0 mg/L) and high (3.0 mg/L) chloramine dose, while P and N represent the addition of orthophosphate and no additional orthophosphate.

C1 and C2 represent coupon one and coupon 2, respectively. Error bars represent standard error (n=3)..

Over the experimental period of this second flow-through, HPC data indicated that both bulk phase microorganisms and coupon-associated biofilms exposed to OP had higher viable cell counts, compared to those which were not (Figures 4.1 and 4.3). Chloramine dose appeared to have little impact on both bulk phase and coupon-associated microorganisms as measured through HPCs. The same trend was true for biofilm reformation potential, for both bulk phase and coupon-associated microorganisms (Figures 4.2 and 4.4). As discussed in Chapter 3, phosphate addition has been shown to routinely impact biofilm diversity and density, even in concentrations as low as 0.03 mg/L (Lehtola et al. 2006; Fang et al. 2009b). The addition of OP, acting as a source of phosphorous, may have allowed for nutrient limitation to be mitigated, increasing potential for growth and diversification in the microorganisms which are exposed (Jansson 1988; Del Olmo et al. 2020).

As previously mention, more diverse biofilms have been shown to exhibit increased resistance to environmental pressures (Boles et al. 2004; Jang et al. 2012), such as chloramine disinfectant, when compared to single-species biofilms (Simões et al. 2010). In this study, the biofilm reformation potential which is exhibited by both bulk phase and coupon-associated microorganisms exposed to OP (Figures 4.2 and 4.4) indicates increased potential to form larger and possibly stronger biofilms, which may lead to an increased community diversity (Waak et al. 2019). The addition of OP appeared to allow for an increased resistance to chloramine in the sampled communities, exhibited through higher viable cell counts and overall biomass as biofilm material reformation. Other studies have discussed the exhibition of higher viable cell counts and overall diversification as a result of chloramine resistance (Bertelli et al. 2018). The decrease in

reformation potential noticed for bulk phase microorganisms and coupon-associated communities between day 63 and day 87 may be indicative of a maturing biofilm, with a shifting diversity, similar to those seen from Section 3 (I. Douterelo et al. 2018; Potgieter et al. 2018).

The lower viable cell counts in samples exposed to chloramine in the absence of added OP (Figures 4.1 and 4.3) suggests that chloramine still acts as a selective pressure, as similar results have been seen in studies focused on chloramine resistance (Chiao et al. 2014; Waak et al. 2019). This type of selective pressure would benefit microbial communities which have an increased chloramine resistance, and allow for lowered competition for resources such as nutrients and space (Berry et al. 2006b). Although these communities may thrive to some extent, lowered viable cell counts, diversity and activity are expected as a consequence of this pressure (Gomez-Alvarez et al. 2016; Ng et al. 2021).

4.2.2 Impact of chloramine dose on microbial community profiles in the presence and absence of orthophosphate

Functional profiling by CLPP:

Further functional monitoring performed using metabolic assays allowed for a range of assessment opportunities for the microbial community at each sampling time (Clairmont and Slawson 2020). As previously stated, BioLog EcoPlates™ were used to determine the community-level physiological profile (CLPP) through average well colour development (AWCD), Shannon Diversity, and carbon guilding (Section 2.2). AWCD of each EcoPlate™ was measured after 5 days of sample incubation, and provides insight into the carbon metabolism occurring within a community over time.

AWCD from the removed coupon-associated biofilms, as shown in Figure 4.5, exhibited higher levels of metabolic activity in the presence of OP. No bulk phase microorganisms exhibited metabolic activity which surpassed threshold readings (Data not shown). Regardless of chloramine levels, resuspended microorganisms from coupons exposed to OP were the only ones to surpass the minimum threshold of metabolism for these assays (As described in Section 2.2). Between day 7 and day 63, metabolic activity for all system communities was stable, with only minor differences in AWCD seen between chloramine doses and coupon replicates. From day 77 onward, however, a noticeable increase in metabolic activity is seen from coupon-associated biofilms exposed to added OP. AWCD increased for these communities from a range of 0.4-0.7, to 0.9-1.5 OD (595nm). Communities not exposed to added OP did not show an increase on day 77, but remained low and below the minimum threshold for metabolic positivity.

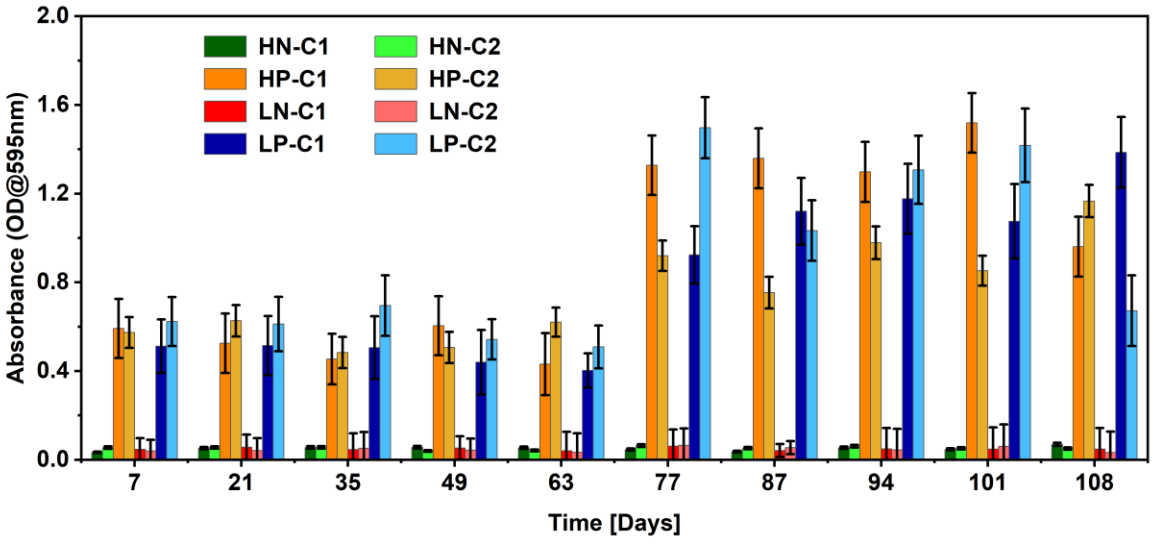

Figure 4.5: Metabolic activity of resuspended coupon-attached communities, as measured through average well colour development (AWCD) from BioLog Ecoplates ™. L and H represent low (2.0 mg/L) and high (3 mg/L) chloramine dose, while P and N represent the addition of orthophosphate and no additional orthophosphate. Error bars represent standard error (n=3). C1 and C1 represent coupon replicate 1 and 2, respectively.

Along with AWCD, Shannon diversity from removed coupon-associated communities was calculated (Figure 4.6). Since the communities unexposed to added OP did not surpass the metabolic positivity threshold, their individual H' scores have been omitted from Figure 4.6. Coupon-associated microorganisms which were exposed to the high chloramine dose exhibited the highest metabolic diversity of all systems, as measured through Shannon Diversity, between days 7 and 77. The coupon-associated communities which were exposed to a low dose of chloramine exhibited H' indices that, unlike the high chloramine exposed communities, did not initially surpass 3.3, indicating lower metabolic diversity. Following day 77, metabolic diversity of communities exposed to the high chloramine concentration decreased, and more closely resembled those exposed to the low concentration of chloramine. However, at day 87, metabolic diversity for the low chloramine-exposed communities actually surpassed those at high chloramine dose, indicating a more metabolically diverse community. Following day 87, no notable difference between H' indices could be observed based on chloramine exposure.

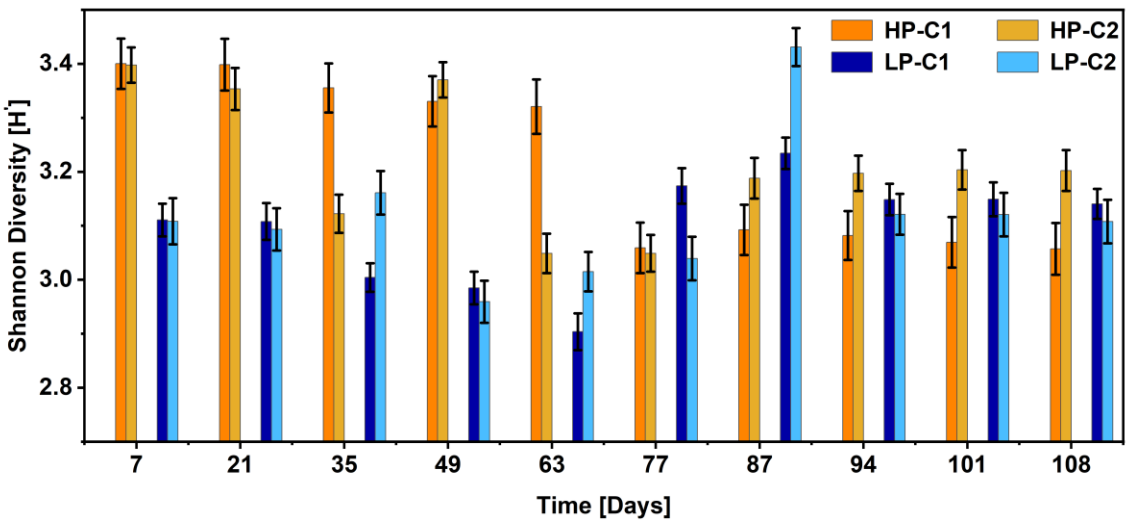

Figure 4.6: Shannon diversity scores of removed biofilm communities. Communities exposed to no added OP have been omitted, due to standard procedures for metabolic monitoring. L and H

represent low (2.0 mg/L) and high (3.0 mg/L) chloramine dose, while P and N represent the addition of orthophosphate and no additional orthophosphate. C1 and C2 represent coupon 1 and 2, respectively. Error bars represent standard error (n=3).

Carbon guilding monitored from EcoPlate^{TM} data indicates which guilds, or groups, of carbon sources were best metabolized, as described in Section 2.2 (Figure 4.7). Initially, coupon-associated biofilms exposed to low chloramine and added OP exhibited between 25-30% utilization of carbohydrates, amino acids and carboxylic acids. Polymer and amines/amides utilization comprised the remaining 15% of overall utilization. At day 63, carbohydrate utilization decreased for these communities, but an increase in polymer, amino acid and carboxylic acid utilization was observed. At day 108, carboxylic acid utilization again increased, along with carbohydrate utilization, and a small decrease in amino acid and polymer utilization. Coupon-associated communities exposed to high chloramine and added OP exhibited relatively comparable polymer and amine/amides utilization throughout the experimental period. Carbohydrate utilization for communities exposed to the high chloramine dose slightly decreased throughout the sampling period, but increases in carboxylic acid and amino acid utilization were noted between day 7 and 63, and day 63 and 108, respectively. Although coupon-associated biofilms which unexposed to added OP did not surpass the minimum threshold readings, their guild data included for comparison in Figure 4.7.

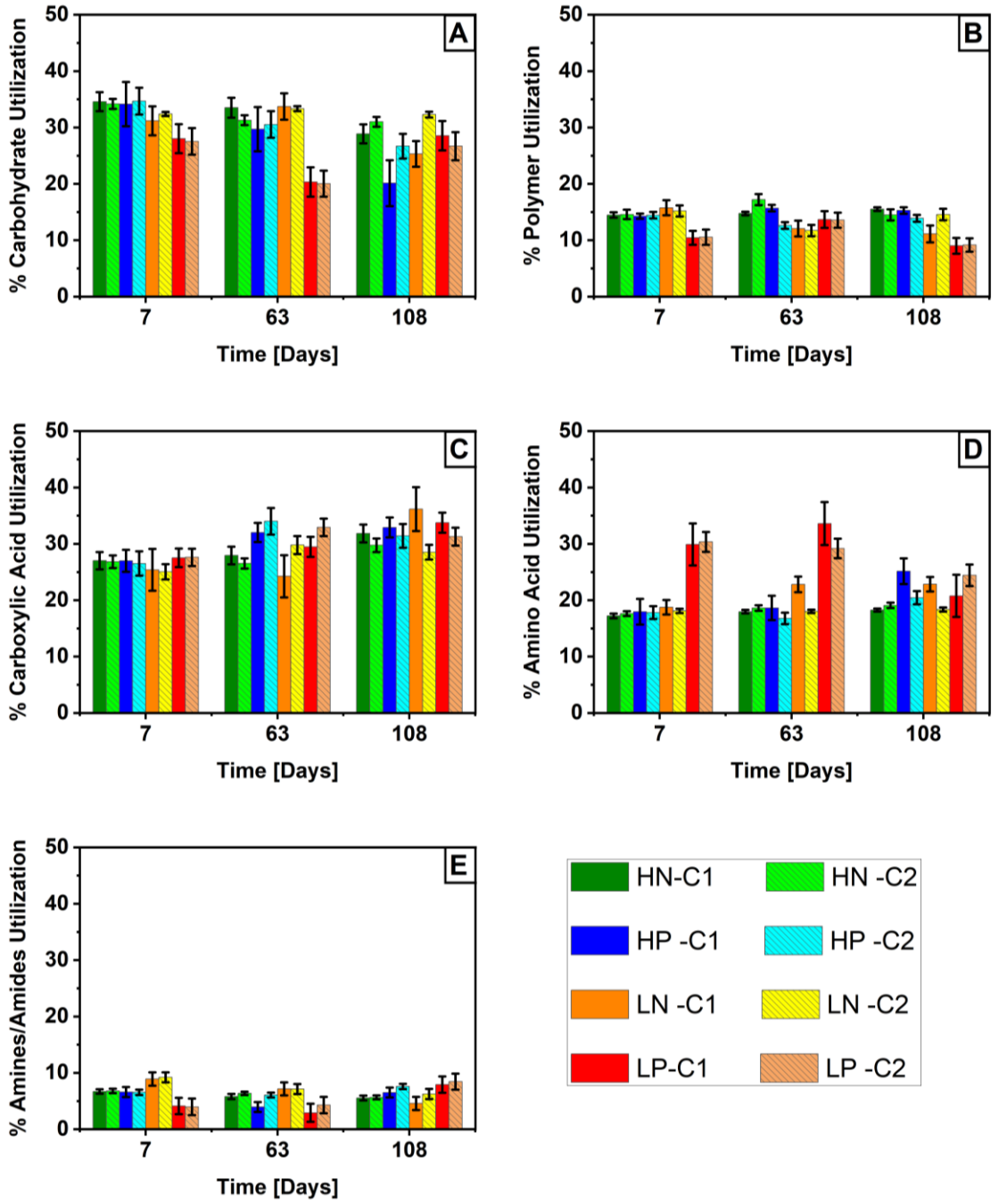

Figure 4.7: Percent usage of carbon substrates (grouped by polymers, carbohydrates, carboxylic and ketonic acids, amino acids, and amines and amides) on Biolog Ecoplates™ by coupon-associated bacterial communities. L and H represent low (2.0 mg/L) and high (3.0 mg/L) chloramine dose, while P and N represent the addition of orthophosphate and no additional orthophosphate. C1 and C2 represent coupon 1 and 2, respectively. Error bars represent standard error (n=3).

The metabolic activity and diversity of the coupon-associated communities increased in the presence of OP and were less affected by chloramine concentration. Microorganisms, both from the bulk phase and coupon-associated biofilms, exposed to no added OP failed to cross the threshold of metabolic activity, indicating lowered metabolic rates for these communities, which has routinely been exhibited in similar studies, focused on microorganisms in the bulk phase (Farkas et al., 2012; K. E. Fish & Boxall, 2018; Liu et al., 2013). On day 77, microorganisms from coupon-associated biofilms exposed to added OP exhibited noticeably increased metabolic activity, which was not reflected in coupon-associated communities unexposed to added OP, or any of the bulk phase microorganisms. This increase is potentially due to a shift in genetic diversity, and is most likely the source of differences in metabolic diversity between samples (Elias and Banin 2012; Mouchet et al. 2012; Pisithkul et al. 2019) , as discussed previously in Chapter 3. The diversification in metabolic profiles of these communities appears to be enhanced by the presence of OP, which may inhibit the selective pressures of chloramine disinfectant (Aggarwal et al. 2018; Zhu et al. 2021).

Results shown in Figure 4.7 highlight that over the duration of the study, carbon guilding profiles of the coupon-associated communities exposed to added OP begin to align with each other, and a greater evenness is exhibited in overall carbon source utilization. Guilding of coupon-associated biofilms not exposed to added OP show evenness over time, however the utilization of each carbon guild matches the ratios of respective carbon sources present in an EcoPlate™ (Sofo & Ricciuti, 2019; Weber & Legge, 2010). Microbial communities exposed to both high chloramine concentrations and added OP more closely resembled carbon utilization ranges which match the ratio of present carbon sources, when compared to communities exposed to low chloramine concentration with added OP. A carbon utilization range which more closely matches

the ratio of carbon sources present may be representative of a more even metabolic range, however these results are due to communities unexposed to added OP failing to surpass the minimum threshold, rather than actually express an even metabolic range. These differences in carbon utilization, between the communities exposed to added OP (Figure 4.7), may indicate that chloramine dose can impact overall diversity, although viable cell count and metabolic activity showed increases associated with added OP (Figures 4.3 and 3.5). Chlorination has been previously shown to impact species diversity in a simulated DWDS, and although chloramine doses differ between studies, these impacts are routinely discussed (Gomez-Alvarez et al. 2016; Zhu et al. 2021). As discussed in the previous experiment (Chapter 3), a more even spread of carbon source utilization is typical of a diversified community, rather than strict carbon utilization profiles which are indicative of a less diverse population (Button et al. 2016; Flynn et al. 2017).

Functional profiling of the coupon-associated and bulk phase microorganisms indicates that those exposed to added OP at a concentration of 2 mg/L produced more metabolically active and diverse biofilms, and are more likely to reform biomass as biofilm material in the event of sloughing (Figures 4.4 through 4.7). This can be attributed to added OP acting as a source of additional phosphorous (Correll 1999; Fang et al. 2009b; Del Olmo et al. 2020), increasing resistance to chloramine disinfectant, and potentially other selective pressures (Rosales et al. 2020). This is further supported when considering the higher viable cell counts, as shown in Figures 4.1 and 4.3, from both bulk phase microorganisms and coupon-associated communities exposed to added OP. As mentioned previously, microorganisms exposed to added OP appear to have advantages over those which were unexposed, such as increased biofilm reformation potential, (Figures 4.4 and 4.2), potentially mitigating the selective pressure of the chloramine

disinfectant. This offset in selective pressure allows for an increase in metabolic diversity, as well as an increase in the number of viable cells which are more metabolically active, and has been shown in research which focused on selective pressures, such as flow rate, on community structure in a DWDS (Douterelo et al. 2013; Zhu et al. 2020; Zhu et al. 2021). The communities not exposed to added OP have been shown to form less metabolically diverse and active profiles, most likely due to the selective pressure of chloramine, which has been exhibited in other literature (Zhu et al. 2021; Chen et al. 2022). These communities are more likely comprised of selected bacteria which can withstand higher concentrations of chloramine in the absence of additional environmental advantages, and, as such, are less numerous and diverse (Ling and Liu 2013; Waak et al. 2019). The lack of added OP to serve as a nutrient for growth may have limited the potential for replication and diversification for these environmentally-selected microorganisms, which has consequence of limiting potential diversity and activity (De la Fuente-Núñez et al. 2013; Zhu et al. 2020; Joshi et al. 2021).

Structural Profiling Using DGGE:

Structural profiling took place using DGGE as a means of assessing genetic shifts over the course of the experimental period. As described in Section 2.2, similarity was compared using hierarchical clustering analysis through GenCompare II, to generate an unweighted pair group method with arithmetic mean (UPGMA) dendrograms. These dendrograms are compared for each treatment over the sampling period, to visualize how the microbial genetic profiles shift, and provides insight into the structural variations as a result of OP presence and chloramine dose.

Overall similarity for coupon-associated communities exposed to the low concentration of chloramine in the presence of added OP, showed the lowest overall genetic similarity between

sampling dates, at 26.4% (Figure 4.8). The most genetically distinct cluster was from samples collected on days 63and 77, sharing 69.7% similarity on these days. Samples from coupon-associated communities at day 87indicate only 40.4% similarity to all other clusters, from other sampling dates. The highest genetic similarity for coupon-associated communities exposed to the low chloramine dose and added OP is shared between samples collected on days 101 and 108, at 98%. Earlier sampling dates (days 7, 21 and 35), share 64% similarity. Samples collected on days 35 and 49 share over 80% genetic similarity with the initial sampling event at day 7, and only 26% similarity to the samples collected at days 63and 77.

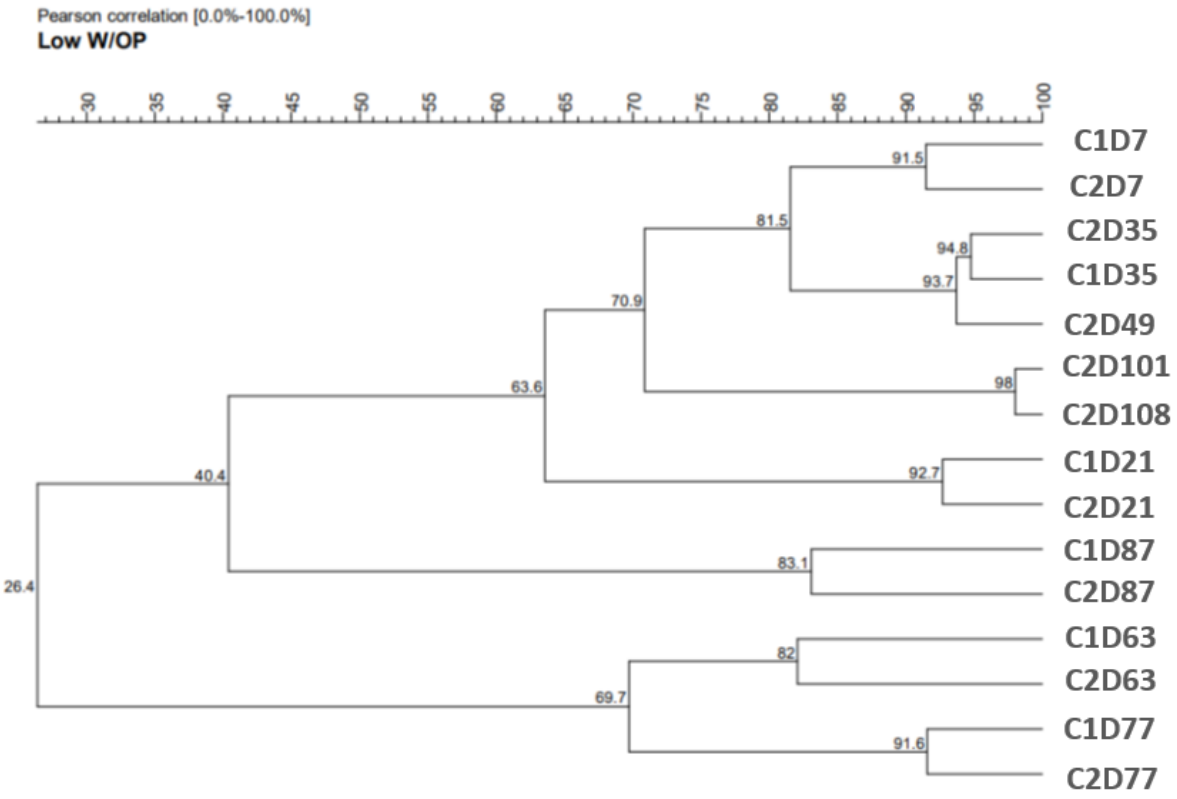

Figure 4.8: Hierarchical cluster analysis of banding patterns obtained from denaturing gradient gel electrophoresis (DGGE) of PCR amplified 16 rDNA extracted from coupon-associated biofilms after exposure to 2 mg/L of orthophosphate and low (2 mg/L) of chloramine, rendered graphically as an UPGMA dendrogram. C= Coupon replicate, D= Isolation day

A similar trend was observed for communities exposed to the higher chloramine dose with additional OP (Figure 4.9). Samples collected at days 63 and 77 showed these two dates share lowest similarity overall, at 46.3%, and have lowered levels of genetic similarity between observed replicate coupons as well. Comparative to communities shown in Figure 4.8, genetic similarity between the communities sampled on day 101 and 108 remains lower. Again, a similar trend to communities exposed to the low chloramine dose and added OP arises between samples within the first 49 days, whereby samples collected between days 7 and day 49 share a high overall similarity (84.7%). Interestingly, day 7 samples are more similar to day 35s and 49 (94%), rather than to day 21 (84.7%). Samples taken between days 87 and 108 show an overall high genetic similarity of 70%, including a 77% similarity for samples between days 87 and 101.

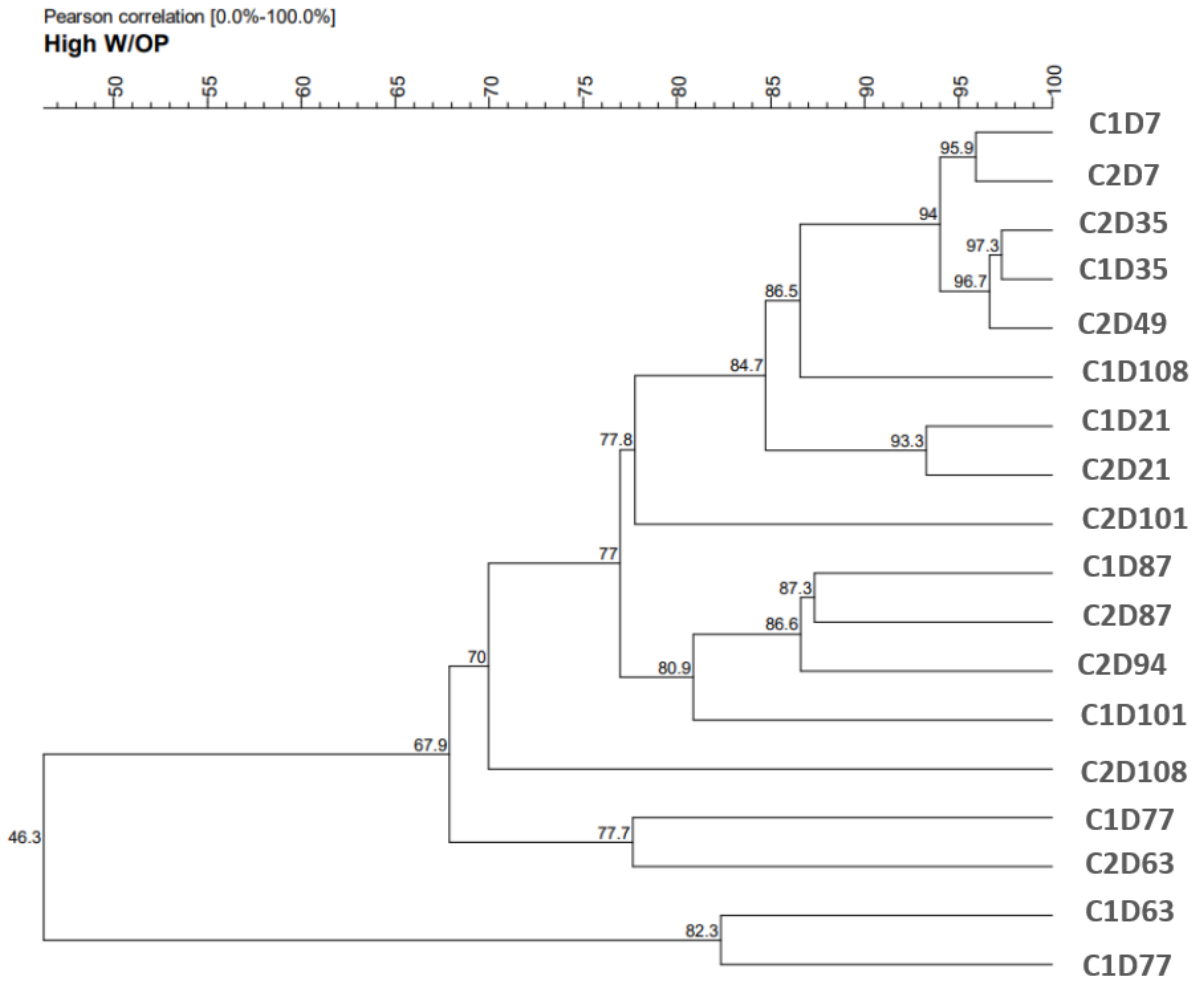

Figure 4.9: Hierarchical cluster analysis of banding patterns obtained from denaturing gradient gel electrophoresis (DGGE) of PCR amplified 16 rDNA extracted from coupon-associated biofilms after exposure to 2 mg/L of orthophosphate and high (3 mg/L) of chloramine, rendered graphically as an UPGMA dendrogram. C= Coupon replicate, D= Isolation day

As shown in Figure 4.10, genetic similarity for coupon-associated communities exposed to the lower chloramine dose, but no added OP remained higher than communities exposed to added OP (Figures 4.8 and 4.9), at 51.8%. Three distinct clusters can be seen, with communities sampled on later dates (days 101 and 108) exhibiting lowest overall genetic similarity (51.8%). When considering experimental replication, day 63 and day 77 share the lowest overall similarity between coupon replicates sampled. The medial cluster of this dendrogram indicates that genetic

similarity decreased slowly between day 7 and day 63, at which point a sharp decrease in similarity between coupon replicates is seen. Samples taken on day 87 and 94 then show an increased similarity to earlier dates, at almost 80%, with coupon replicates exhibiting an increase in genetic similarity.

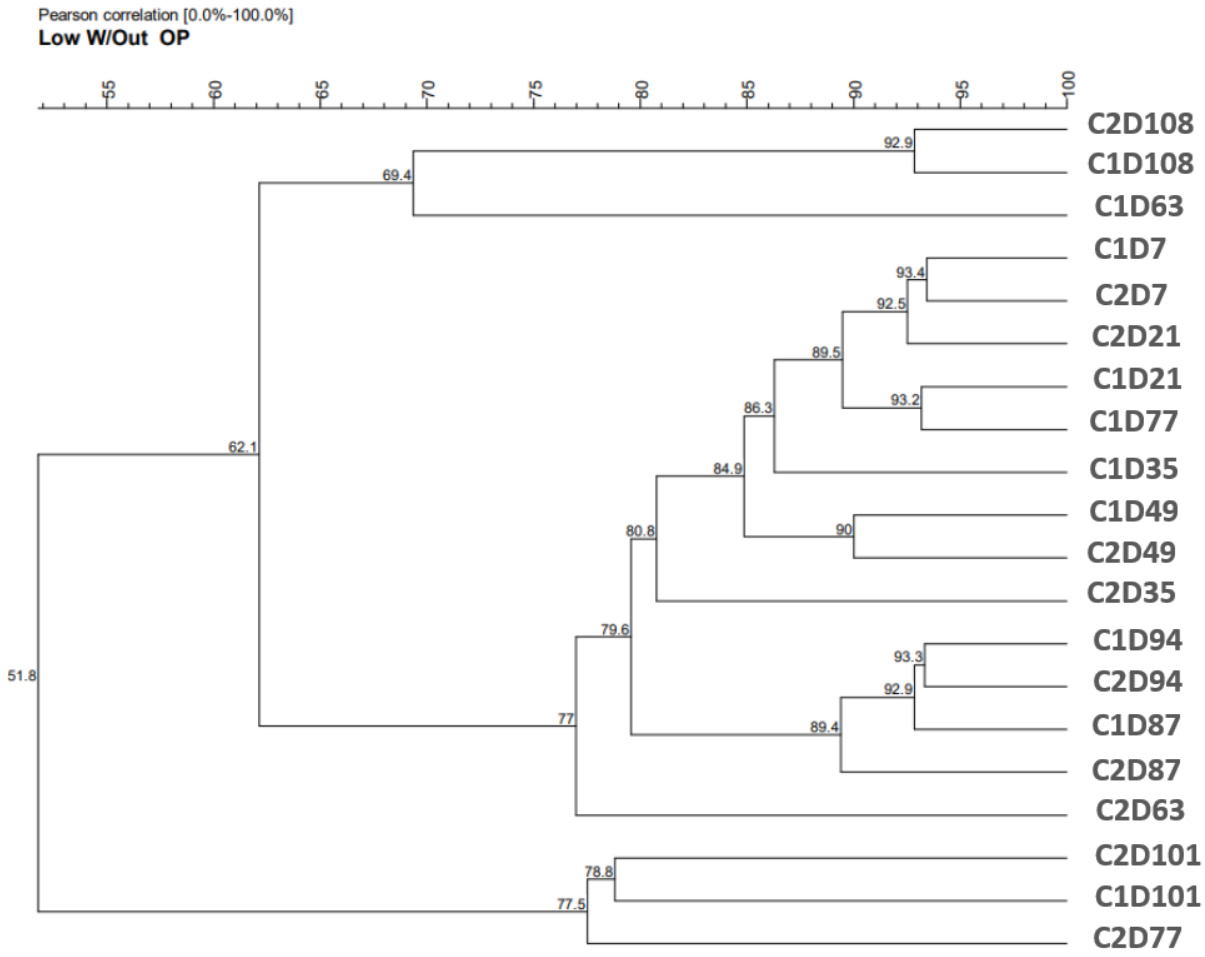

Figure 4.10: Hierarchical cluster analysis of banding patterns obtained from denaturing gradient gel electrophoresis (DGGE) of PCR amplified 16 rDNA extracted from coupon-associated biofilms after exposure to no additional orthophosphate and low (2 mg/L) of chloramine, rendered graphically as an UPGMA dendrogram. C= Coupon replicate, D= Isolation day

Lastly, coupon-associated communities exposed to the high concentration of chloramine, in the absence of OP, exhibited the highest overall genetic similarity, at 72.9% (Figure 4.11). This

similarity increased for all communities over time, excluding a sole coupon replicate for days 108 and 77, to 83.9% similarity overall. Distinct clusters become difficult to distinguish when similarity between dates is high, however it does show that structural similarity for samples taken on day 63, 87 and 94 is closer to that of the initial sampling, on day 7, compared to samples collected on days 21 and 35.

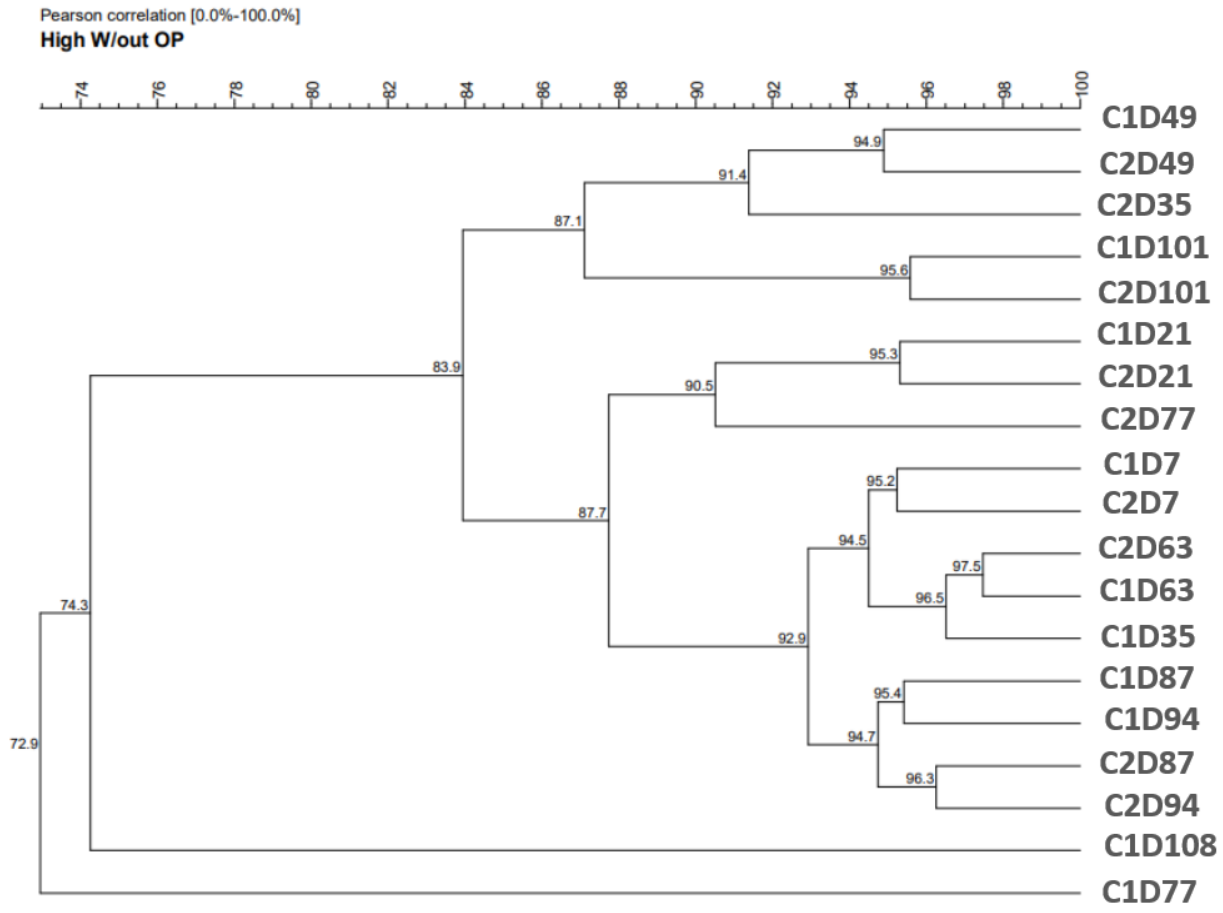

Figure 4.11: Hierarchical cluster analysis of banding patterns obtained from denaturing gradient gel electrophoresis (DGGE) of PCR amplified 16 rDNA extracted from coupon-associated biofilms after exposure to no additional orthophosphate and high (3 mg/L) of chloramine, rendered graphically as an UPGMA dendrogram. C= Coupon replicate, D= Isolation day

Genetic diversity over the sampling period increased in the presence of added OP, with coupon-associated communities exposed to the low chloramine dose having low genetic similarity

throughout the sampling period (Figures 4.8 and 4.9). This further demonstrates the potential for OP to increase overall community diversity. The increased similarity in structural profiles of coupon-associated communities exposed to chloramine in the absence of OP reinforces previous research, which shows that chloramine disinfectant can act as a selective pressure on the genetic diversity of communities (Gomez-Alvarez et al. 2016; Waak et al. 2019; Ng et al. 2021).

Coupon-associated communities exposed to the low chloramine concentration and added OP diversified structurally in a shorter time period of 63 days (Figure 4.8). It appears that the speed at which these coupon-associated communities diversify is a consequence of both OP addition and chloramine dose, as the development of diversification between sampling dates for the communities exposed to low chloramine and no added OP was similar to those exposed to high chloramine and OP (Figures 4.9 and 4.10). Similarity in community structure decreased for these communities over the 108 days, but was seen in both instances to increase sometime around day 63. It is possible that the increased chloramine dose was able to impose a selective pressure (Berry et al. 2006b; Waak et al. 2019), which overcame the advantage of added OP for these communities at this date. The selective pressure of the lower of the two chloramine doses seems to be comparable to that observed at the high dose in the presence of OP. It is likely that the environmental pressure is selective of a community with increased chloramine tolerance, however full genomic identification through sequencing, which is common in research of DWDS microbial communities (Douterelo et al. 2014), would allow for a full comprehension of the taxa present.

The communities unexposed to added OP, and exposed to the high chloramine concentration, exhibited the lowest overall diversity in structure. As OP has been shown to increase diversity of coupon-associated biofilms at concentrations of 2 mg/L (Chapter 3), the lower genetic similarity

in association with a lack of added OP was expected. It appears as if the selective pressure of high chloramine slows the genetic diversification of a community, when compared to those exposed to OP and low chloramine. This diversity impacts of this pressure may also be reversible in times of lowered chloramine presence, which has been exhibited in research focused on longer-term impacts of chloramination of a DWDS (Liu et al. 2012). The increase in overall similarity for these coupon-associated communities exposed to high chloramine and no added OP, when compared to those exposed to low chloramine (Figures 4.10 and 4.11, respectively), from 51.8% to 72.9%, further supports the concept of selective pressure on genetic diversity associated with an increasing chloramine dose in the absence of OP.

Comparison of Profiles:

The comparison of both functional and structural profiles allows for an in-depth analysis of monitored data. Since these profiles are not strictly independent, comparison between trends for both structural and functional data may help tease apart aspects of the complex interactions which may otherwise go unnoticed (Clairmont and Slawson 2020).

Profiles of communities exposed to lower chloramine and OP exhibited overall higher genetic diversity and metabolic diversity (Figures 4.6 and 4.7, and Figures 4.8 through 4.11). Although metabolic diversity of these communities was lower than those exposed to the high chloramine dose, they did reach a similar level of metabolic diversity after day 77. At day 63, where the low chloramine and OP-exposed coupon-associated communities experienced the lowest genetic similarity, metabolic profiles exhibited results suggestive of a shift towards a more diverse and active community as well (Figures 4.3 and 4.7). Metabolic diversity increased following this date, as did overall metabolic activity. These increases also coincide with a decrease in biofilm formation potential (Figures 4.2 and 4.4). The coupon-associated communities exposed to the

high level of chloramine exhibited similar trends between structural and functional profiles, of decreased genetic diversity, and similar carbon utilization profiles, compared to communities exposed to the low chloramine dose and added OP. One exception to this was the metabolic diversity, which was initially higher for coupon-associated communities exposed to the high chloramine concentration and added OP when compared to coupon-associated communities exposed to the high chloramine concentration and no added OP.

Bulk phase microorganisms and coupon-associated communities which were not exposed to added OP had less diverse and robust genetic and metabolic profiles throughout the sampling dates in comparison to those which were exposed to OP. This comes, most likely as a result in the lowered nutrient load in the systems, when compared to systems with added OP. Overall viable cell counts, biofilm formation potential, and metabolic activity were lower for OP-unexposed microorganisms throughout all sampling dates. Genetic diversity for OP unexposed coupon-associated communities increased at a later date when compared to those exposed to added OP (Figures 4.10 and 4.11). As seen in Figure 4.4, this may have also had implications on the biofilm formation potential (Goller and Romeo 2008; I. Douterelo et al. 2018). Unfortunately, bulk phase and coupon-associated communities exposed to no added OP did not surpass the positivity threshold for metabolism (Section 2.2), and as such, data which can be meaningfully analyzed is sparse.

One potential concern related to the increase in activity and diversity of microorganisms in a DWDS is the prevalence of nitrifying taxa (Keshvardoust et al. 2020). The metabolization of ammonia from chloramine residuals by nitrifying bacteria results in free chlorine, which, as previously mentioned (Section 1), is a less effective disinfectant residual against biofilm communities, as penetration into the interior levels of the biofilm is decreased (Ozekin et al.

1996; Zhang and Edwards 2009; Khiari 2016). Similar to that noted in the first experiment (Chapter 3), OP addition increased free ammonia in the systems (Appendix B1), as a consequence of increasing monochloramine decay (Appendix B2). This did not correlate with an increase in measured nitrites and nitrates (Appendix B3 and B4), when compared to data from the first experiment (Appendix A) (Chapter 3). A possible relationship between added OP and free ammonia can be seen, whereby ARs with added OP had higher measured levels of free ammonia. As pH was consistent between the AR systems, these increases of free ammonia are more likely microbially-driven, through liberation of ammonia from chloramine molecules. These results suggest that more robust and diverse microbial communities, such as those in this study exposed to added OP, to degrade chloramine disinfectant residuals (Zhang and Edwards 2009; Sawade et al. 2016).

4.3 Chapter Summary and Conclusions

The diverse nature of drinking water treatment requires the monitoring of parameters which are closely related and complex. The addition of OP as a corrosion inhibitor to finished water with two different chloramine doses was monitored to assess the impact on microbial communities present, which prior research has routinely debated (Miettinen et al. 1997; Fang et al. 2009a; Douterelo et al. 2016; Aghasadeghi et al. 2021). In conclusion, this portion of the research addressed the second and third objectives; to establish microbial response to the presence and absence of chloramine as a disinfectant through culture and molecular-based approaches, as well as compared and contrasted biofilm response to chloramine in the presence of orthophosphate by comparing community profiles. In doing so, we can provide insight into the complex microbial interactions at play and help strengthen our answer to the question of the impact of orthophosphate addition on microbial communities in a DWDS. This second experimental phase

investigated the impact of a high and low chloramine dose on the profiles of microorganisms present in a DWDS, in the presence and absence of OP as a corrosion inhibitor. Both bulk phase microorganisms and coupon-associated communities exposed to added OP exhibited higher viable cell counts, biofilm reformation potential, metabolic diversity and activity regardless of chloramine dose. Those which were not exposed to added OP routinely exhibited lower viable cell counts, biofilm reformation potential, and metabolic activity. A higher chloramine dose appeared to exhibit a stronger environmental pressure on these groups. Genetic diversity was dependent on both OP and chloramine dose, with coupon-associated communities exhibiting lower diversity in the presence of a higher chloramine dose and no added OP. This study supports current research which states that chloramine acts to select for microorganisms which can ultimately tolerate higher chloramine doses (Berry et al. 2006a; Isabel Douterelo et al. 2018; Chen et al. 2022) As well, this research shows that exposure to OP serves as a nutrient for growth and diversification of microorganisms in a DWDS (Fang et al. 2009b; Aghasadeghi et al. 2021).

Chapter 5: Long-Term Pipe Loop Study

5.1 Experimental Overview:

In December of 2019, an opportunity arose for microbiological sampling at the conclusion of a 68-week long pipe loop study, which had focused on the physico-chemical impacts of four corrosion inhibitors on lead release from lead service lines. Although microbiological data was not sampled during the operation of the system, this did allow for a breakdown comparison of established biofilm material on the pipe wall when exposed to different corrosion inhibitors over a period of 68 weeks.

Lead service lines, sacrificed during a replacement program from a municipality in Southern Ontario, served as the pipe material used for the study. Finished water, from another source as the water used in previous chapters and treated with chlorine disinfectant residual, was dosed with one of two sodium silicate corrosion inhibitors, A (SiO_2/Na_2O wt. ratio: 3.2:1) and B (SiO_2/Na_2O wt. ratio: 4.3:1) (National Silicates, Etobicoke, ON, Canada*), orthophosphate (OP) or had routine pH adjustments as a means of corrosion inhibition. The pipe segments exposed to pH adjustment reflect one control strategy for lead, and also acted as a means of comparison of the impact of silicates on lead release, versus the impacts of pH changes associated with silicate dosing (Aghasadeghi *et al.,* 2021). Over the course of 62 weeks, water amended with one corrosion inhibitor was pumped through segments of pipe material as described by Aghasadeghi *et al*. 2021. All treatments were studied using duplicate pipes, excluding sodium silicate B due to limitations of available pipe material. At the completion of the 62 week period, the final 3 inches of pipe material was swabbed using sterile cotton-tipped applicators which were pre-moistened

in 0.9% (w/v) sterile saline. These swabs were then placed in 100mL of the sterile saline solution and transported on ice to the laboratory. The glass bottles containing the saline solution and swabs were sonicated (Bransonic® Ultrasonic Cleaner, Model 5210) for 2 min at 47 kHz at 20°C (Gagnon and Slawson, 1999) and serial diluted to be plated in duplicate on R2A agar for enumeration of HPCs, as described by standard method 9215 (Rice *et al.,* 2012). Microbial community profiling (CLPP) was also performed on 3 pipe segments representing Silicate A-1, pH adjustment 2, OP 1, as described in Section 2.2.

5.2 Results and Discussion

The impact of the tested corrosion control materials on biofilm formation within the pipe loop system was assessed at the end of the experimental period during disassembly of the experimental apparatus. Based on HPC enumeration, loops dosed with silicate A supported the lowest microbial accumulation, as seen in Figure 5.1 with values of 3.28 and 3.02 log CFU/cm^2 for loop segments 1 and 2, respectively. In contrast, pipe loops dosed with orthophosphate supported the highest viable biomass (log CFU/cm^2 values, 4.54 and 4.66). The pipe loop system dosed with silicate B supported 3.96 log CFU/cm^2. Both silicate A and silicate B segments supported lower or equal amounts of biofilm accumulation when compared to that found in unamended control pH adjusted loops. Overall, orthophosphate-treated loops resulted in more than 0.5 log higher biological accumulation, when compared to those treated with silicates.

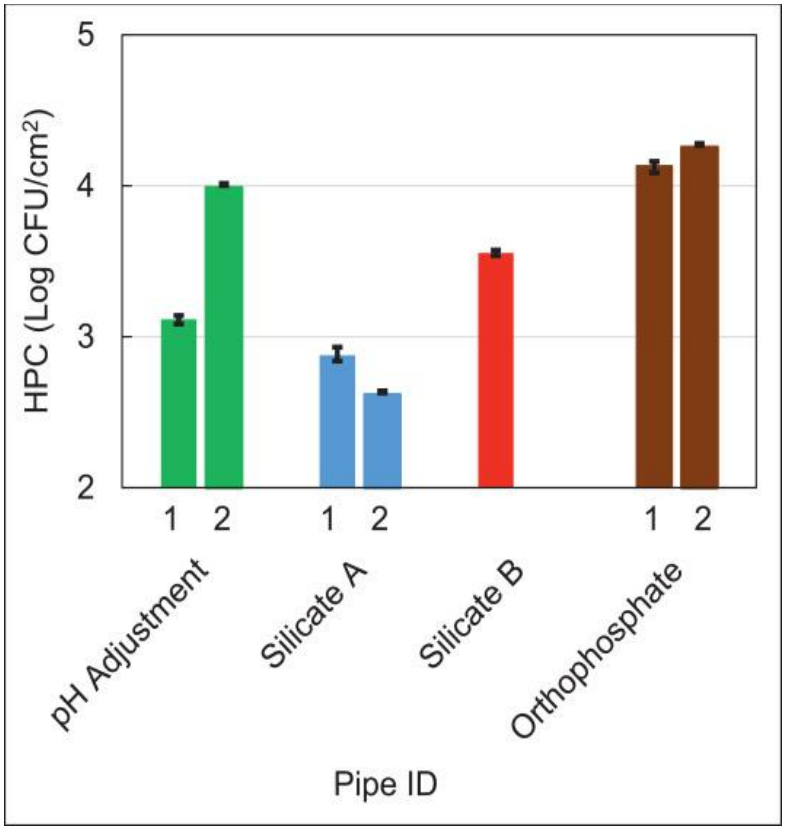

Figure 5.1: Heterotrophic plate counts (HPCs) of swabbed pipe segments, measured in Log CFU/cm^2. Silicate B was limited to one pipe segment replicate due to limitations in pipe availability. Samples were plated in duplicate on R2A agar. Error bars represent maximum and minimum values (n=2). Taken from Ahgasadeghi *et al*., 2021.

Shannon Diversity indices, as measured through EcoPlate™ readings at 72 hours, showed that microbial communities removed from the pipe segment exposed to OP had the lowest metabolic diversity, with an index of 2.61, when compared to those exposed to sodium silicate A and the routine pH adjustment (Figure 5.2). Pipe segment communities exposed to sodium silicate A exhibited the highest H', at 3.22, with an index only 0.07 higher than those exposed to the

control loop pH adjustment. The single pipe segment dosed with sodium silicate B was not assessed due to limitations of material.

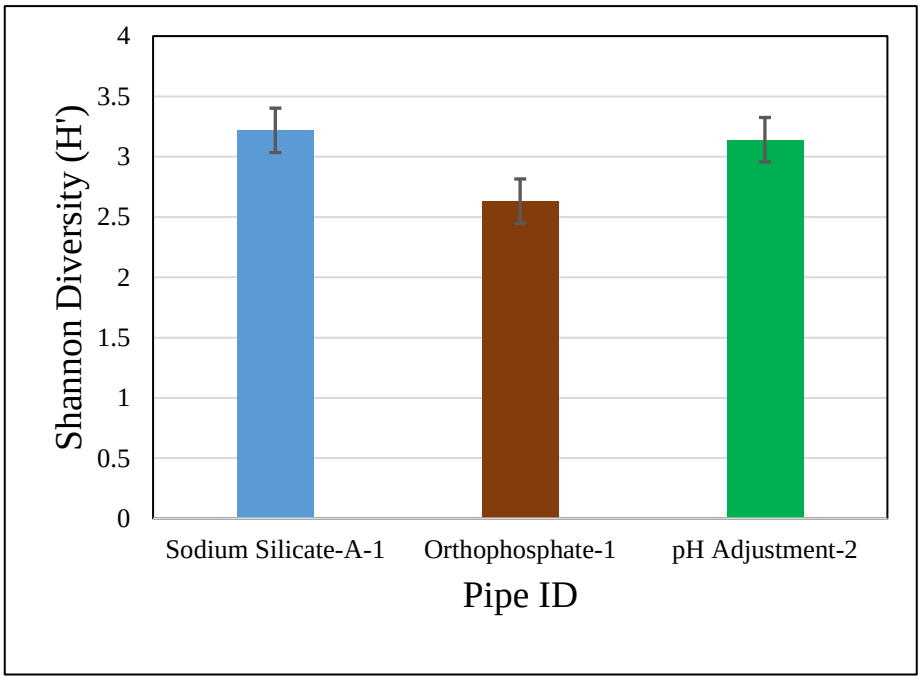

Figure 5.2: Metabolic diversity of communities from swabbed pipe segments, as measured by Shannon Diversity (H'). Higher H' scores represent an increased metabolic diversity. The sole pipe segment dosed with sodium silicate B was not assessed. Error bars represent standard error (n=3).

Carbon source utilization was assessed through the number of sole carbon sources which had been metabolized by the collected communities after 72-hours of incubation. This assessment differs from carbon guilding described in Section 2.2, counting the number of carbon sources which are utilized rather than categorizing them. Individual well absorbance readings which surpassed 0.250 at an OD of 595nm were counted as a positive source utilization (Section 2.2). Of the 31 possible carbon sources, communities exposed to routine pH adjustment were able to

metabolize 22 (Figure 5.3). In contrast, communities exposed to OP and sodium silicate A metabolized 13 and 6 carbon sources, respectively.

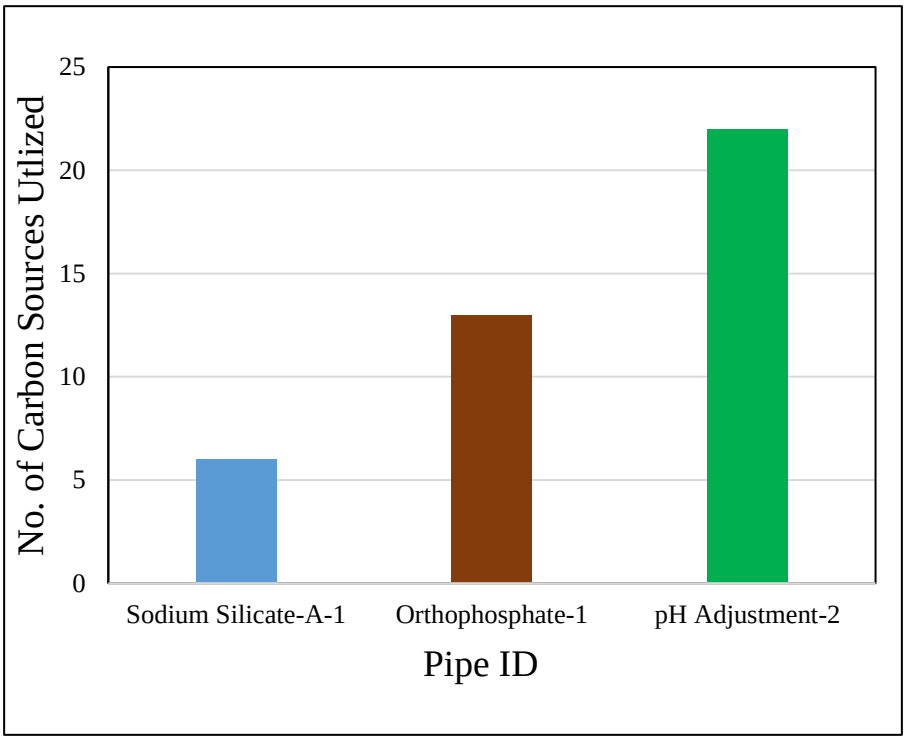

Figure 5.3: Carbon source utilization, as measured through carbon sources which were metabolized from BioLog Ecoplates. The threshold of utilization is an absorbance reading >0.250 @OD595 at 72 hours. The sole pipe segment dosed with sodium silicate B was not assessed. Error bars represent standard error.

The Shannon Diversity score of each biofilm community is reflective of the number of carbon sources utilized, and the degree to which they are utilized (Kela P. Weber and Legge 2010; Russo et al. 2012). As seen in Figures 5.2 and 5.3, the communities collected from pipe segments amended with sodium silicate A exhibited a high Shannon diversity, along with a low amount of carbon sources utilized. This indicates that the communities exposed to sodium silicate A metabolized the 6 carbon sources in similar abundance (Kela P. Weber and Legge 2010; Frąc et

al. 2012; Button et al. 2016). The lower H' seen from the collected communities of the orthophosphate-exposed pipe segment, and considering the 13 carbon sources utilized, indicates that although the overall carbon source utilization was higher than for sodium silicate A (Figure 5.1.2), the evenness to which these sources were utilized was much lower (Leflaive et al. 2008; Frąc et al. 2012). Although the utilization of all 13 carbon sources surpassed the threshold, H' indicates that a portion of the carbon sources were either metabolized at a much higher or lower ratio (Frąc et al. 2012; Russo et al. 2012). pH-adjusted communities exhibited the highest carbon source utilization, and when considered with H' (Figure 5.2), indicate that these communities have a more diverse metabolic profile than those exposed to OP or sodium silicate A. As the pipe segment chosen for metabolic profiling from pH adjustment exposures was the replicate with the highest viable cell count (Figure 5.1), the sampling of the primary pH adjustment pipe segment, which had lower viable cell count (Figure 5.1) may have had contrasting results, as this data is dependant on biomass from a single sampling event.

Biofilm accumulation on pipe walls, and the subsequent diversity of these communities, can be influenced by a number of factors including pipe material, water chemistry and flow conditions (Fish & Boxall, 2018)). In natural waters, growth of microbial organisms is largely determined by limiting nutrients such as phosphorus (Sathasivan & Ohgaki, 1999). There are a number of aspects to be considered in biofilm formation, including those which affect initial adherence to wall material (Lehtola et al. 2002). In this study, metabolic profiling and HPC values were examined in a single breakdown sampling event. HPC data are presented (Figure 5.1) which indicates that pipe loop segments exposed to the addition of phosphate resulted in higher viable CFUs. Those exposed to sodium silicate A, while having the highest overall metabolic diversity as measured through H' (Figure 5.2), had a much stricter carbon source utilization (Figure 5.3)

and lower HPCs. Although only one pipe segment from pH adjustment loops was assessed for metabolic diversity, communities from this loop were seen to have the highest overall carbon source utilization (Figure 5.3) and diversity higher than those exposed to OP (5.2).

Understanding the dynamics of biofilm formation from study onset would require more extensive sampling, but it is widely accepted that distribution system conditions are nutrient-limited (Berry & Raskin, 2006). The results of this study indicate that the addition of a previously limiting nutrient, such as phosphate, resulted in higher levels of viable accumulation, and metabolic carbon utilization. Sodium silicate materials, in contrast, contain no macronutrients required for microbial growth (Zhou et al. 2018). Recent studies have identified sodium silicate as having a possible antimicrobial effect in other systems and may play a role in microbial load reduction and carbon source utilization limits (Vattem et al. 2012). Further studies would need to be performed to fully assess whether the reduced viable cell loads and metabolic activity measured in silicate-impacted pipe loops were due to antimicrobial effects, or the lack of an additional nutrient in the form of phosphorus.

5.3 Chapter Summary and Conclusions:

Though this experiment was a one-time sampling of a pipe loop system, that took place during its deconstruction, it still provides insight to the long-term impact of multiple corrosion inhibitors on microbial communities adhered to pipe wall material. These long-term studies are important in fully comprehending the interactions between microbial communities, which may otherwise go unnoticed. In conclusion, this portion of the research helped answer the overarching question on the impact of orthophosphate as a corrosion inhibitor on microbial communities in a DWDS, from an extended point of view. Overall, pipe loops dosed with orthophosphate saw higher

viable cell counts attached to pipe material, comparative to pipe loops dosed with either sodium silicate species or pH adjusted pipes. However, the pipe loops which were treated with sodium silicate A as a means of a control exhibited the highest metabolic diversity, as measured through Shannon diversity, although only metabolizing 6 of the potential 31 carbon sources monitored. Pipe loops treated with pH adjustment harboured communities on pipe wall material which were able to metabolize 22 of the 31 available carbon sources. Literature suggests that sodium silicate-based compounds may exhibit an antimicrobial effect on communities (Vattem et al. 2012; Zhou et al. 2018), and although this research can not support these claims, it is shown that the use of sodium silicates as corrosion inhibitors do not support levels of microbial growth or metabolic activity seen from OP dosing. A long-term pipe loop study, similar to this, focused on microbiological monitoring approach, may uncover more information.

Chapter 6: Summary, Conclusions and Future Directions

6.1 Research Summary:

This research was designed to further our knowledge of microbial communities in a DWDS, specifically regarding the impact of common treatment practices. To this end we asked the question: How are the structural and functional profiles of microorganisms in a DWDS impacted by corrosion control measures, specifically the addition of orthophosphate (OP), at concentrations typically seen in a DWDS?

Coupon-associated communities from the first experiment exhibited shifts towards more diverse and active metabolic and genetic profiles, which were related to OP exposure. Increasing concentrations of OP above 1 mg/L allowed for these communities to replicate to higher viable cell counts, and reform biomass at an increased rate. Increases in metabolic activity and diversity were also driven by higher levels of OP, which were not observed to the same extent in communities exposed to lower OP doses. Genetic diversity was also seen to be influenced by OP concentration and increases in OP corresponded to an increased genetic diversity. Physico-chemical parameters indicated that monochloramine decay increased in relation to OP dose, which was confounded by the fact that pH decreased in relation to increases in OP addition, rather than microbial interactions..

The most notable difference in community profiles were seen during the middle of the experimental period, such as at day 56, where biofilm reformation potential decreased, and metabolic activity, along with genetic and metabolic diversity, increased. These are all potential indicators of a maturing biofilm community and were only seen in the microbial communities exposed to the higher OP doses. These shifts in both genetic and metabolic profiles, related to

OP exposure, indicate that profiles of microorganisms in a DWDS, when exposed to OP as a corrosion inhibitor at and above 2 mg/L, shift towards that of a more robust and diverse community.

The second major experiment was aimed at understanding microbial community response to disinfectant dose in the presence of added OP. We asked the question: How do chloramine disinfectant concentrations impact microbial profiles, in both the presence and absence of OP as a corrosion inhibitor?

Similar to observations made during the first experiment, community profile shifts were exhibited when exposed to added OP. Viable cell count, biomass reformation, and metabolic activity and diversity all increased in the presence of OP. Exposure to higher concentrations of chloramine disinfectant had minimal impacts on communities when in the presence of OP, potentially linking OP availability to an increased disinfectant resistance. Coupon-associated communities unexposed to additional OP exhibited less diverse metabolic and genetic profiles overall. However, the differences in profiles observed between the tested chloramine doses, reinforce theories that chloramine acts as a selective pressure in a DWDS. Interestingly, microbial communities exposed to high levels of chloramine and OP exhibited genetic profiles which more closely resembled those unexposed to OP than those exposed to a lower chloramine dose, further reinforcing this theory.

The termination of a lead service pipe loop experiment allowed for an interesting opportunity to examine biofilm communities exposed to different corrosion inhibitors. Although microbial sampling only took place at the end of the study during deconstruction, it still allowed for an examination of the impact of different corrosion inhibitors, such as sodium-silicate compounds, on microbial growth. Microbial samples swabbed from pipe walls exposed to OP had higher

viable cell counts and utilized more carbon sources than those swabbed from pipe material exposed to sodium silicates. Although the diversity of carbon source utilization was higher for communities exposed to sodium silicates, the reduced carbon utilization range and lowered cell counts provide another perspective on the impact of different corrosion inhibitors on microbial communities.

Overall conclusions of this research include that community profiles of microorganisms from a DWDS become more diverse, both genetically and metabolically, in the presence of OP as a corrosion inhibitor. These more diverse communities have been found to form greater biomass as both viable cells and biofilm material and, as a consequence of this increased robustness, are more resistant to chloramine as a disinfectant residual. Additionally, an increase in chloramine disinfectant dose acts to select for less genetically diverse communities, however, this selection is inhibited by OP addition.

6.2 Future Recommendations:

The presence of OP as a corrosion inhibitor was shown to impact the profiles of microbial communities in such a way that there is a possibility of negative impacts on treated water quality. This, however, comes from the assessment of a short-term study, when compared to the life and treatment regimens of a full-scale DWDSs. Longer-term studies, such as the investigation from Chapter 5 are typically more costly and require more initial preparation, but may be more applicable for a comparison to a DWDS treatment regime. AR designs allow for routine sampling of biofilm communities, yet their lifespan is limited by the number of coupons available for sampling. Investigating other aspects of treatment such as water retention time and

temperature variation, may be beneficial to more fully comprehend impacts on the profiles of microbial communities present. It may also be valuable to investigate the more significant community differences, such as those seen between communities exposed to 1 and 2 mg/L OP, in a long-term pipe loop study, with greater opportunity for microbial sampling. Pipe loop designs often make routine biofilm monitoring difficult, as deconstruction is required for the swabbing of inner pipe walls, however, their long-term focus is often more applicable to a DWDS. A long-term study, aimed at understanding the impacts of drinking water treatment discussed from this research, may ultimately bridge the gaps in knowledge on microbial communities in our drinking water distribution systems

Application of different corrosion inhibitors, such as silicate-based compounds, may be a step towards reducing dissolved lead with minimal impact on the microbial communities. This expansion away from OP could potentially mitigate microbially-mediated changes in finished water quality. As OP is a common corrosion inhibitor, the likelihood of a full-scale change of treatment regime is low. A more realistic option for municipalities is the lower amounts of OP which is added to treated water, potentially below current levels, which may reduce the amount of microbial activity, while still actively reducing amounts of dissolved lead.

Chapter 7: Integrative Nature of This Research

This research took place as the major component to a Masters degree in Integrative Biology. As the title suggests, the integration of multiple disciplines, faculties along with collaborative efforts is a focus intended to help students broaden their scope within the field of biology. Biology, by nature, is integrative, but this program is intended to encourage a further understanding of how this integration impacts and is impacted by our research. Biology clearly integrates key aspects of chemistry, physics, environmental sciences, maths and physiology to name a few. However, a reflection on exactly which disciplines have been involved in my specific research expanded on my initial understanding of the type of integration possible.

My committee included experienced researchers from a number of disciplines, including engineering, analytical chemistry, as well as micro and molecular biology, all who have integral individual backgrounds, ideas and solutions to problems. Through this diverse committee, I was able to understand how aspects of, water treatment engineering, analytical chemistry, genetics, applied microbiology, molecular biology and even history have impacted my research.

I would be remiss to not mention the extension of my research into communication with members of the water treatment industry. The inclusion of members of the water treatment industry, who may have little background in the field of biology, has only broadened my field of view when thinking about my research.

While this research is certainly no “latchkey” discovery, it does highlight the integral and complex nature of microbiology in an applied field.

*Disclaimer of Endorsement

Any reference obtained from this research to a specific commercial product, process, tradename or service does not constitute or imply an endorsement of the commercial product, process, tradename or service, or its producer or provider.

Chapter 8: References

Aggarwal S, Gomez-Smith CK, Jeon Y, Lapara TM, Waak MB, Hozalski RM. 2018. Effects of Chloramine and Coupon Material on Biofilm Abundance and Community Composition in Bench-Scale Simulated Water Distribution Systems and Comparison with Full-Scale Water Mains. Environ Sci Technol. doi:10.1021/acs.est.8b02607.

Aghasadeghi K, Peldszus S, Trueman BF, Mishrra A, Cooke MG, Slawson RM, Giammar DE, Gagnon GA, Huck PM. 2021. Pilot-scale comparison of sodium silicates, orthophosphate and pH adjustment to reduce lead release from lead service lines. Water Res. doi:10.1016/j.watres.2021.116955.

Akin EW, Hoff JC, Lippy EC. 1982. Waterborne outbreak control: which disinfectant? Environ Health Perspect. doi:10.2307/3429415.

Araya R, Tani K, Takagi T, Yamaguchi N, Nasu M. 2003. Bacterial activity and community composition in stream water and biofilm from an urban river determined by fluorescent in situ hybridization and DGGE analysis. FEMS Microbiol Ecol. doi:10.1016/S0168-6496(02)00394-X.

Ashbolt NJ. 2015. Microbial Contamination of Drinking Water and Human Health from Community Water Systems. Curr Environ Heal reports. doi:10.1007/s40572-014-0037-5.

AWWA. 2013. Nitrification Prevention and Control in Drinking Water. In: American Water Works Association.

Bååth E, Kritzberg E. 2015. pH tolerance in freshwater bacterioplankton: Trait variation of the community as measured by leucine incorporation. Appl Environ Microbiol. doi:10.1128/AEM.02236-15.

Banks MK, Bryers JD. 1991. Bacterial species dominance within a binary culture biofilm. Appl Environ Microbiol. doi:10.1128/aem.57.7.1974-1979.1991.

Bannister JW, Clairmont LK, Stevens KJ, Slawson RM. 2021. Exposure to elevated nutrient load results in structural and functional changes to microbial communities associated with riparian wetland plants Phalaris arundinaceae and Veronica anagallis-aquatica. Rhizosphere. doi:10.1016/j.rhisph.2021.100350.

Beitelshees M, Hill A, Jones CH, Pfeifer BA. 2018. Phenotypic variation during biofilm formation: Implications for anti-biofilm therapeutic design. Materials (Basel). doi:10.3390/ma11071086.

Berman T. 1988. Differential uptake of orthophosphate and organic phosphorus substrates by

bacteria and algae in Lake Kinneret. J Plankton Res. doi:10.1093/plankt/10.6.1239.

Berry D, Xi C, Raskin L. 2006a. Microbial ecology of drinking water distribution systems. Curr Opin Biotechnol. doi:10.1016/j.copbio.2006.05.007.

Berry D, Xi C, Raskin L. 2006b. Microbial ecology of drinking water distribution systems. Curr Opin Biotechnol. doi:10.1016/j.copbio.2006.05.007.

Bertelli C, Courtois S, Rosikiewicz M, Piriou P, Aeby S, Robert S, Loret JF, Greub G. 2018. Reduced chlorine in drinking water distribution systems impacts bacterial biodiversity in biofilms. Front Microbiol. doi:10.3389/fmicb.2018.02520.

Van Blerk GN, Leibach L, Mabunda A, Chapman A, Louw D. 2011. Rapid and specific detection of Salmonella in water samples using real-time PCR and High Resolution Melt (HRM) curve analysis. Water Sci Technol. doi:10.2166/wst.2011.838.

Boe-Hansen R, Albrechtsen HJ, Arvin E, Jørgensen C. 2002. Bulk water phase and biofilm growth in drinking water at low nutrient conditions. Water Res. doi:10.1016/S0043-1354(02)00191-4.

Boles BR, Thoendel M, Singh PK. 2004. Self-generated diversity produces “insurance effects” in biofilm communities. Proc Natl Acad Sci U S A. doi:10.1073/pnas.0407460101.

Brileya KA, Camilleri LB, Zane GM, Wall JD, Fields MW. 2014. Biofilm growth mode promotes maximum carrying capacity and community stability during product inhibition syntrophy. Front Microbiol. doi:10.3389/fmicb.2014.00693.

Button M, Weber K, Nivala J, Aubron T, Müller RA. 2016. Community-Level Physiological Profiling of Microbial Communities in Constructed Wetlands: Effects of Sample Preparation. Appl Biochem Biotechnol. doi:10.1007/s12010-015-1921-7.

CASIDA LE. 1960. Microbial oxidation and utilization of orthophosphite during growth. J Bacteriol.

Chan S, Pullerits K, Keucken A, Persson KM, Paul CJ, Rådström P. 2019. Bacterial release from pipe biofilm in a full-scale drinking water distribution system. npj Biofilms Microbiomes. doi:10.1038/s41522-019-0082-9.

Chandki R, Banthia P, Banthia R. 2011. Biofilms: A microbial home. In: Journal of Indian Society of Periodontology.

Chao Y, Mao Y, Wang Z, Zhang T. 2015. Diversity and functions of bacterial community in drinking water biofilms revealed by high-throughput sequencing. Sci Rep. doi:10.1038/srep10044.

Chen J, Li W, Tan Q, Sheng D, Li Y, Chen S, Zhou W. 2022. Effect of disinfectant exposure and starvation treatment on the detachment of simulated drinking water biofilms. Sci Total Environ. doi:10.1016/j.scitotenv.2021.150896.

Chiao TH, Clancy TM, Pinto A, Xi C, Raskin L. 2014. Differential resistance of drinking water bacterial populations to monochloramine disinfection. Environ Sci Technol. doi:10.1021/es4055725.

Clairmont LK, Slawson RM. 2020. Contrasting Water Quality Treatments Result in Structural and Functional Changes to Wetland Plant-Associated Microbial Communities in Lab-Scale Mesocosms. Microb Ecol. doi:10.1007/s00248-019-01389-5.

Correll DL. 1999. Phosphorus: A rate limiting nutrient in surface waters. Poult Sci. doi:10.1093/ps/78.5.674.

Cruz MC, Woo Y, Flemming HC, Wuertz S. 2020. Nitrifying niche differentiation in biofilms from full-scale chloraminated drinking water distribution system. Water Res. doi:10.1016/j.watres.2020.115738.

Deininger RA, Lee JY. 2001. Rapid Determination of Bacteria in Drinking Water Using an ATP Assay. F Anal Chem Technol. doi:10.1002/fact.1020.

Delahaye E, Welté B, Levi Y, Leblon G, Montiel A. 2003. An ATP-based method for monitoring the microbiological drinking water quality in a distribution network. Water Res. doi:10.1016/S0043-1354(03)00288-4.

Depetris A, Peter H, Bordoloi AD, Bernard H, Niayifar A, Kühl M, de Anna P, Battin TJ. 2021. Morphogenesis and oxygen dynamics in phototrophic biofilms growing across a gradient of hydraulic conditions. iScience. doi:10.1016/j.isci.2021.102067.

Douterelo Isabel, Calero-Preciado C, Soria-Carrasco V, Boxall JB. 2018. Whole metagenome sequencing of chlorinated drinking water distribution systems. Environ Sci Water Res Technol. doi:10.1039/c8ew00395e.

Douterelo I., Fish KE, Boxall JB. 2018. Succession of bacterial and fungal communities within biofilms of a chlorinated drinking water distribution system. Water Res. doi:10.1016/j.watres.2018.04.058.

Douterelo I, Husband S, Loza V, Boxall J. 2016. Dynamics of biofilm regrowth in drinking water distribution systems. Appl Environ Microbiol. doi:10.1128/AEM.00109-16.

Douterelo I, Jackson M, Solomon C, Boxall J. 2017. Spatial and temporal analogies in microbial communities in natural drinking water biofilms. Sci Total Environ. doi:10.1016/j.scitotenv.2016.12.118.

Douterelo I, Sharpe R, Boxall J. 2014. Bacterial community dynamics during the early stages of biofilm formation in a chlorinated experimental drinking water distribution system: Implications for drinking water discolouration. J Appl Microbiol. doi:10.1111/jam.12516.

Douterelo I, Sharpe RL, Boxall JB. 2013. Influence of hydraulic regimes on bacterial community structure and composition in an experimental drinking water distribution system. Water Res. doi:10.1016/j.watres.2012.09.053.

Douterelo I, Sharpe RL, Husband S, Fish KE, Boxall JB. 2019. Understanding microbial ecology to improve management of drinking water distribution systems. Wiley Interdiscip Rev Water. doi:10.1002/wat2.1325.

Drinking water distribution systems: Assessing and reducing risks. 2007.

Eichner CA, Erb RW, Timmis KN, Wagner-Döbler I. 1999. Thermal gradient gel electrophoresis

analysis of bioprotection from pollutant shocks in the activated sludge microbial community. Appl Environ Microbiol.

El-Chakhtoura J, Prest E, Saikaly P, van Loosdrecht M, Hammes F, Vrouwenvelder H. 2015. Dynamics of bacterial communities before and after distribution in a full-scale drinking water network. Water Res. doi:10.1016/j.watres.2015.02.015.

Elias S, Banin E. 2012. Multi-species biofilms: Living with friendly neighbors. FEMS Microbiol Rev. doi:10.1111/j.1574-6976.2012.00325.x.

Fang W, Hu JY, Ong SL. 2009a. Influence of phosphorus on biofilm formation in model drinking water distribution systems. J Appl Microbiol. doi:10.1111/j.1365-2672.2008.04099.x.

Fang W, Hu JY, Ong SL. 2009b. Influence of phosphorus on biofilm formation in model drinking water distribution systems. J Appl Microbiol. doi:10.1111/j.1365-2672.2008.04099.x.

Farkas A, Dragan-Bularda M, Muntean V, Ciataras D, Tigan S. 2012. Microbial activity in drinking water-associated biofilms. Cent Eur J Biol. doi:10.2478/s11535-013-0126-0.

Faust MA, Correll DL. 1976. Comparison of bacterial and algal utilization of orthophosphate in an estuarine environment. Mar Biol. doi:10.1007/BF00390757.

Fehér PP, Purgel M, Lengyel A, Stirling A, Fábián I. 2019. The mechanism of monochloramine disproportionation under acidic conditions. Dalt Trans. doi:10.1039/c9dt03789f.

Fish K, Osborn AM, Boxall JB. 2017. Biofilm structures (EPS and bacterial communities) in drinking water distribution systems are conditioned by hydraulics and influence discolouration. Sci Total Environ. doi:10.1016/j.scitotenv.2017.03.176.

Fish KE, Boxall JB. 2018. Biofilm microbiome (re)growth dynamics in drinking water distribution systems are impacted by chlorine concentration. Front Microbiol. doi:10.3389/fmicb.2018.02519.

Fish KE, Osborn AM, Boxall J. 2016. Characterising and understanding the impact of microbial biofilms and the extracellular polymeric substance (EPS) matrix in drinking water distribution systems. Environ Sci Water Res Technol. doi:10.1039/c6ew00039h.

Fish KE, Reeves-McLaren N, Husband S, Boxall J. 2020. Unchartered waters: the unintended impacts of residual chlorine on water quality and biofilms. npj Biofilms Microbiomes. doi:10.1038/s41522-020-00144-w.

Flemming HC, Percival SL, Walker JT. 2002. Contamination potential of biofilms in water distribution systems. In: Water Science and Technology: Water Supply.

Flynn TM, Koval JC, Greenwald SM, Owens SM, Kemner KM, Antonopoulos DA. 2017. Parallelized, Aerobic, single carbon-source enrichments from different natural environments contain divergent microbial communities. Front Microbiol. doi:10.3389/fmicb.2017.02321.

Frąc M, Oszust K, Lipiec J. 2012. Community level physiological profiles (CLPP), characterization and microbial activity of soil amended with dairy sewage sludge. Sensors. doi:10.3390/s120303253.

Gagnon GA, Slawson RM. 1999. An efficient biofilm removal method for bacterial cells

exposed to drinking water. J Microbiol Methods. doi:10.1016/S0167-7012(98)00089-X.

Garland JL, Mills AL. 1991. Classification and characterization of heterotrophic microbial communities on the basis of patterns of community-level sole-carbon-source utilization. Appl Environ Microbiol. doi:10.1128/aem.57.8.2351-2359.1991.

Goller CC, Romeo T. 2008. Environmental influences on biofilm development. Curr Top Microbiol Immunol. doi:10.1007/978-3-540-75418-3_3.

Gomes IB, Simões M, Simões LC. 2014. An overview on the reactors to study drinking water biofilms. Water Res. doi:10.1016/j.watres.2014.05.039.

Gomez-Alvarez V, Pfaller S, Pressman JG, Wahman DG, Revetta RP. 2016. Resilience of microbial communities in a simulated drinking water distribution system subjected to disturbances: Role of conditionally rare taxa and potential implications for antibiotic-resistant bacteria. Environ Sci Water Res Technol. doi:10.1039/c6ew00053c.

Gomez-Alvarez V, Revetta RP. 2020. Monitoring of Nitrification in Chloraminated Drinking Water Distribution Systems With Microbiome Bioindicators Using Supervised Machine Learning. Front Microbiol. doi:10.3389/fmicb.2020.571009.

Green SJ, Leigh MB, Neufeld JD. 2010. Denaturing Gradient Gel Electrophoresis (DGGE) for Microbial Community Analysis. In: Handbook of Hydrocarbon and Lipid Microbiology.

He H, Cooper JN, Mishra A, Raskin DM. 2012. Stringent response regulation of biofilm formation in vibrio cholerae. J Bacteriol. doi:10.1128/JB.00014-12.

Health Canada. 2012. Guidelines for Canadian Drinking Water Quality Summary Table Prepared by the Federal-Provincial-Territorial Committee on Drinking Water of the Federal-Provincial-Territorial Committee on Health and the Environment March 2006. Environments.

Honsa ES, Cooper VS, Mhaissen MN, Frank M, Shaker J, Iverson A, Rubnitz J, Hayden RT, Lee RE, Rock CO, et al. 2017. Rela mutant enterococcus faecium with multiantibiotic tolerance arising in an immunocompromised host. MBio. doi:10.1128/mBio.02124-16.

How ZT, Linge KL, Busetti F, Joll CA. 2016. Organic chloramines in drinking water: An assessment of formation, stability, reactivity and risk. Water Res. doi:10.1016/j.watres.2016.02.006.

Huang J, Hu B, Qi K, Chen W, Pang X, Bao W, Tian G. 2016. Effects of phosphorus addition on soil microbial biomass and community composition in a subalpine spruce plantation. Eur J Soil Biol. doi:10.1016/j.ejsobi.2015.12.007.

Hwang C, Ling F, Andersen GL, LeChevallier MW, Liu WT. 2012a. Microbial community dynamics of an urban drinking water distribution system subjected to phases of chloramination and chlorination treatments. Appl Environ Microbiol. doi:10.1128/AEM.01892-12.

Hwang C, Ling F, Andersen GL, LeChevallier MW, Liu WT. 2012b. Microbial community dynamics of an urban drinking water distribution system subjected to phases of chloramination and chlorination treatments. Appl Environ Microbiol. doi:10.1128/AEM.01892-12.

Jang HJ, Choi YJ, Ro HM, Ka JO. 2012. Effects of phosphate addition on biofilm bacterial

communities and water quality in annular reactors equipped with stainless steel and ductile cast iron pipes. J Microbiol. doi:10.1007/s12275-012-1040-x.

Jansson M. 1988. Phosphate uptake and utilization by bacteria and algae. Hydrobiologia. doi:10.1007/BF00024904.

Javier L, Pulido-Beltran L, Kruithof J, Vrouwenvelder JS, Farhat NM. 2021. Phosphorus concentration in water affects the biofilm community and the produced amount of extracellular polymeric substances in reverse osmosis membrane systems. Membranes (Basel). doi:10.3390/membranes11120928.

Jin Q, Kirk MF. 2018. pH as a primary control in environmental microbiology: 1. thermodynamic perspective. Front Environ Sci. doi:10.3389/fenvs.2018.00021.

Joshi RV, Gunawan C, Mann R. 2021. We Are One: Multispecies Metabolism of a Biofilm Consortium and Their Treatment Strategies. Front Microbiol. doi:10.3389/fmicb.2021.635432.

Kaplan JB. 2010. Biofilm Dispersal: Mechanisms, Clinical Implications, and Potential Therapeutic Uses. J Dent Res. doi:10.1177/0022034509359403.

Kelly JJ, Minalt N, Culotti A, Pryor M, Packman A. 2014. Temporal variations in the abundance and composition of biofilm communities colonizing drinking water distribution pipes. PLoS One. doi:10.1371/journal.pone.0098542.

Keshvardoust P, Huron VAA, Clemson M, Barraud N, Rice SA. 2020. Nitrite production by ammonia-oxidizing bacteria mediates chloramine decay and resistance in a mixed-species community. Microb Biotechnol. doi:10.1111/1751-7915.13628.

Khiari D. 2016. The role and behavior of chloramines in drinking water. Water Res Found.

Kjelleberg S, Albertson N, Flärdh K, Holmquist L, Jouper-Jaan Å, Marouga R, Östling J, Svenblad B, Weichart D. 1993. How do non-differentiating bacteria adapt to starvation? Antonie Van Leeuwenhoek. doi:10.1007/BF00871228.

Kolter R, Siegele DA, Tormo A. 1993. The stationary phase of the bacterial life cycle. Annu Rev Microbiol. doi:10.1146/annurev.mi.47.100193.004231.

Konstantinidis KT, Tiedje JM. 2004. Trends between gene content and genome size in prokaryotic species with larger genomes. Proc Natl Acad Sci U S A. doi:10.1073/pnas.0308653100.

Kragh KN, Alhede M, Kvich L, Bjarnsholt T. 2019. Into the well—A close look at the complex structures of a microtiter biofilm and the crystal violet assay. Biofilm. doi:10.1016/j.bioflm.2019.100006.

Kwon S, Moon E, Kim TS, Hong S, Park HD. 2011. Pyrosequencing demonstrated complex microbial communities in a membrane filtration system for a drinking water treatment plant. Microbes Environ. doi:10.1264/jsme2.ME10205.

De la Fuente-Núñez C, Reffuveille F, Fernández L, Hancock REW. 2013. Bacterial biofilm development as a multicellular adaptation: Antibiotic resistance and new therapeutic strategies. Curr Opin Microbiol. doi:10.1016/j.mib.2013.06.013.

LeChevallier MW, Schulz W, Lee RG. 1991. Bacterial nutrients in drinking water. Appl Environ Microbiol. doi:10.1128/aem.57.3.857-862.1991.

LeChevallier MW, Seidler RJ, Evans TM. 1980. Enumeration and characterization of standard plate count bacteria in chlorinated and raw water supplies. Appl Environ Microbiol.

Lee WH, Pressman JG, Wahman DG. 2018. Three-Dimensional Free Chlorine and Monochloramine Biofilm Penetration: Correlating Penetration with Biofilm Activity and Viability. Environ Sci Technol. doi:10.1021/acs.est.7b05215.

Leflaive J, Danger M, Lacroix G, Lyautey E, Oumarou C, Ten-Hage L. 2008. Nutrient effects on the genetic and functional diversity of aquatic bacterial communities. FEMS Microbiol Ecol. doi:10.1111/j.1574-6941.2008.00593.x.

Lehtola MJ, Laxander M, Miettinen IT, Hirvonen A, Vartiainen T, Martikainen PJ. 2006. The effects of changing water flow velocity on the formation of biofilms and water quality in pilot distribution system consisting of copper or polyethylene pipes. Water Res. doi:10.1016/j.watres.2006.04.010.

Levy K, Woster AP, Goldstein RS, Carlton EJ. 2016. Untangling the Impacts of Climate Change on Waterborne Diseases: A Systematic Review of Relationships between Diarrheal Diseases and Temperature, Rainfall, Flooding, and Drought. Environ Sci Technol. doi:10.1021/acs.est.5b06186.

Li J, Nedwell DB, Beddow J, Dumbrell AJ, McKew BA, Thorpe EL, Whitby C. 2015. amoA gene abundances and nitrification potential rates suggest that benthic ammonia-oxidizing bacteria and not archaea dominate N cycling in the Colne estuary, United Kingdom. Appl Environ Microbiol. doi:10.1128/AEM.02654-14.

Li L, Jeon Y, Lee SH, Ryu H, Santo Domingo JW, Seo Y. 2019. Dynamics of the physiochemical and community structures of biofilms under the influence of algal organic matter and humic substances. Water Res. doi:10.1016/j.watres.2019.04.014.

Li N, Ren NQ, Wang XH, Kang H. 2010. Effect of temperature on intracellular phosphorus absorption and extra-cellular phosphorus removal in EBPR process. Bioresour Technol. doi:10.1016/j.biortech.2010.03.008.

Li P, Wu J. 2019. Drinking Water Quality and Public Health. Expo Heal. doi:10.1007/s12403-019-00299-8.

Li Q, Yu S, Li L, Liu G, Gu Z, Liu M, Liu Z, Ye Y, Xia Q, Ren L. 2017. Microbial communities shaped by treatment processes in a drinking water treatment plant and their contribution and threat to drinking water safety. Front Microbiol. doi:10.3389/fmicb.2017.02465.

Li X, Upadhyaya G, Yuen W, Brown J, Morgenroth E, Raskin L. 2010. Changes in the structure and function of microbial communities in drinking water treatment bioreactors upon addition of phosphorus. Appl Environ Microbiol. doi:10.1128/AEM.01232-10.

Li Y, Kim KS, Deschamps J, Briandet R, Trubuil A. 2015. Spatio-temporal Interaction of Bacteria Mixture within Biofilms. Procedia Environ Sci. doi:10.1016/j.proenv.2015.05.009.

Liao X, Chen C, Wang Z, Chang CH, Zhang X, Xie S. 2015. Bacterial community change

through drinking water treatment processes. Int J Environ Sci Technol. doi:10.1007/s13762-014-0540-0.

Ling F, Liu WT. 2013. Impact of chloramination on the development of laboratory-grown biofilms fed with filter-pretreated groundwater. Microbes Environ. doi:10.1264/jsme2.ME12095.

Liu G, Verberk JQJC, Van Dijk JC. 2013a. Bacteriology of drinking water distribution systems: An integral and multidimensional review. Appl Microbiol Biotechnol. doi:10.1007/s00253-013-5217-y.

Liu G, Verberk JQJC, Van Dijk JC. 2013b. Bacteriology of drinking water distribution systems: An integral and multidimensional review. Appl Microbiol Biotechnol. doi:10.1007/s00253-013-5217-y.

Liu R, Yu Z, Zhang H, Yang M, Shi B, Liu X. 2012. Diversity of bacteria and mycobacteria in biofilms of two urban drinking water distribution systems. Can J Microbiol. doi:10.1139/W11-129.

Liu S, Jiang Z, Deng Y, Wu Y, Zhang J, Zhao C, Huang D, Huang X, Trevathan-Tackett SM. 2018. Effects of nutrient loading on sediment bacterial and pathogen communities within seagrass meadows. Microbiologyopen. doi:10.1002/mbo3.600.

Lührig K, Canbäck B, Paul CJ, Johansson T, Persson KM, Rådström P. 2015. Bacterial community analysis of drinking water biofilms in southern Sweden. Microbes Environ. doi:10.1264/jsme2.ME14123.

Manuel CM, Nunes OC, Melo LF. 2007. Dynamics of drinking water biofilm in flow/non-flow conditions. Water Res. doi:10.1016/j.watres.2006.11.007.

Marois-Fise JT, Carabin A, Lavoie A, Dorea CC. 2013. Effects of temperature and pH on reduction of bacteria in a pointof- use drinking water treatment product for emergency relief. Appl Environ Microbiol. doi:10.1128/AEM.03696-12.

Martiny AC, Jørgensen TM, Albrechtsen HJ, Arvin E, Molin S. 2003. Long-Term Succession of Structure and Diversity of a Biofilm Formed in a Model Drinking Water Distribution System. Appl Environ Microbiol. doi:10.1128/AEM.69.11.6899-6907.2003.

Merritt JH. 2015. Growing and analyzing static biofilms supplemental. Curr Protoc Microbiol.

Miettinen IT, Vartiainen T, Martikainen PJ. 1997. Phosphorus and bacterial growth in drinking water. Appl Environ Microbiol.

Mirjam Blokker EJ, Van Der Wielen PWJJ. 2018. Modelling steady-state biofilm in a drinking water distribution system. In: 1st International WDSA / CCWI 2018 Joint Conference.

Mohammed HA, Ismail SF. 2021. Design and implementation of remotely monitoring system for pH level in Baghdad drinking water networks. Telkomnika (Telecommunication Comput Electron Control. doi:10.12928/TELKOMNIKA.v19i3.12921.

Mouchet MA, Bouvier C, Bouvier T, Troussellier M, Escalas A, Mouillot D. 2012. Genetic difference but functional similarity among fish gut bacterial communities through molecular and biochemical fingerprints. FEMS Microbiol Ecol. doi:10.1111/j.1574-6941.2011.01241.x.

Muhammad MH, Idris AL, Fan X, Guo Y, Yu Y, Jin X, Qiu J, Guan X, Huang T. 2020. Beyond Risk: Bacterial Biofilms and Their Regulating Approaches. Front Microbiol. doi:10.3389/fmicb.2020.00928.

Muyzer G. 1999. DGGE/TGGE a method for identifying genes from natural ecosystems. Curr Opin Microbiol. doi:10.1016/S1369-5274(99)80055-1.

Muyzer G, De Waal EC, Uitterlinden AG. 1993. Profiling of complex microbial populations by denaturing gradient gel electrophoresis analysis of polymerase chain reaction-amplified genes coding for 16S rRNA. Appl Environ Microbiol. doi:10.1128/aem.59.3.695-700.1993.

Németh A, Szirányi B, Krett G, Janurik E, Kosáros T, Pekár F, Márialigeti K, Borsodi AK. 2014. Prokaryotic phylogenetic diversity of Hungarian deep subsurface geothermal well waters. Acta Microbiol Immunol Hung. doi:10.1556/AMicr.61.2014.3.9.

Ng WJ, Tan CT, Bae S. 2021. Effects of monochloramine on culturability, viability and persistence of Pseudomonas putida and tap water mixed bacterial community. Appl Microbiol Biotechnol. doi:10.1007/s00253-021-11251-9.

Nguyen D, Joshi-Datar A, Lepine F, Bauerle E, Olakanmi O, Beer K, McKay G, Siehnel R, Schafhauser J, Wang Y, et al. 2011. Active starvation responses mediate antibiotic tolerance in biofilms and nutrient-limited bacteria. Science (80-). doi:10.1126/science.1211037.

Nriagu JO. 1972. Lead Orthophosphates. L Solubility and Hydrolysis of Secondary Lead Orthophosphate. Inorg Chem. doi:10.1021/ic50116a041.

O'Toole GA. 2010. Microtiter dish Biofilm formation assay. J Vis Exp. doi:10.3791/2437.

Ollos PJ, Slawson RM, Huck PM. 1998. Bench scale investigations of bacterial regrowth in drinking water distribution systems. In: Water Science and Technology.

Del Olmo G, Ahmad A, Jensen H, Karunakaran E, Rosales E, Calero Preciado C, Gaskin P, Douterelo I. 2020. Influence of phosphate dosing on biofilms development on lead in chlorinated drinking water bioreactors. npj Biofilms Microbiomes. doi:10.1038/s41522-020-00152-w.

Oszust K, Frac M, Gryta A, Bilińska N. 2014. The influence of ecological and conventional plant production systems on soil microbial quality under hops (Humulus lupulus). Int J Mol Sci. doi:10.3390/ijms15069907.

Ozekin K, Valentine RL, Vikesland PJ. 1996. Modeling the Decomposition of Disinfecting Residuals of Chloramine. ACS Symp Ser. doi:10.1021/bk-1996-0649.ch008.

Park SK, Kim YK, Choi SC. 2008. Response of microbial growth to orthophosphate and organic carbon influx in copper and plastic based plumbing water systems. Chemosphere. doi:10.1016/j.chemosphere.2008.04.006.

Pasteur L. 2000. The History of Drinking Water Treatment. Public Health.

Pisithkul T, Schroeder JW, Trujillo EA, Yeesin P, Stevenson DM, Chaiamarit T, Coon JJ, Wang JD, Amador-Noguez D. 2019. Metabolic remodeling during biofilm development of bacillus subtilis. MBio. doi:10.1128/mBio.00623-19.

Potgieter S, Pinto A, Sigudu M, du Preez H, Ncube E, Venter S. 2018. Long-term spatial and

temporal microbial community dynamics in a large-scale drinking water distribution system with multiple disinfectant regimes. Water Res. doi:10.1016/j.watres.2018.03.077.

Prest Emmanuelle I., Hammes F, van Loosdrecht MCM, Vrouwenvelder JS. 2016. Biological stability of drinking water: Controlling factors, methods, and challenges. Front Microbiol. doi:10.3389/fmicb.2016.00045.

Prest E. I., Weissbrodt DG, Hammes F, Van Loosdrecht MCM, Vrouwenvelder JS. 2016. Long-term bacterial dynamics in a full-scale drinking water distribution system. PLoS One. doi:10.1371/journal.pone.0164445.

Reuben RC, Roy PC, Sarkar SL, Ha S Do, Jahid IK. 2019. Multispecies interactions in biofilms and implications to safety of drinking water distribution system. Microbiol Biotechnol Lett. doi:10.4014/mbl.1907.07007.

Revetta RP, Gomez-Alvarez V, Gerke TL, Curioso C, Santo Domingo JW, Ashbolt NJ. 2013. Establishment and early succession of bacterial communities in monochloramine-treated drinking water biofilms. FEMS Microbiol Ecol. doi:10.1111/1574-6941.12170.

Rickard AH, McBain AJ, Stead AT, Gilbert P. 2004. Shear rate moderates community diversity in freshwater biofilms. Appl Environ Microbiol. doi:10.1128/AEM.70.12.7426-7435.2004.

Rooney LM, Amos WB, Hoskisson PA, McConnell G. 2020. Intra-colony channels in E. coli function as a nutrient uptake system. ISME J. doi:10.1038/s41396-020-0700-9.

Rosales E, Del Olmo G, Calero Preciado C, Douterelo I. 2020. Phosphate Dosing in Drinking Water Distribution Systems Promotes Changes in Biofilm Structure and Functional Genetic Diversity. Front Microbiol. doi:10.3389/fmicb.2020.599091.

Rose J, Grimes J. 2001. Reevaluation of Microbial Water Quality : Powerful New Tools for Detection and Risk Assessment.

Rusin PA, Rose JB, Gerba CP. 1997. Health significance of pigmented bacteria in drinking water. In: Water Science and Technology.

Russo SE, Legge R, Weber KA, Brodie EL, Goldfarb KC, Benson AK, Tan S. 2012. Bacterial community structure of contrasting soils underlying Bornean rain forests: Inferences from microarray and next-generation sequencing methods. Soil Biol Biochem. doi:10.1016/j.soilbio.2012.05.021.

Sakcham B, Kumar A, Cao B. 2019. Extracellular DNA in Monochloraminated Drinking Water and Its Influence on DNA-Based Profiling of a Microbial Community. Environ Sci Technol Lett. doi:10.1021/acs.estlett.9b00185.

Salgar-Chaparro SJ, Lepkova K, Pojtanabuntoeng T, Darwin A, Machuca LL. 2020. Nutrient level determines biofilm characteristics and subsequent impact on microbial corrosion and biocide effectiveness. Appl Environ Microbiol. doi:10.1128/AEM.02885-19.

Salzer A, Keinhörster D, Kästle C, Kästle B, Wolz C. 2020. Small Alarmone Synthetases RelP and RelQ of Staphylococcus aureus Are Involved in Biofilm Formation and Maintenance Under Cell Wall Stress Conditions. Front Microbiol. doi:10.3389/fmicb.2020.575882.

Sawade E, Monis P, Cook D, Drikas M. 2016. Is nitrification the only cause of microbiologically induced chloramine decay? Water Res. doi:10.1016/j.watres.2015.11.016.

Schleich C, Chan S, Pullerits K, Besmer MD, Paul CJ, Rådström P, Keucken A. 2019. Mapping dynamics of bacterial communities in a full-scale drinking water distribution system using flow cytometry. Water (Switzerland). doi:10.3390/w11102137.

Schmeisser C, Stöckigt C, Raasch C, Wingender J, Timmis KN, Wenderoth DF, Flemming HC, Liesegang H, Schmitz RA, Jaeger KE, et al. 2003. Metagenome Survey of Biofilms in Drinking-Water Networks. Appl Environ Microbiol. doi:10.1128/AEM.69.12.7298-7309.2003.

Schneider OD, Lechevallier MW, Reed HF, Corson MJ. 2007. A comparison of zinc and nonzinc orthophosphate-based corrosion control. J / Am Water Work Assoc. doi:10.1002/j.1551-8833.2007.tb08084.x.

Schock MR. 1989. Understanding corrosion control strategies for lead. J Am Water Work Assoc. doi:10.1002/j.1551-8833.1989.tb03244.x.

Schofield WB, Zimmermann-Kogadeeva M, Zimmermann M, Barry NA, Goodman AL. 2018. The Stringent Response Determines the Ability of a Commensal Bacterium to Survive Starvation and to Persist in the Gut. Cell Host Microbe. doi:10.1016/j.chom.2018.06.002.

Shukla SK, Rao TS. 2017. An Improved crystal violet Assay for Biofilm Quantification in 96-Well Microtitre Plate. bioRxiv. doi:10.1101/100214.

Simões LC, Simões M, Vieira MJ. 2010. Influence of the diversity of bacterial isolates from drinking water on resistance of biofilms to disinfection. Appl Environ Microbiol. doi:10.1128/AEM.00872-10.

Sofo A, Ricciuti P. 2019. A standardized method for estimating the functional diversity of soil bacterial community by Biolog® EcoPlatesTM assay-The case study of a sustainable olive orchard. Appl Sci. doi:10.3390/app9194035.

Srinivasan S, Harrington GW, Xagoraraki I, Goel R. 2008. Factors affecting bulk to total bacteria ratio in drinking water distribution systems. Water Res. doi:10.1016/j.watres.2008.04.025.

Stefanowicz A. 2006. The biolog plates technique as a tool in ecological studies of microbial communities. Polish J Environ Stud.

Szewzyk U, Szewzyk R, Manz W, Schleifer K-H. 2000. Microbiological Safety of Drinking Water. Annu Rev Microbiol. doi:10.1146/annurev.micro.54.1.81.

Trogolo D, Arey JS. 2017. Equilibria and Speciation of Chloramines, Bromamines, and Bromochloramines in Water. Environ Sci Technol. doi:10.1021/acs.est.6b03219.

Tsvetanova Z. 2020. Quantification of the bacterial community of drinking water-associated biofilms under different flow velocities and changing chlorination regimes. Appl Water Sci. doi:10.1007/s13201-019-1086-6.

Vattem DA, Maitin V, Richardson CR. 2012. Evaluation of antibacterial and toxicological effects of a novel sodium silicate complex. Res J Microbiol. doi:10.3923/jm.2012.191.198.

Volk CJ, LeChevallier MW. 1999. Impacts of the reduction of nutrient levels on bacterial water quality in distribution systems. Appl Environ Microbiol. doi:10.1128/aem.65.11.4957-4966.1999.

Waak MB, Hozalski RM, Hallé C, Lapara TM. 2019. Comparison of the microbiomes of two drinking water distribution systems - With and without residual chloramine disinfection. Microbiome. doi:10.1186/s40168-019-0707-5.

Weber KP, Gehder M, Legge RL. 2008. Assessment of changes in the microbial community of constructed wetland mesocosms in response to acid mine drainage exposure. Water Res. doi:10.1016/j.watres.2007.06.055.

Weber Kela P., Legge RL. 2010. Community-level physiological profiling. Methods Mol Biol. doi:10.1007/978-1-60761-439-5_16.

Weber Kela P, Legge RL. 2010. Bioremediation - Methods and Protocols. Methods Mol Biol.

Wilczak A, Jacangelo JG, Marcinko JP, Odell LH, Kirmeyer GJ, Wolfe RL. 1996. Occurrence of nitrification in chloraminated distribution systems. J / Am Water Work Assoc. doi:10.1002/j.1551-8833.1996.tb06586.x.

Wingender J, Flemming HC. 2004. Contamination potential of drinking water distribution network biofilms. Water Sci Technol. doi:10.2166/wst.2004.0861.

Wolfe RL, Means EG, Davis MK, Barrett SE. 1988. Biological nitrification in covered reservoirs containing chloraminated water. J / Am Water Work Assoc. doi:10.1002/j.1551-8833.1988.tb03105.x.

XUE D, YAO H-Y, GE D-Y, HUANG C-Y. 2008. Soil Microbial Community Structure in Diverse Land Use Systems: A Comparative Study Using Biolog, DGGE, and PLFA Analyses. Pedosphere. doi:10.1016/s1002-0160(08)60060-0.

Yee LF, Abdullah P, Ata S, Abdullah A. 2008. Chlorination and chloramines formation. Malaysian J Anal Sci.

Yuan S, Yu Z, Pan S, Huang J, Meng F. 2020. Deciphering the succession dynamics of dominant and rare genera in biofilm development process. Sci Total Environ. doi:10.1016/j.scitotenv.2020.139961.

Zak JC, Willig MR, Moorhead DL, Wildman HG. 1994. Functional diversity of microbial communities: A quantitative approach. Soil Biol Biochem. doi:10.1016/0038-0717(94)90131-7.

Zhang HL, Fang W, Wang YP, Sheng GP, Xia CW, Zeng RJ, Yu HQ. 2013. Species of phosphorus in the extracellular polymeric substances of EBPR sludge. Bioresour Technol. doi:10.1016/j.biortech.2013.05.068.

Zhang HL, Fang W, Wang YP, Sheng GP, Zeng RJ, Li WW, Yu HQ. 2013. Phosphorus removal in an enhanced biological phosphorus removal process: Roles of extracellular polymeric substances. Environ Sci Technol. doi:10.1021/es403227p.

Zhang Y, Edwards M. 2009. Accelerated chloramine decay and microbial growth by nitrification in premise plumbing. J / Am Water Work Assoc. doi:10.1002/j.1551-8833.2009.tb09990.x.

Zhang Y, Love N, Edwards M. 2009. Nitrification in drinking water systems. Crit Rev Environ Sci Technol. doi:10.1080/10643380701631739.

Zhou X, Shen Y, Fu X, Wu F. 2018. Application of sodium silicate enhances cucumber resistance to Fusarium wilt and alters soil microbial communities. Front Plant Sci. doi:10.3389/fpls.2018.00624.

Zhu Z, Shan L, Hu F, Li Z, Zhong D, Yuan Y, Zhang J. 2020. Biofilm formation potential and chlorine resistance of typical bacteria isolated from drinking water distribution systems. RSC Adv. doi:10.1039/d0ra04985a.

Zhu Z, Shan L, Zhang X, Hu F, Zhong D, Yuan Y, Zhang J. 2021. Effects of bacterial community composition and structure in drinking water distribution systems on biofilm formation and chlorine resistance. Chemosphere. doi:10.1016/j.chemosphere.2020.128410.

Appendices

Appendix A

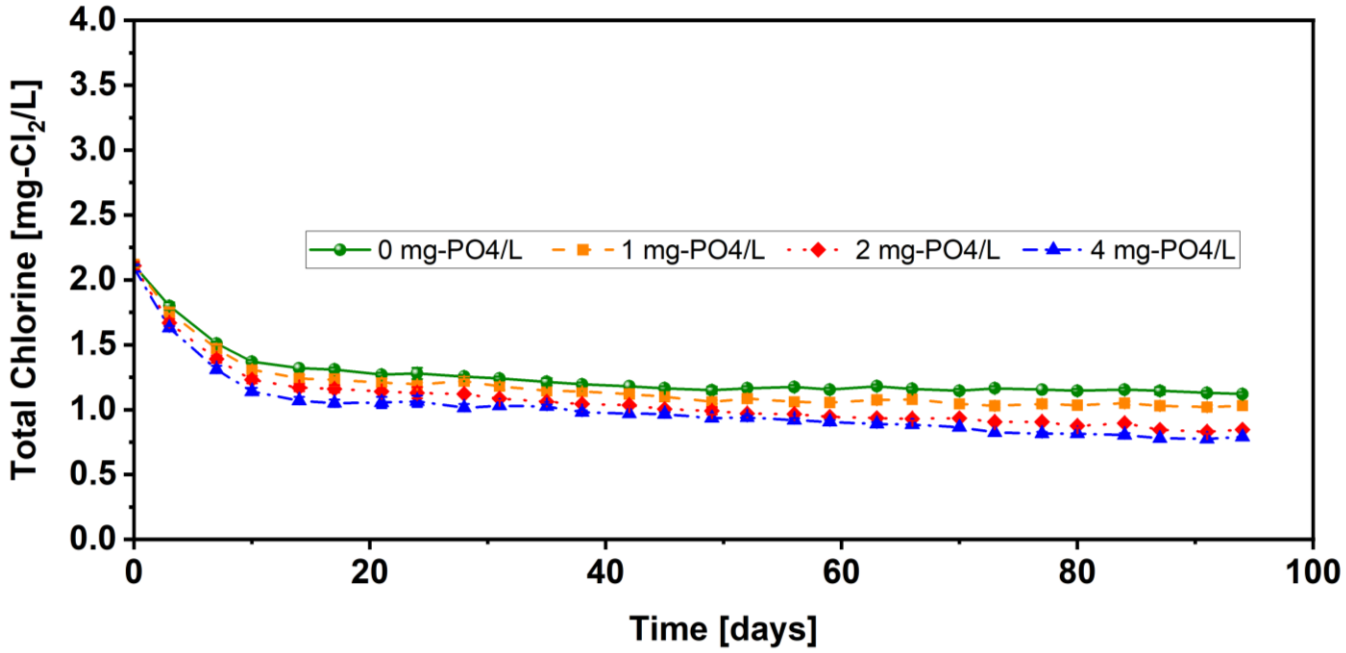

Appendix A1: Total chlorine (as CL_2) decay curve, dependant on orthophosphate dose in annular reactor (AR) systems. Supplied by Mahmoud Badawy, 2021.

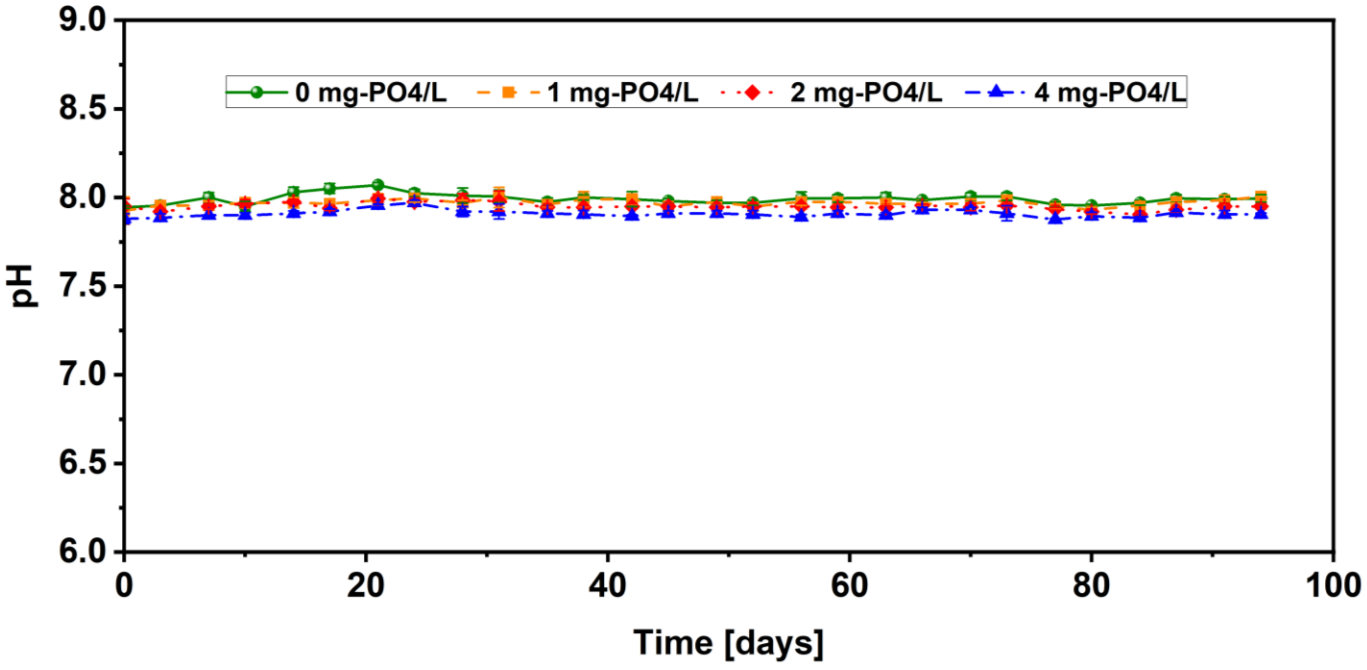

Appendix A2: pH stability of treated water, dependant on orthophosphate dose in annular reactor (AR) systems. Supplied by Mahmoud Badawy, 2021.

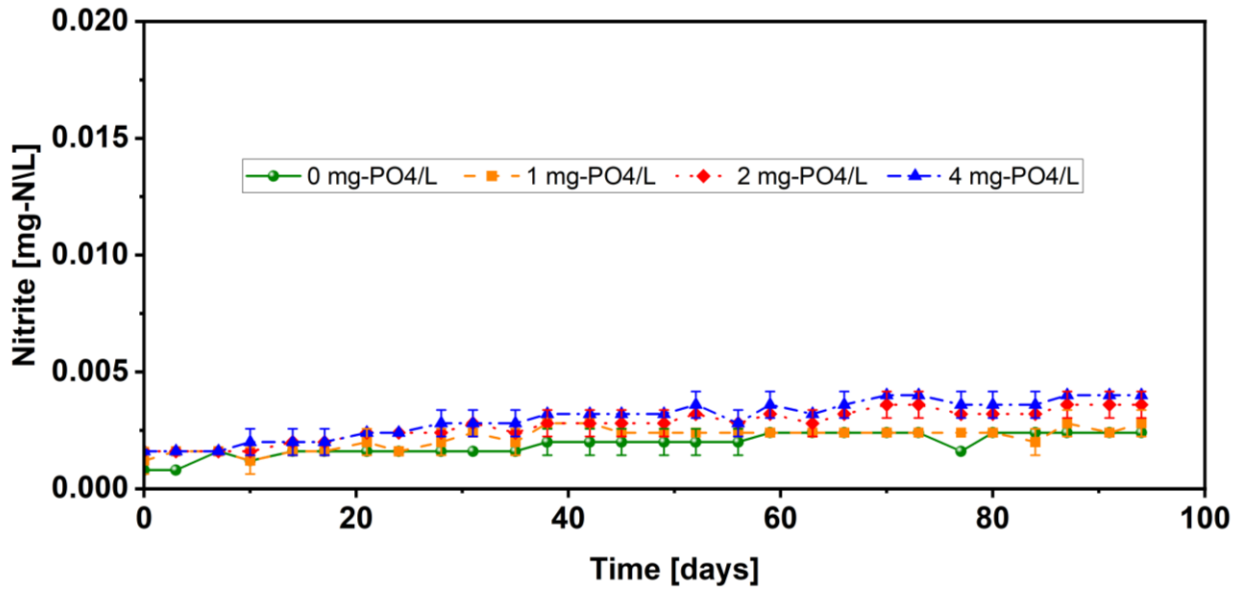

Appendix A3: Nitrite concentration, dependant on orthophosphate dose in annular reactor (AR) systems. Supplied by Mahmoud Badawy, 2021.

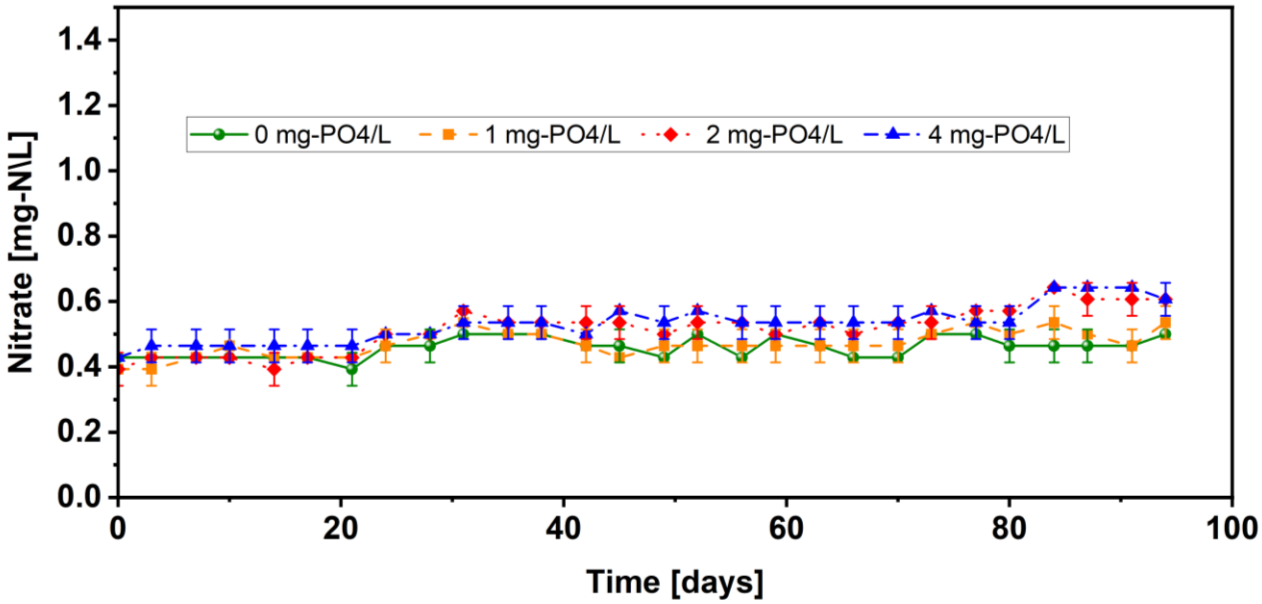

Appendix A4: Nitrate concentration, dependant on orthophosphate dose in annular reactor (AR) systems. Supplied by Mahmoud Badawy, 2021.

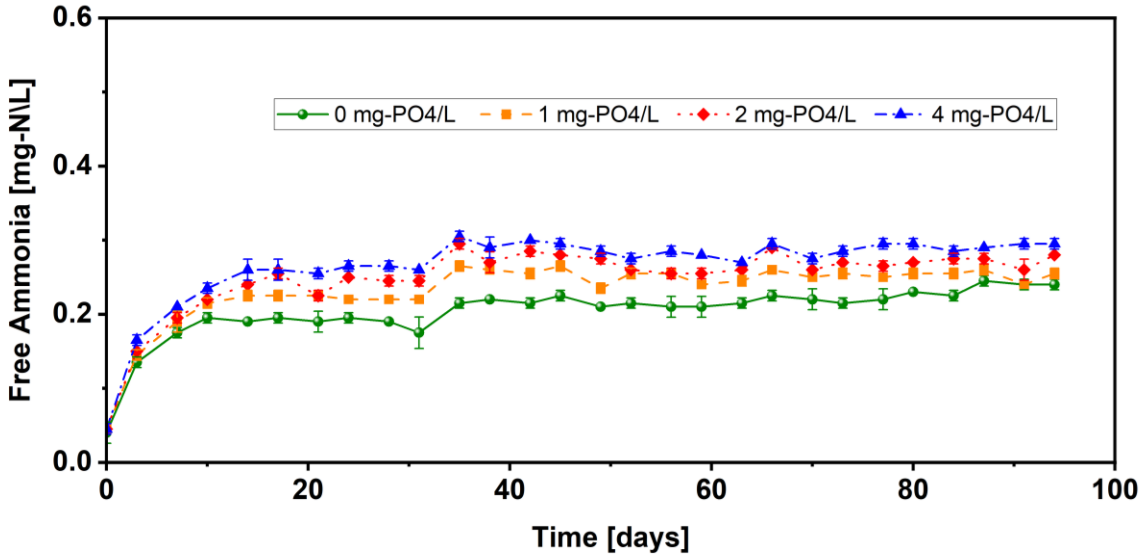

Appendix A5: Calculated free ammonia concentration from total chlorine losses, dependent on orthophosphate dose in annular reactor (AR) systems. Supplied by Mahmoud Badawy, 2021.

Appendix B

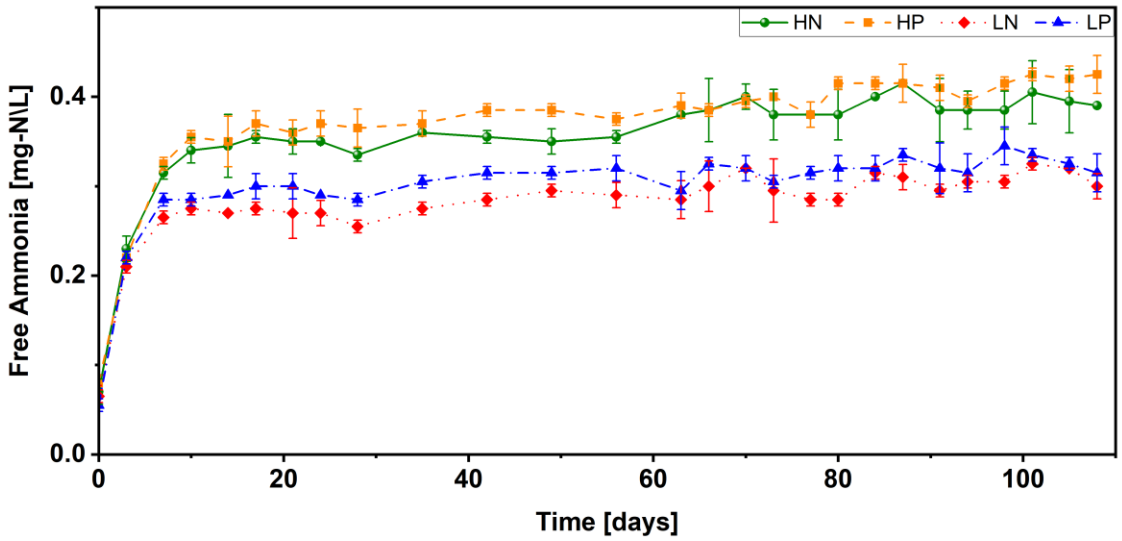

Appendix B0.1: Measured free ammonia in water sampled from annular reactors (ARs) dosed with 2 mg/L of orthophosphate. High MC= 3.0 mg/L chloramine as Cl_2. Low MC= 2.0 mg/L chloramine as Cl_2 Courtesy of Mahmoud Badawy, 2021.

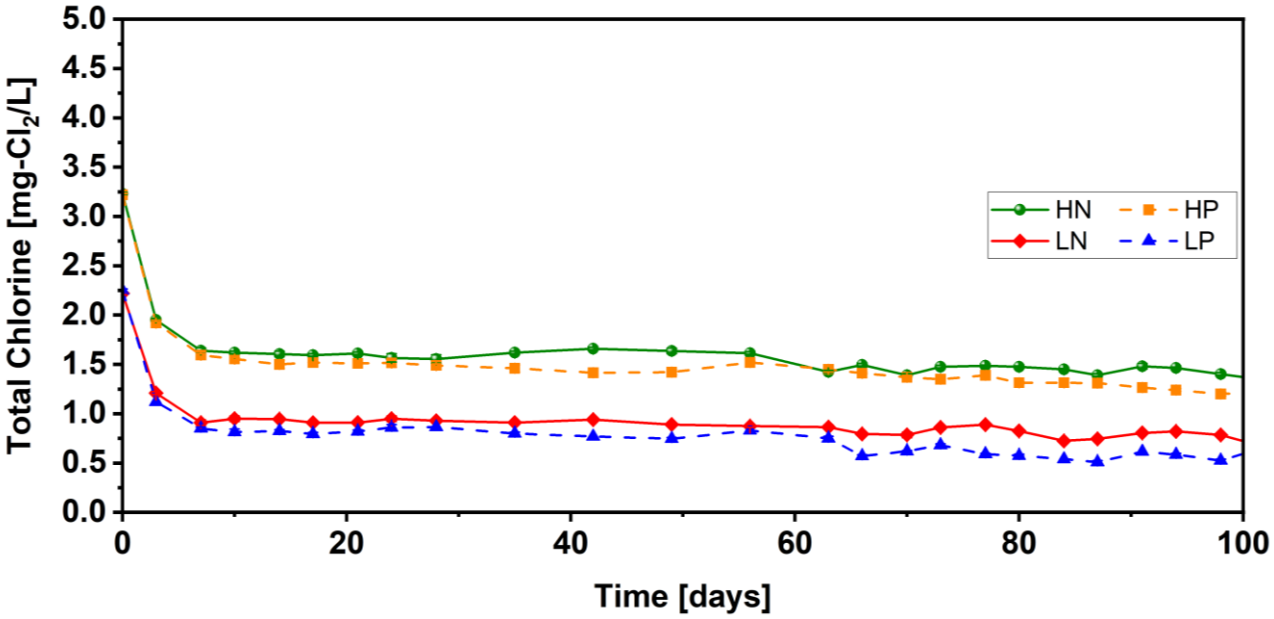

Appendix B2: Total chlorine (as CL2) decay curve in water sampled from annular reactors (ARs) dosed with 2 mg/L of orthophosphate. High MC= 3.0 mg/L chloramine as Cl_2. Low MC= 2.0 mg/L chloramine as Cl_2. Courtesy of Mahmoud Badawy, 2021.

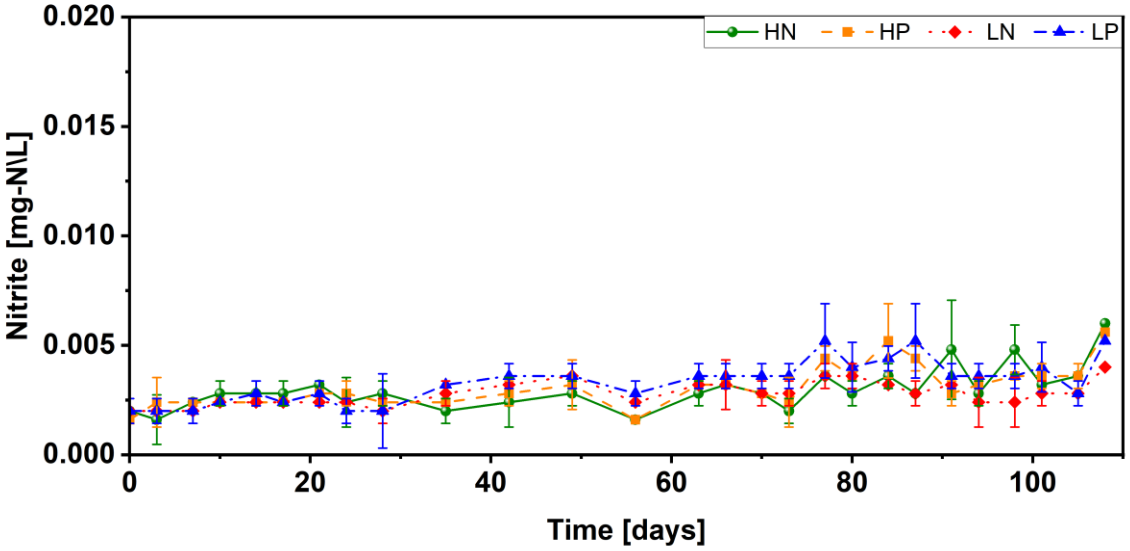

Appendix B3: Measured nitrites in water sampled from annular reactors (ARs) dosed with 2 mg/L of orthophosphate. High MC= 3.0 mg/L chloramine as Cl_2. Low MC= 2.0 mg/L chloramine as Cl_2. Courtesy of Mahmoud Badawy, 2021.

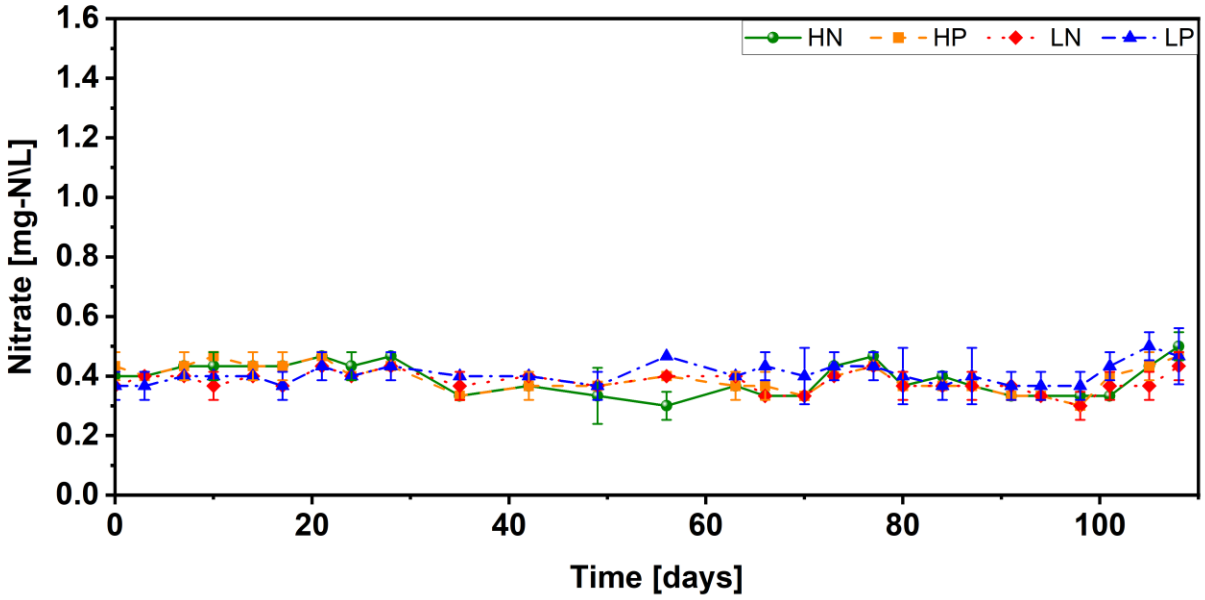

Appendix B4: Measured nitrates in water sampled from annular reactors (ARs) dosed with 2 mg/L of orthophosphate. High MC= 3.0 mg/L chloramine as Cl_2. Low MC= 2.0 mg/L chloramine as Cl_2. Courtesy of Mahmoud Badawy, 2021.

Appendix C

To roughly determine if phosphorous was a limiting nutrient, and if the addition of orthophosphate would impact microbial growth at concentrations typically seen in a DWDS, flasks containing sampled water (taken in early February 2021), before the addition of disinfectant, were dosed with OP at concentrations of 0, 1, 2, 3, 4 and 5 mg/L (0, 0.33, 0.66, 1, 1.33 and 1.66 mg/L of Phosphorus, respectively). Over 21 days, HPC were preformed to understand the addition of OP on the microbial communities present. Appendix C shows the results of this batch test, where samples dosed with OP exhibited higher viable cell counts, when compared to the control.

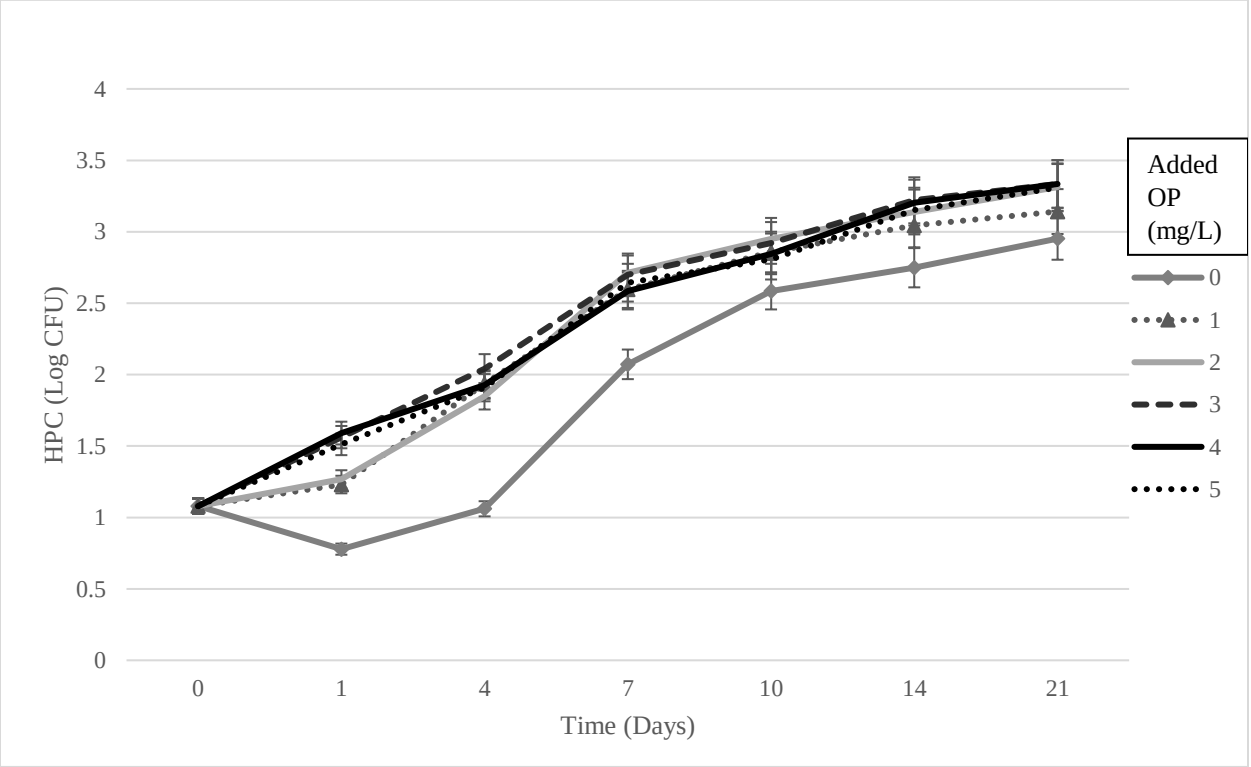

Appendix C1: Heterotrophic plate counts (HPCs) of batch test sampled dosed with orthophosphate (OP). Samples from batch flasks were plated in duplicate. Error bars represent standard error (n=2).